

**Sediment Magnetic Record of Post-colonial Environmental Change
in Frenchman's Bay, Lake Ontario**

**SEDIMENT MAGNETIC RECORD OF
POST-COLONIAL ENVIRONMENTAL CHANGE IN
FRENCHMAN'S BAY, LAKE ONTARIO**

By

Christina Clark, B. Sc. (Hons.)

A Thesis

Submitted to the School of Graduate Studies

In Partial Fulfilment of the Requirements

For the Degree

Master of Science

McMaster University

© Copyright by Christina Clark, September 2004

MASTER OF SCIENCE (2004)

McMASTER UNIVERSITY

(Geology)

Hamilton, Ontario

TITLE: Sediment Magnetic Record of Post-colonial Environmental Change in
Frenchman's Bay, Lake Ontario

AUTHOR: Christina Clark (McMaster University)

SUPERVISOR: Dr. J. I. Boyce

NUMBER OF PAGES: xv + 157

ABSTRACT

Frenchman's Bay is a shallow coastal lagoon (0.84 km²) located near the eastern limits of the Toronto urban area. Wholesale land clearance in the 1850's and subsequent industrialization and urbanization of the watershed have had severely impacted wetland habitats and degraded sediment and water quality. Prior to implementation of remediation work, a detailed sedimentologic and magnetic property study was conducted to determine the impacts of post-colonial land use changes in Frenchman's Bay. 11 vibrocores (2-4.5 m length) were extracted from the lagoon and 35 magnetic susceptibility profiles were collected using a probe driven 1-2 m in the lagoon floor. The core lithofacies were logged in detail and magnetic susceptibility (κ , χ) and remanence parameters (NRM, SIRM, Bcr) were measured at 2 cm intervals. Magnetic property and lithofacies data were integrated with geochemical analyses (TOC, CO₃) and ²¹⁰Pb dating of core in order to reconstruct the lagoon lithostratigraphy and the thickness of the post-colonial 'anthropogenic layer'.

The stratigraphic succession in the lagoon consists of a thick upper sequence of marly gyttja and peat-rich silty marls overlying Holocene laminated marls. The post-colonial layer (Unit 1) is recognized as an uppermost high magnetic susceptibility ($\chi = \sim 200\text{-}300 \times 10^{-8} \text{ m}^3/\text{Kg}$) gyttja layer that extends to 1-1.5 m depth. The base of the unit has a ²¹⁰Pb age of 1850 (± 55.6), corresponding with the main phase of land clearance and onset of industrialization of the harbour. Titanomagnetite, maghemite and magnetite spherules are the primary magnetic minerals, indicating soil erosion and coal burning as the predominant sources of magnetic particles. The underlying Unit 2 consists of peaty marls with abundant plant fragments recording a more extensive marsh. Unit 3 consists of

more carbonate-rich laminated sands (magnetic susceptibility $\chi \approx 6000 \times 10^{-8} \text{ m}^3/\text{Kg}$) deposited in a low energy oligotrophic lagoon. The basal layer (Unit 4) consists of high magnetic susceptibility massive pebbly muds, which record a pre-lagoon phase of higher water levels in post-glacial Lake Iroquois (ca. 13,500 Ka).

Isopach mapping of the magnetostratigraphic units clearly identifies that the anthropogenic layer (Unit 1; post-1850) is thickest within a central basin which has acted as trap for sediment carried into the lagoon by several streams. The total volume of impacted anthropogenic sediment is estimated at $4 \times 10^5 \text{ m}^3$. Isopach maps also identify two thin ($< 2 \text{ m}$) wedges of sand ($9.6 \times 10^4 \text{ m}^3$) near the north and southern shores of the bay that records periodic overwash and growth of the beach barrier.

The major environmental changes in the lagoon since its inception (ca. 2.7 Ka) include: 1. The formation of a shallow coastal embayment following water level rise from a mid-Holocene low-stand in Lake Ontario (Unit 4); 2. Development of a spit and beach barrier by eastward longshore transport (Unit 3); 3. Closure of the lagoon and development of a stabilized marsh habitat with low sedimentation levels (Unit 2); 4. Destruction of marsh habitats and eutrophication of the lagoon coinciding with land clearance (post-1850's) and an increase in the influx of sediments eroded from the catchment area.

ACKNOWLEDGEMENTS

I would like to thank Dr. J.I. Boyce for providing funding for this research through a NSERC research grant, and the unique concept for this thesis.

I need to offer a special thanks to Dr. W.A. Morris for always asking the sometimes infuriatingly tough questions because he knew it was in us to answer them. Your confidence and guidance has been invaluable over the past few years, and it's been awesome working with you and getting to know you. And thank you again for coming in on your vacation to help me fix problems!!

I would also like to thank Dr. Eduard Reinhardt for opening up his labs to me over the past two years, and for the continual use of a variety of his equipment. I doubt that I will ever miss the coulter counter or the sound of the core fridge compressor, but I do appreciate being able to use them!

A big thank you is sent to Shawn Collins for helping, listening and challenging my ideas because it certainly helped strengthen my work. I'm glad we had each other to work through frustrations and share the masters experience. Shawn and the Geophysics Lab (Vicki, Kristi, Heather, Dickie, Steve) have been a huge support over the past two years, so thanks for the help, distractions, and especially the memories!

There are a number of people who volunteered to help me collect my data out on Frenchman's Bay, and without their help I would have been in deep trouble. So I would like to thank the following people for helping with the coring, probing or general tinkering with my equipment in and out of the field; Greg Potter, Shawn Collins, Mahsa Moghaddas, Jen Clark (even though you broke my equipment!), Vicki Thomson, Sean Dickie, Gloria Lopez, Andrew Kingston, Tammera Kostya, Bev Goodman, Mike Doughty and Dr. Nick Eyles.

Now for my roommates, who you may notice were also dragged out into the field. Thanks to Mahsa, Jen and Dickie for putting up with my crazy hours and frustrations at random times, and for all the edits and for listening to my thesis 'stuff' so much that Dickie isn't the only one who could ace a mag final! You guys are awesome!

Of course Jen isn't just a roommate, she's my twin sister who has been a great support to me our whole life. You understand me better than myself sometimes, and you helped keep me grounded and enjoying the bigger picture throughout my masters. Thank you for that.

My final thanks is saved for Bry. Thank you for everything you've done in that wonderfully supportive nature that you have, who knows maybe one day it will rub off on me! And thanks so much for all of the extra things you do, which includes editing my thesis on the shores of the Detroit river for *many* hours!!

TABLE OF CONTENTS

TITLE PAGE	I
ABSTRACT	III
ACKNOWLEDGEMENTS	V
TABLE OF CONTENTS	VII
LIST OF FIGURES	XI
LIST OF TABLES	XIV
LIST OF EQUATIONS	XIV
LIST OF ABBREVIATIONS	XV
PREFACE	XVI
CHAPTER 1: INTRODUCTION	1
1.1 Background and Rationale	1
1.1.1 Environmental Magnetism	5
1.2 Study area	10
1.2.1 Physical Setting.....	10
1.2.2 Geology	10
1.2.3 Previous Work	12
1.2.4 Historical Background.....	14
1.2.5 Types of Magnetic Behaviour.....	15
1.2.6 Hysteresis.....	19
1.2.7 Domains.....	22
1.2.8 Magnetic Parameters	24
<i>Magnetic Susceptibility (χ or κ)</i>	24
<i>% Frequency Dependence of Magnetic Susceptibility ($\chi_{fd\%}$)</i>	25
<i>Natural Remanent Magnetization (NRM)</i>	26
<i>Viscous Remanent Magnetization (VRM)</i>	27
<i>Isothermal Remanence Magnetization (IRM)</i>	27
<i>Remanent Coercive Force (Bcr)</i>	28
1.2.9 Magnetic Bivariate Ratios and Plots	28
<i>IRM/SIRM</i>	28
<i>S-Ratio (IRM-100mT/SIRM)</i>	29
<i>S-Ratio versus χ Plot</i>	31
<i>SIRM/χ</i>	31
<i>SIRM/χ versus Bcr Plot</i>	32

	<i>χ</i> versus Bcr Plot.....	33
	<i>χ</i> versus TOC + CO ₃ Plot.....	33
	Gradient of IRM Acquisition Curve.....	34
1.2.10	Environmental Applications of Magnetics.....	34
	Magnetic Mineral Concentration, Minerology and Grain Size.....	35
	Magnetic Susceptibility.....	37
1.3	Methods.....	39
1.3.1	Sampling Procedures.....	39
	Coring.....	39
	Proto-type Probe.....	44
1.3.2	Geotechnical Analyses.....	45
	Lithology.....	45
	Grain Size.....	47
	Loss on Ignition (LOI).....	52
	²¹⁰ Pb Dating.....	54
	ESEM and XRD.....	55
1.3.3	Magnetic Property Analyses.....	57
	Bulk Magnetic Susceptibility (<i>χ</i>).....	57
	Volume Magnetic Susceptibility (<i>κ</i>).....	57
	Natural Remanence Magnetization (NRM).....	58
	Isothermal Remanence Magnetization (IRM).....	58
CHAPTER 2: RAPID IN-SITU MEASUREMENT OF MAGNETIC SUSCEPTIBILITY IN		
LAKE SEDIMENTS: A CASE STUDY FROM FRENCHMAN'S BAY, LAKE		
ONTARIO, CANADA.....		
2.1	Abstract.....	60
2.2	Introduction.....	61
2.3	Methods.....	63
2.3.1	Probe Construction.....	63
	Effective Sensing Volume.....	65
	Response to Thick and Thin Beds.....	68
2.3.2	Study Area.....	69
2.4	Results.....	72
2.4.1	Probe Response.....	72
2.4.2	Frenchman's Bay.....	75
2.5	Conclusions.....	81

CHAPTER 3: A MULTI-PROXY RECORD OF POST-COLONIAL AND LATE HOLOCENE ENVIRONMENTAL CHANGE IN FRENCHMAN'S BAY, LAKE ONTARIO, CANADA	83
3.1 Abstract	83
3.2 Introduction	85
3.2.1 Study Area and Geologic Setting.....	88
<i>Physical Setting</i>	88
<i>Settlement History</i>	88
<i>Geology</i>	92
3.3 Methods	94
3.3.1 Coring.....	94
3.3.2 Magnetic Properties.....	94
3.3.3 Chronology	96
3.3.4 ESEM and XRD.....	96
3.4 Results	97
3.4.1 Lithology	98
<i>Unit 1</i>	98
<i>Unit 2</i>	107
<i>Unit 3</i>	107
<i>Unit 4</i>	108
3.4.2 Chronology	108
3.4.3 ESEM and XRD.....	109
3.4.4 Magnetostratigraphy.....	114
3.4.5 Magnetic Properties.....	118
<i>Magnetic Susceptibility</i>	118
<i>SIRM/χ vs Bcr Biplot</i>	119
<i>χ vs Bcr Bivariate plot</i>	122
<i>S-ratio vs χ Bivariate Plot</i>	122
<i>SIRM vs χ Bivariate Plot</i>	127
<i>χ vs. TOC+CO₃ Bivariate Plot</i>	131
<i>Gradient of IRM acquisition curve</i>	131
<i>Dominant Magnetic Characteristics of Each Unit</i>	134
3.5 Discussion/ Environmental Interpretation	136
3.5.1 Stage 1: FMB Basin Formation (Unit 4).....	136
3.5.2 Stage 2: Rapid Lake Level Rise.....	138
3.5.3 Stage 3: Formation of Beach Barrier (Unit 3)	138
3.5.4 Stage 4: Stable Oligotrophic Lagoon (Unit 2).....	139
3.5.5 Stage 5: The Modern Lagoon (Unit 1).....	142

	<i>Water Level History</i>	146
3.6	Conclusion	146
CHAPTER 4:	CONCLUSIONS	148
CHAPTER 5:	REFERENCES	152
APPENDIX A:	LITHOLOGIC LOG TEMPLATE	A - 1
APPENDIX B:	EXAMPLE PRINTOUT FROM THE BECKMAN-COULTER LS 230 LASER PARTICLE SIZE ANALYSER	B - 1
APPENDIX C:	DETAILED LITHOLOGIC LOGS FOR FRENCHMAN’S BAY	C - 1

LIST OF FIGURES

Figure 1.1: Frenchman’s Bay study area showing the extent of the watershed and lagoon.	11
Figure 1.2: Schematic diagrams showing the distribution of magnetization vectors in crystals that experience spontaneous magnetization (Walden <i>et al.</i> , 1999).	17
Figure 1.3: The TiO ₂ -FeO-Fe ₂ O ₃ ternary diagram showing the composition of common iron-titanium oxides (Walden <i>et al.</i> , 1999; p. 20 Fig 2.9).	18
Figure 1.4: M-H plot for ferromagnetic material showing hysteresis parameters (Walden <i>et al.</i> , 1999).	21
Figure 1.5: Magnetic susceptibility response in the sediment profile of Hamilton Harbour (Versteeg, 1994).	38
Figure 1.6: Lake-based vibracoring in a boat and floating platform.	40
Figure 1.7: Measurements required to determine uncompacted core length and elevation calculations.	43
Figure 1.8: Equipment required to split aluminium sediment cores obtained from the field.	46
Figure 1.9: The automated Beckman-Coulter LS 230 laser particle size analyzer. An example grain size analysis print out is available in Appendix B:	50
Figure 2.1: A. Probe housing for the MS2-F probe shown on the right. Probe tip is attached to 5 m long PVC and ABS pole. B. Probe in use in the field for in-situ measurements of sediment volume magnetic susceptibility (κ). Probe is advanced into sediment at 2 cm intervals.	64
Figure 2.2: Diagram showing sand columns used to test probe response. A. Probe response and effective sensing volume determined using sand-filled cylinders of decreasing diameters. Effective probe sensing volume is a hemisphere with a 2.1 cm radius. B. Response of the probe to thin sand beds (1.5, 3 cm thickness, $\chi = 39.7 \times 10^{-8}$ SI) within low susceptibility ($\chi = 23.5 \times 10^{-8}$ SI) sand.	66
Figure 2.3: Map showing the location of Frenchman's Bay, coring and sediment probe locations and lagoon bathymetry.	70
Figure 2.4: A. Detailed lithologic log for borehole FMB4 with approximate sediment ages based on ²¹⁰ Pb dating. B. The bulk (laboratory) magnetic	

<p>susceptibility (χ) measured at ca. 2 cm intervals down the core. C. Laboratory volume magnetic susceptibility (κ) profile. D. In-situ volume susceptibility profile measured with probe at location #14.....</p>	73
<p>Figure 2.5: Linear regression of laboratory versus in-situ field magnetic susceptibility from FMB-4 and probe #14. Linear equation is used to calibrate in-situ volume magnetic susceptibility measurements against laboratory values.....</p>	76
<p>Figure 2.6: A North-south magnetostratigraphic section showing correlated volume magnetic susceptibility profiles (κ). The post-colonial sediment layer is identified by a κ increase of 50-100 $\times 10^{-5}$ SI in the upper 50-120 cm of the profiles. Another feature that had a shorter wavelength (8-20 cm) and higher intensity (100-500 $\times 10^{-5}$ SI) was identified as a sand and sandy silt layer. The location of the transect is shown in Figure 2.3A.....</p>	78
<p>Figure 2.7: Isopach maps showing A. the post-colonial sediment layer in Frenchman's Bay, and B. the location of sandy overwash deposits from the modern and possibly relict beach barriers.....</p>	80
<p>Figure 3.1: The locations of cores, magnetic susceptibility (k) profiles and transects in Frenchman's Bay.....</p>	89
<p>Figure 3.2: Frenchman's Bay watershed showing the extent of urban cover and main sources of urban effluents. Source data obtained from (PlantownConsultantsLtd., 1975; Eyles <i>et al.</i>, 2002; Gerrie <i>et al.</i>, 2003).....</p>	90
<p>Figure 3.3: A number of transgressive shoreline positions and changes in wetland extent and land use (see inset) in the Frenchman's Bay area are shown on the earlier 1954 aerial photograph (Photo from (Hunting, 1954). Red = 1954 wetland and shoreline position, Yellow = 1995 wetland and shoreline position.....</p>	93
<p>Figure 3.4: The lithologic log for core FMB1 along with data for sediment and magnetic parameters used to identify four distinct units in Frenchman's Bay.....</p>	99
<p>Figure 3.5: The lithologic log for core FMB2 along with data for sediment and magnetic parameters used to identify four distinct units in Frenchman's Bay.....</p>	101
<p>Figure 3.6: The lithologic log for core FMB3 along with data for sediment and magnetic parameters used to identify four distinct units in Frenchman's Bay.....</p>	103
<p>Figure 3.7: The lithologic log for core FMB4 along with data for sediment and magnetic parameters used to identify four distinct units in Frenchman's Bay.....</p>	105

Figure 3.8: Sediment accumulation rates determined for Frenchman’s Bay from ²¹⁰ Pb analysis.	109
Figure 3.9: ESEM images and XRD spectra of grains found in units 1 and 2.	110
Figure 3.10: A north-south transect showing correlated sediment facies and magnetic properties. Location of the transect is shown in Figure 3.1.....	115
Figure 3.11: Isopach maps of A. the post-colonial sediment layer in Frenchman’s Bay, and B. the location of sand and storm overwash sediments from the modern and possibly relict beach barriers.	117
Figure 3.12: Biplot of SIRM/ χ versus remanent acquisition coercivity (Bcr) for cubet subsamples from cores FMB1 and FMB4.....	120
Figure 3.13: Bivariate plot of bulk magnetic susceptibility (χ) versus remanent acquisition coercivity (Bcr) for cubet subsamples obtained from cores FMB1 and FMB4.....	123
Figure 3.14: Bivariate plot of S-ratio versus χ for cubet subsamples from cores FMB1 and FMB4.	125
Figure 3.15: Bivariate plot of SIRM versus χ for cubet subsamples from cores FMB1 and FMB4.	128
Figure 3.16: Bivariate plot of X versus weight percent organic and carbonate matter for subsamples from cores FMB1, FMB2, FMB3, and FMB4.....	132
Figure 3.17: The gradient of IRM acquisition curve for a sediment sample from unit 1 (depth = 10.5 cm) in core FMB1.....	133
Figure 3.18: Frenchman’s Bay Sediment model.....	145

LIST OF TABLES

Table 1.1: Magnetic and compositional properties of some common minerals	8
---	----------

LIST OF EQUATIONS

Equation 1.1: % Frequency Dependence of Magnetic Susceptibility	25
Equation 1.2: Calculating the uncompacted length of a core.....	42
Equation 1.3: Weight percent organic matter.....	53
Equation 1.4: Weight percent carbonate content.....	53
Equation 1.5: Bulk Magnetic Susceptibility (χ).....	57

LIST OF ABBREVIATIONS

Bcr	Remanent coercive force; the field at which the IRM of a previously saturated sample is reduced to zero in the backfield direction (outside inducing field)
Bcr'	Remanence acquisition coercive force; the field necessary to reach half of the saturation IRM during initial acquisition (approx. equals Bcr) (Robertson and France 1994; Stockhausen 1998)
FMB	Frenchman's Bay
H	The applied field; used when inducing a magnetization (mT)
Hc	Coercive force (inside inducing field)
Hcr	Coercivity of remanence (inside inducing field)
Hs	Applied Saturation Field; the applied field required to induce Ms (inside inducing field parameter)
IRM	Isothermal Remanent Magnetism
k or κ	Volume Magnetic Susceptibility (10^{-6} SI) *note κ is unitless
M	Overall Magnetization
Mr	Remanent Magnetisation (outside inducing field) (A/m)
Mrs	Saturation Remanent Magnetism (similar to SIRM, but a constant temperature is not maintained) (A/m)
Ms	Saturation Magnetisation (inside inducing field) (A/m)
NRM	Natural Remanent Magnetism
SIRM	Saturation Isothermal Remanent Magnetism (similar to Mrs, but a constant temperature is maintained)
S-Ratio	$IRM_{-100 \text{ mT}} / SIRM$; the isothermal remanent magnetism acquired after a backfield of 100 mT is applied to the sample, divided by the SIRM of the same sample
Tc	Curie Temperature ($^{\circ}\text{C}$)
$\chi_{fd\%}$	Percent Frequency Dependence of Magnetic Susceptibility
χ	Bulk Magnetic Susceptibility ($10^{-8} \text{ m}^3/\text{kg}$)

PREFACE

Chapters 2 to 3 in this thesis have been prepared for publication in various academic journals. As required by McMaster University regulations, this section outlines what work was performed by the author, and the contributions of the co-authors.

Chapter 2: Rapid In-situ Measurement of Magnetic Susceptibility in Lake Sediments: A Case Study from Frenchman's Bay, Lake Ontario, submitted to *Journal of Applied Geophysics*. Laboratory experiments and field work was designed, conducted and analysed by the author. Co-author Dr. J. I. Boyce provided funding through a research grant from the Natural Science and Engineering Research Council of Canada, the concept for the project, and various edits.

Chapter 3: A multi-proxy record of post-colonial and Late Holocene environmental change in Frenchman's Bay, Lake Ontario, Canada, submitted to *Journal of Paleolimnology*. All experimental data and geotechnical analysis was collected or performed by the author. Co-author Dr. J. I. Boyce provided funding through a research grant from the Natural Science and Engineering Research Council of Canada, as well as the concept for the project. Co-author Dr. E. G. Reinhardt provided the use of his laboratory facilities and equipment, while also assisting with core collection and providing all of the micropaleontological analysis. Dr. W.A. Morris provided the use of his paleomagnetic laboratory facilities while also offering insightful discussion sessions regarding magnetic theory and providing critical reviews of the magnetic analyses and final interpretations.

Chapter 1: INTRODUCTION

1.1 Background and Rationale

Land use changes associated with colonization and the subsequent growth of urban areas have dramatic effects on coastal habitats in western Lake Ontario. The Greater Toronto urban area now supports 1 out of 5 Canadians and is one of the most rapidly growing urban centres in North America. Management of the environmental impacts of urbanization is a major problem facing Toronto and other Canadian communities and municipalities. The restoration of waterfront areas is a growing concern and requires that municipal planning departments have access to high quality environmental information to allow them to develop effective land use plans and remediation policies. One of the most significant challenges facing planners and environmental scientists is the restoration of urban-impacted lagoons and river mouths, since they are the primary receiving basins and accumulation areas for contaminants carried into Lake Ontario by urbanized streams. These small enclosed water bodies are often characterized by highly degraded water and sediment quality as a result of historical loadings from storm sewer systems and effluents from industrial and agricultural sources. An important requirement prior to remediation of these habitats is a good understanding of both the pre-colonization conditions in the watershed and the natural variability of the systems. This baseline information includes knowledge of past hydrologic conditions, changes in water levels, sedimentation rates, lake status and habitat health. From a practical remediation standpoint, an understanding of contaminated sediment loadings

and accumulation areas is one of the most critical requirements for planning a remediation strategy, as it dictates what type of strategy will be used to deal with contaminated sediments.

In eastern Greater Toronto Area, the City of Pickering has recently begun a process to restore waterfront habitats within the Frenchman's Bay watershed area (Fig. 1). Frenchman's Bay is a shallow coastal lagoon on the Lake Ontario shoreline and has a long history (>150 years) of urban and industrial development. The lagoon is known to local residents as 'the toilet bowl' due high levels of bacteria, sporadically strong odours, and high concentrations of urban pollutants that have rendered the bay unsuitable for many recreational purposes. In response the City of Pickering in 2001, initiated an environmental study of the lagoon with a view to developing a strategy for restoration of the bay and its habitats. The study is a multi-disciplinary effort involving a collaboration between the City of Pickering, McMaster University and University of Toronto. The primary objectives of the study were to establish the current limnological and biological conditions within the lagoon and to identify specific areas of environmental concern. A related objective which is the topic of this thesis, is to establish the geological framework of the lagoon and to document the paleoenvironmental changes associated with colonization and urbanization of Frenchman's Bay. The specific aims of the thesis are:

1. To map the distribution and vertical changes in the lagoon bottom sediments, and to construct a depositional model which accounts for the observed stratigraphy;

2. To evaluate the use of in-situ measurement of magnetic susceptibility as a method for mapping the thickness and distribution of contaminant-impacted ‘anthropogenic’ sediments in the lagoon;
3. To reconstruct the paleoenvironmental changes and human impacts on Frenchman’s Bay, including the effects of changes in landuse and urbanization, using a multi-parameter magnetic and sediment physical property data.

The objectives were accomplished through a multi-proxy study that integrates analysis of sediment magnetic properties, sedimentology and sediment geochemistry to reconstruct the changes in the paleoenvironment of Frenchman’s Bay

This information is critical to the planned remediation efforts as it defines the baseline environmental conditions and changes in the lagoon environment over time. Increased knowledge of the lagoon subsurface geology (Objective 1) is critical for planned remediation work because the lagoon bottom sediments are the primary repository for urban pollutants. An understanding of sediment distribution, grain size and other characteristics (e.g. organic content) is also important for predicting contaminant migration and the mobility of some contaminants in the subsurface.

The second objective evaluates the use of enviromagnetic methods (see Section 1.1.1) for mapping anthropogenic sediments in the lagoon. A new approach is presented for mapping urban-sourced lake sediments using in-situ measurements with a magnetic suscpetibility probe driven into the lake bottom. This new and innovative technique provides a rapid means of assessing and calculating the volume of urban-impacted

sediments prior to remediation. The third focus of the thesis (Objective 3) is to reconstruct changes in the paleoenvironmental conditions within the lagoon resulting from land use changes. The approach employed made use of a number of paleoenvironmental proxy indicators including sediment (magnetic properties, sediment facies, geochemistry and ^{210}Pb dating) to achieve a more complete understanding of human-induced changes in the lagoon. This approach is adopted because use of single parameter (e.g. lithology, microfaunal evidence) can sometimes lead to non-unique or incomplete characterization of environmental system. The following sections outline the principle methods used in the multi-proxy approach adopted in this thesis. Environmental magnetic methods are explained in some detail as they are the primary environmental proxy employed. Further references and detailed case studies of environmental magnetic applications are given by Evans and Heller (2003).

1.1.1 Environmental Magnetism

The magnetic properties of sediments mainly depend on geological processes such as erosion and weathering, diagenetic processes such as oxidation or reductive dissolution, biogenic magnetism, or limnological parameters such as lake status and water chemistry (Snowball 1994; Reynolds and King 1995; Last and Smol 2001). All of these factors can change the concentration, mineralogy and particle-size distribution (and therefore domain state) of the magnetic minerals present in the sediment and can be measured by analysis of the rock magnetic properties (Walden et al. 1999). The study of magnetic properties along with the investigation of how changes in processes and environments lead to the development of the final suite of magnetic properties is referred to as environmental magnetism. Magnetic properties investigated during this study are discussed later in section 1.2.5. The properties were analyzed alone or in conjunction with other magnetic or sediment properties in order to isolate and filter out even more information about processes and paleoenvironments that have existed in FMB.

Early research (Beckwith et al. 1986; Locke and Bertine 1986) in environmental magnetism identified elevated levels of magnetic oxides in soils were due to atmospheric sources of magnetic minerals associated with magnetite spherules produced during oxidation of pyrite in industrial processes that included combustion of organic matter (eg. coal, oil). It was also discovered that aeolian transport could distribute the ~10 μm spherules far from their sources due to their small size, which is why their widespread presence is noted with slash burning during colonization and at higher concentrations

with the onset of industrialization. Several subsequent studies confirmed these findings and showed a direct correlation between the magnetic susceptibility (ease of magnetization) of contaminated soils and the presence of hydrocarbons, heavy metals (Cu, Fe, Pb, Zn, Cd and Cr) or other combustion-related pollutants (Morris et al. 1995; Chan et al. 1998; Heller et al. 1998; Petrovsky et al. 2000; Desenfant et al. 2004). Magnetic measurements have also proven to be a useful indicator of anthropogenic effects in lake basins, including the onset of land clearance (Boar and Harper 2002), roadside pollution (Hoffmann et al. 1999; Petrovsky et al. 2000), forest fires (Rummery 1983), and soil enhancement & erosion (Shenggao 2000). A technique for rapid remote collection of high resolution sediment magnetic property data for sediments in Hamilton Harbour was recently demonstrated for proxy contaminant mapping by Pozza et al. (2004).

Environmental magnetic methods are being employed in this study in order to characterize the sediment record of anthropogenic impacts on Frenchman's Bay. Baseline conditions and historical changes in sediment sources and processes are determined from ex-situ core and in-situ sediments.

There are a number of magnetic parameters that can be examined alone or in combination to determine the concentration, mineralogy and grain size of magnetic materials in sediment. The end of this chapter summarizes the main magnetic parameters employed in this study and their interpretation and significance for environmental reconstruction. As an introduction to this section, the basic principles of magnetism and

properties of magnetic minerals are first discussed in section 1.2.5. Table 1.1 lists the magnetic and compositional properties of some common minerals to aid in the discussion and later interpretation of magnetic parameters.

There are a number of possible sources for magnetic mineral inputs to Frenchman's Bay that can alter the magnetic properties of the sediment. Some important sources of magnetite include:

- Fossil fuel combustion processes (eg. cars, fireplaces) that involve the oxidization of pyrite to magnetite;
- Atmospheric fall-out;
- Forest fires;
- Soil erosion;
- Urban runoff to streams.

Hoffman et al. (1999) identify highly magnetic spherules produced during processes such as combustion (fly-ash) welding, steel production, smelting, etc. as anthropogenic sources of ferrimagnetic particles. Built in the late 1940s, Hwy 401 expanded from a two lane to a four-lane highway, which draws more cars with their exhaust and requires much more road salt or sand to de-ice the roads in the winter. The Canadian Pacific and Canadian National Railways also cross through Frenchman's Bay's watershed, and can provide additional sources of magnetic mineral sediment and chemical input to the lagoon from their cargo or general disruptive movement through the area. Marsh vegetation traps incoming sediment so that the sediment supply to the bay is reduced, but the degradation of marshland in FMB has resulted in a much higher sediment supply of coarser grain sediments and volume to the lagoon in the more recent years.

Table 1.1: Magnetic and compositional properties of some common minerals.

Mineral ¹	Composition _{1,2}	Magnetism	Density ¹ (g/cm ³)	χ ² (10 ⁻⁶ m ³ Kg ⁻¹)	Ms ^{1,3} (kA/m)	Tc ¹ (°C)	(Mrs) SIRM ² (Am ² Kg ⁻¹)	Avg Bcr ⁴ (mT)	Avg SIRM/ χ ⁴ (kA/m)
Iron	α Fe	Ferrimagnetic	7.874	276000	1715	765			
Magnetite	Fe ₃ O ₄	Ferrimagnetic	5.197	400 – 1000	480	580	10 - 40	24.4	11.3
Maghemite	γ Fe ₂ O ₃	Ferrimagnetic	5.074	250 – 450	380	590 – 675	5 – 35 ² ~ 6.8 ⁴	20.8	11
Titanomagnetite	Fe _{2.4} Ti _{0.6} O ₄	Ferrimagnetic	4.939	169 - 290	125	150	~ 5.2 ⁴	41.4	21.0
Titanomaghaemite		Ferrimagnetic							
Titanohematite	Fe ₂ O ₃ – FeTiO ₄	Ferrimagnetic		281 – 315					
Pyrrhotite	Fe ₇ S ₈	Ferrimagnetic	4.662	50 – 53	~80	320	~ 5.0 ⁴	45.3	209
Greigite	Fe ₃ S ₄	Ferrimagnetic	4.079	~169	~125	~330	~ 5.4 ⁴	67.1	70.7
Hematite	α Fe ₂ O ₃	Canted Anti-ferromagnetic	5.271	0.3 – 2.0	~2.5	675	0.2 – 0.3	318	261
Goethite	α FeOOH	Canted Anti-ferromagnetic	4.264	0.3 – 1.3	~2	120	0.01 – 1.00 ² ~ 0.05 ⁴	1972	57.4
Ulvospinel	Fe ₂ TiO ₄	Paramagnetic							
Ilmenite	FeTiO ₃	Paramagnetic		1.7 – 2					
Lepidocrocite	γ FeOOH	Paramagnetic		0.5 – 0.75					
Pyrite	FeS ₂	Paramagnetic		0.3					
Chalcopyrite	CuFeS ₂	Paramagnetic		0.03					
Biotite	Mg, Fe, Al silicate	Paramagnetic		0.05 – 0.95					
Amphibole	Mg, Fe, Al silicate	Paramagnetic		0.16 – 0.69					
Carbonates of Fe & Mn		Paramagnetic							
Calcite	CaCO ₃	Diamagnetic		-0.0048					
Alkali-feldspar	Ca, Na, K,	Diamagnetic		-0.005					

Mineral ¹	Composition _{1,2}	Magnetism	Density ¹ (g/cm ³)	χ ² (10 ⁻⁶ m ³ Kg ⁻¹)	Ms ^{1,3} (kA/m)	Tc ¹ (°C)	(Mrs) SIRM ² (Am ² Kg ⁻¹)	Avg Bcr ⁴ (mT)	Avg SIRM/ χ ⁴ (kA/m)
	Al silicate								
Plastic		Diamagnetic		-0.005					
Quartz	SiO ₂	Diamagnetic		-0.0058					
Water	H ₂ O	Diamagnetic		-0.009					
Halite	NaCl	Diamagnetic		-0.009					

¹ (Dunlop and Ozdemir 1997)

² (Walden et al. 1999)

³ (Evans and Heller 2003)

⁴ (Peters and Dekkers 2003)

1.2 Study area

1.2.1 Physical Setting

Frenchman's Bay is a shallow coastal lagoon located on the northwestern shore of Lake Ontario. The lagoon is separated from Lake Ontario by a narrow beach barrier with a maintained navigational channel at its eastern end. The lagoon extends over 0.84 km² with about 0.55 km² of open water (Eyles et al. 2002) and a maximum water depth of about 3.5 m. The northern part of the bay includes 15 ha of graminoid marshes which have been designated as a Provincially significant wetland area (Eyles et al. 2002).

The lagoon receives inflow from four small streams (Amberlea, Dunbarton, Pine and Krosno creeks) that drain the 22 km² catchment area (Figure 1.1). The watershed area is heavily urbanized (>80%) and currently supports a population of 47,000 people (Pickering 2001; Eyles et al. 2002). Land use within the watershed is a mixture of residential and commercial with few remaining open green spaces. The northern area of the bay supports a marshland dominated by broad-leaved cat-tail and graminoid marsh grasses and sedges. The other greenspace around the bay is made up of low lying scrublands dominated by Manitoba maples (*Acer negundo*), black willow (*Salix nigra*) and goldenrod (*Solidago spp.*) (McCarthy 1986; Eyles and Chow-Fraser 2003).

1.2.2 Geology

Frenchman's Bay was formed between 3000 to 4000 ybp during a period of rapid lake level rise associated with a phase of the cooler, wetter Neoglacial climate in Southern Ontario (Eyles et al. 2002). The bay was created as the lower reaches of a

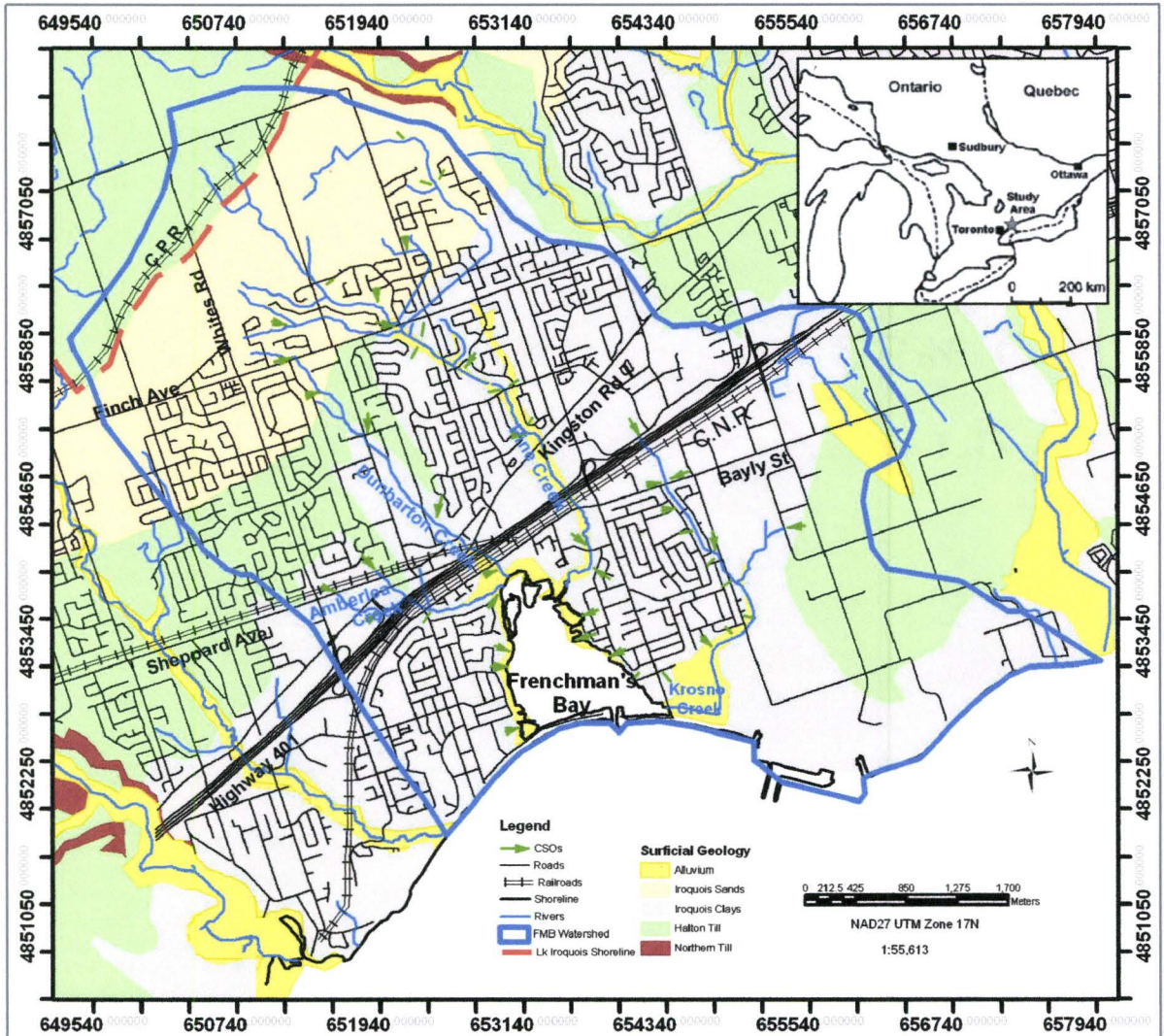


Figure 1.1: Frenchman's Bay study area showing the extent of the watershed and lagoon.

paleoriver valley were flooded and then transformed into a lagoon when a barrier beach formed across the mouth due to longshore drift. Longshore drift from the west continues to deliver sediment to the beach barrier and mouth of the harbour today (Greenwood, 1987).

The sediments within the bay consist of succession of Late Holocene muds and organic deposits overlying post-glacial lake sediments of Lake Iroquois (Eyles 2002). The Lake Iroquois deposits in turn rest on Late Wisconsin glacial sediments (Halton till) and underlying Paleozoic shale bedrock (Whitby Formation). Radiocarbon dating of peats from the base of the lagoon sequence yielded an age of 2750 ybp, indicating a Late Holocene age for the initial formation of the lagoon (see below; McCarthy, 1986).

1.2.3 Previous Work

Several previous studies have investigated the record of post-glacial lakes in the Lake Ontario basin. Anderson and Lewis (1985) reconstructed the postglacial water-level history of the Lake Ontario basin and documented several phases of higher and lower levels of ancestral Lake Ontario. The highest level post-glacial lake, Lake Iroquois stood approximately 25-30 m above present lake levels and inundated a large area north of the present Lake Ontario shoreline. Lake Iroquois was formed at about 12,500 YBP and was followed by a series of lower lake levels as the ice retreated and opened an outlet along the St. Lawrence. The lagoon at Frenchman's Bay was initiated between 3000 and 4000 YBP as water levels rose from a mid-Holocene minimum (Lake Admiralty Phase;

Anderson and Lewis, 1985). The earlier high-level Lake Iroquois phase is recorded by laminated silty clays which form the basal lacustrine sequence below the lagoon.

McCarthy (1986) investigated the Late Holocene water level record from several small lagoons in the Toronto Area, including Frenchmans's Bay. A single core extracted from Frenchman's Bay containing a sequence of lagoon marls overlying sands that were interpreted as a higher energy nearshore environment. A basal peat layer at the base of the lagoon muds yielded a radiocarbon age of 2750 YBP, indicating a Late Holocene age for the lagoon. The onset of colonization is indicated in McCarthy's (1986) core data by the presence of *Ambrosia* (pollen) at approximately 1.1 m depth. By correlating the sedimentary sequence with other lagoons (i.e. Grenadier and Parrott's Ponds) she established a record of accelerated water level rise occurring at about 3000 YBP.

More recent work has focused on development issues, water quality and aquatic habitat restoration in the Frenchman's Bay (Nelson et al. 1991; Stenson 1991; Yeung 1991). The historical development of Frenchman's Bay and the changes in landuse in the area were examined in a detailed report by Skibicki et al., (1991).

The poor water quality and aesthetics of Frenchman's Bay has more recently prompted the City of Pickering to take measures to abate effluent discharges and to restore the Bay's aquatic habitats. As part of the clean-up program, a series of studies have been conducted to document the existing conditions and to identify human impacts on the system (Eyles et al., 2003; Eyles and Chow-Fraser, 2003). The present study is

part of a wider multidisciplinary examination of the historic environmental changes in the wetland in order to put the modern impacts into context.

1.2.4 Historical Background

Native settlement of the lagoon by the Huron and Five Nations Iroquois has been dated to at least 4000 ybp, when FMB was surrounded by extensive wetlands and a forested landscape. The first European traders arrived in 1669, but a long-term settlement was not established until the early 1800s with the arrival of immigrants from England, Ireland and Scotland (Skibicki 1991). European settlers cleared the land for agriculture, mills, inns and businesses so that by 1848 there were 26 sawmills operating (around the east and west shores of FMB). By 1851 over half the township was cleared of trees (Skibicki 1991). Development declined in the later part of the 19th century until the 1960's when the construction of the Pickering Nuclear Generating Station (PNGS) stimulated the growth of urban residential and commercial development around FMB. The large volumes of sediment excavated during the construction of the PNGS were used to infill a large area of the wetlands at the mouth of Krosno Creek (Eyles et al. 2002).

The watershed is underlain by a variety of glacial, glaciofluvial, and alluvial deposits which can be sources of sediment input to FMB if erosion occurs. Additional sources of sediment input is supplied by storm sewer outfalls during large precipitation events, as overland flow washes chemicals and angular road sand from surrounding roads and highways into the sewers to be released directly into FMB. There have been many land-use changes in the area surrounding Frenchman's Bay in the recent past. Many new

residential developments have been added, which is greatly reducing the surface vegetation while increasing erosion and runoff to FMB through storm drains and sewer systems (Eyles and Chow-Fraser 2003). As the spatial extent of the residential developments increased from 1939 to 1993, the spatial extent of the emergent and submergent wetlands in FMB decreased.

1.2.5 Types of Magnetic Behaviour

All substances, including rock forming minerals have magnetic properties which are due to diamagnetism, paramagnetism or ferromagnetism (Walden et al. 1999). *Diamagnetism* is exhibited by a substance with no unpaired electrons in the various electron shells of their constituent atoms (Walden et al. 1999). The weak and negative magnetic behaviour is only observed when an external (natural or artificial) field is applied and the electron orbits become aligned in order to oppose the external field (Butler 1992; Versteeg 1994).

If a substance has some atoms with unpaired electrons that cause a net magnetic moment due to both its electron spin and orbit, then *paramagnetism* can exist. The interaction of these atomic magnetic moments with each other is very small because the distances between atoms with unpaired electrons within the substances are relatively large and with no externally applied field, the magnetic moment of a paramagnetic substance is zero due to the random orientation of such magnetic moments (Walden et al. 1999). When an applied field is present the magnetic moments tend to align in the same direction producing a weak positive magnetism (~ one or two orders of magnitude greater

than diamagnetism), but return to a random orientation (with no net moment) when the field is removed.

Ferromagnetism is a term for a group of related magnetic phenomena observed in substances with unpaired electrons in atoms that are closely and regularly spaced so that strong interaction (coupling) between unpaired electron spins occur. The interaction of forces between unpaired electrons in adjacent atoms allows their spins to become aligned even in the absence of an externally applied field (called ‘spontaneous magnetization’) (Walden et al. 1999). Due to the influence of the Pauli Principle¹, the crystal structure and density of packing for substances containing transition elements determines whether paramagnetism or ferromagnetism will dominate; increased density results in increased ferromagnetism (Butler 1992). These crystalline substances are normally compounds of the transition metals, especially iron, cobalt or nickel (Walden et al. 1999).

Ferromagnetism can be further divided according to the distribution of magnetization vectors in crystals resulting from spontaneous magnetization when the following interactions occur as illustrated by Figure 1.2:

- a) Parallel coupling (Ferromagnetism)
- b) Antiparallel coupling (Antiferromagnetism)
- c) Antiparallel coupling with layers of unequal magnetism (Ferrimagnetism)
- d) Imperfect antiferromagnetism arises due to defects in sublattices, etc. so a moderate net magnetism arises (Canted Antiferromagnetism)

¹ The Pauli Principle identifies that only one electron per atom can have a particular set of the four quantum numbers; if pressed together electrons of adjacent atoms try to satisfy the rule at the same time so the electron states and magnetic moments become strongly coupled.

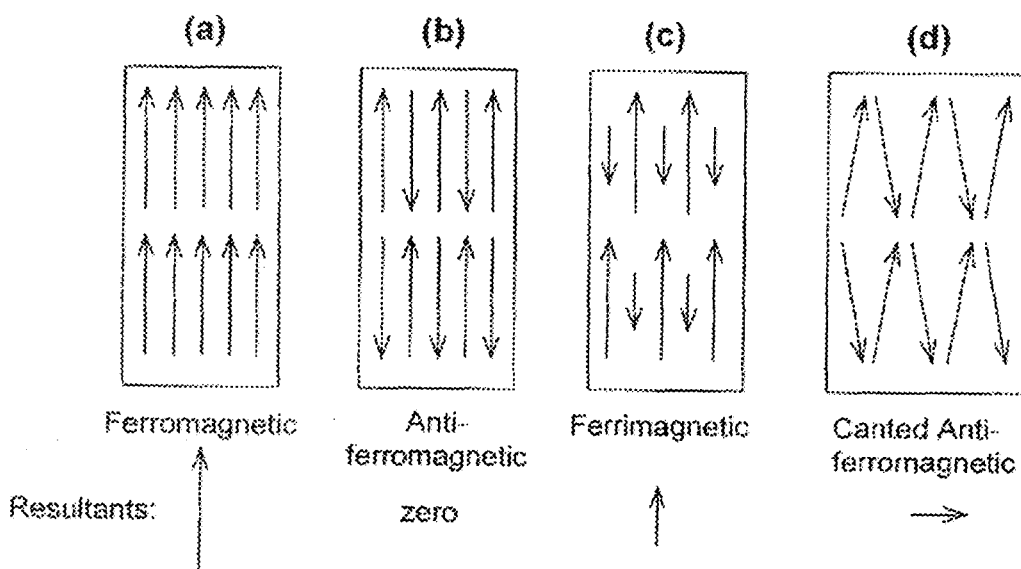


Figure 1.2: Schematic diagrams showing the distribution of magnetization vectors in crystals that experience spontaneous magnetization (Walden et al. 1999).

Ferrimagnetism is the magnetism in most naturally occurring magnetic minerals, which consists of antiparallel coupling with layers of unequal magnetic moments (Versteeg 1994). Its behaviour is the result of incompletely filled 3d shells of first transition series elements (atoms therefore possess magnetic moments), mainly iron and manganese, as well as the shape of the crystal structure (Butler 1992; Versteeg 1994).

Ferromagnetic solids have the ability to record the direction of an applied magnetic field, and when the magnetizing field is removed, magnetization does not return to 0, but retains a record of the applied field (Butler 1992). The most important ferromagnetic minerals due to their abundance in the environment are the iron-titanium oxides shown in the $\text{TiO}_2\text{-FeO-Fe}_2\text{O}_3$ ternary diagram in Figure 1.3.

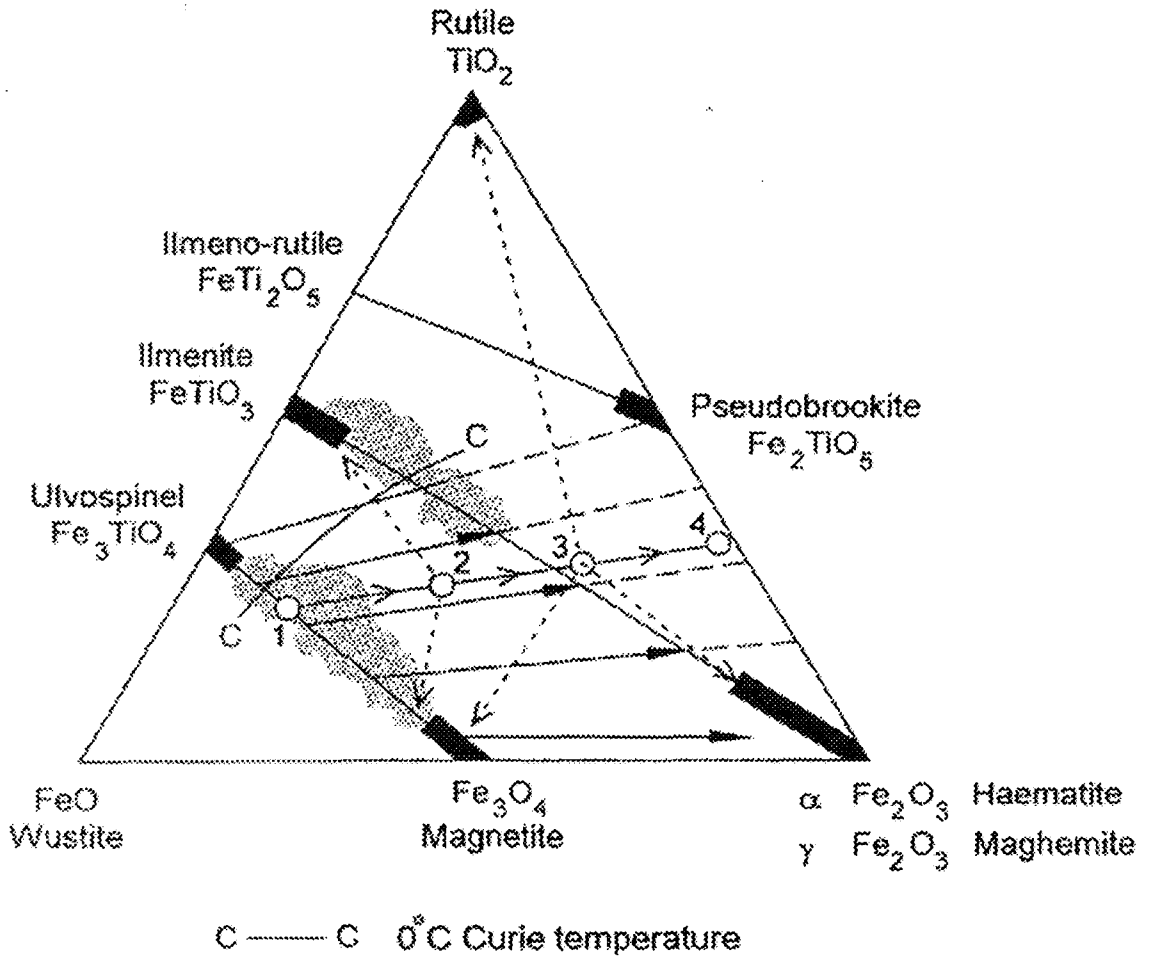


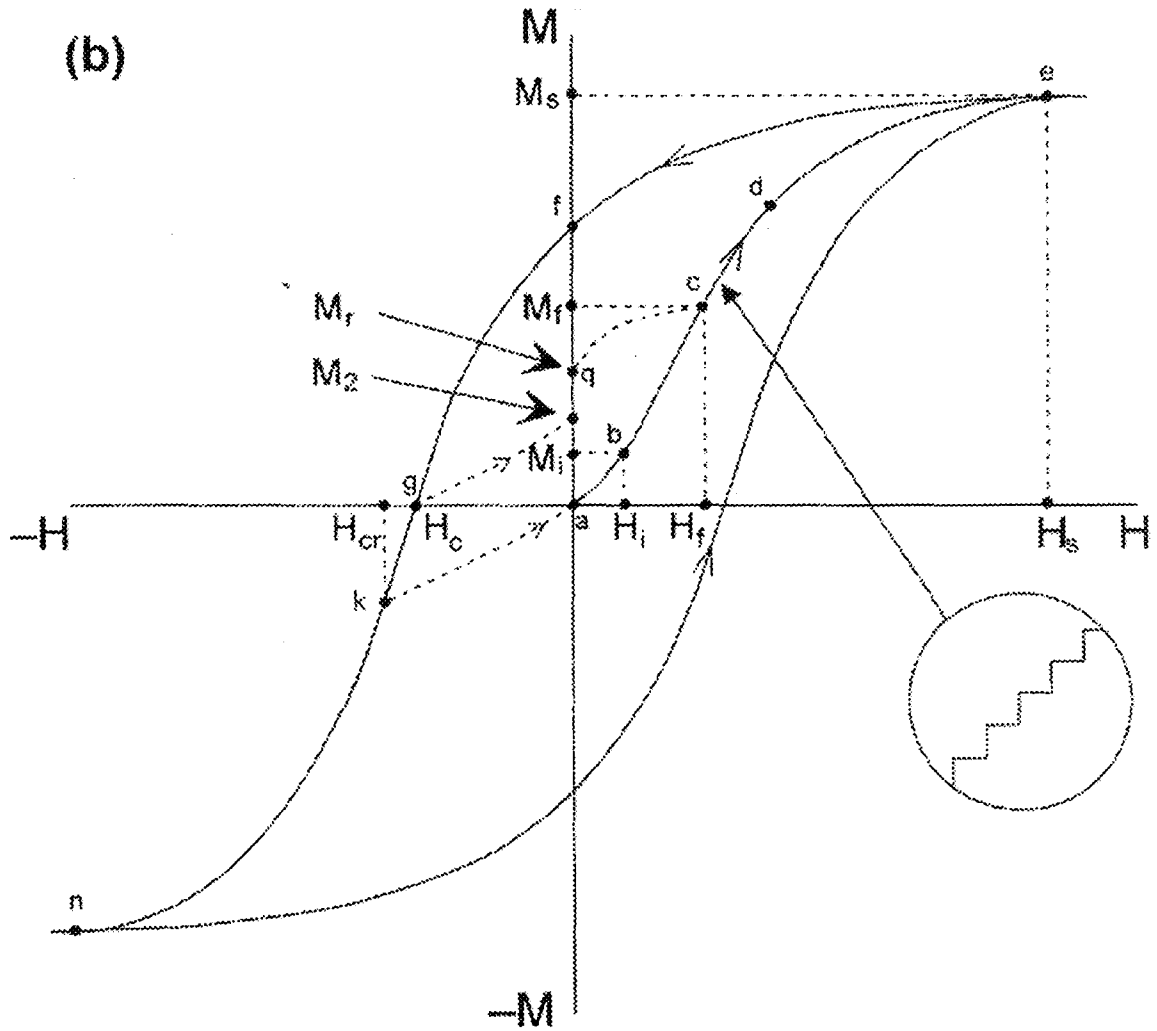
Figure 1.3: The TiO₂-FeO-Fe₂O₃ ternary diagram showing the composition of common iron-titanium oxides (Walden et al. 1999; p. 20 Fig 2.9).

1.2.6 Hysteresis

Ferromagnetic solids have the ability to record magnetism in the direction of an applied magnetic field, but certain conditions must be met first. The magnetization acquired by a ferromagnet when exposed to an external magnetic field is proportional to the strength of the applied field as long as the applied field remains below a maximum point (the saturating field, or H_s) (Versteeg 1994). As the applied field strength increases, the acquired magnetization peaks so that increasing the applied field strength does not produce an increase in the magnetization. This maximum in the acquired magnetization is called saturation magnetization (M_s). For small applied fields the magnetization is reversible so that if the field is removed, the magnetization will reduce to zero. If a large enough field is applied (greater than coercive force), then removing the external field results in a remanent magnetization (M_r). A large enough field is required to cause multi-domain walls to relocate themselves, via translation or rotation, to cross energy barriers and reach new minimum energy positions. The domain walls are then unable to recross the energy barrier when the field is removed, and remanence has therefore been induced in the grain. But if the applied field is able to move the domain wall(s) out of its minimum energy position but has not crossed an energy barrier (energy barrier to rotation of M_s), the former domain pattern will re-establish itself once the applied field is removed (Walden et al. 1999). If the application of the applied field is at constant room temperature, then the M_r represents the isothermal remanent magnetization of the material, noted as IRM_{100mT} , where 100mT denotes the H used to

induce the remanence. The maximum remanent magnetization would be acquired following the removal of a saturating magnetic field and is called the saturation remanent magnetization (M_{rs}) or the Saturation Isothermal Remanent Magnetization (SIRM) if at a constant temperature.

Saturation magnetization decreases with increasing temperature until it becomes zero at the Curie temperature (T_c) because above the curie temperature the material becomes paramagnetic (Butler 1992). Each ferromagnetic material has its own characteristic curie temperature (Butler 1992). SIRM is related to the concentrations of all remanence carrying minerals in the sample but is also dependent upon the assemblage of mineral types and their magnetic grain size (Walden and Addison 1995). The SIRM can be reduced to zero by applying a magnetic field in the opposite direction to the original magnetizing field. The strength of the magnetic field required to reduce the SIRM to zero is called the coercive force or coercivity, H_c . The negative applied field value required to completely remove the remanence so there is no net magnetization when the applied field is removed, is called the coercivity or remanence (H_{cr}). Note that H_c is an 'in-field' parameter, while H_{cr} is measured for conditions in the absence of an applied field. Figure 1.4 shows the complete hysteresis cycle which includes all of the parameters mentioned above. Ferrimagnetic minerals acquire remanence relatively easy at lower applied fields so they are described as magnetically 'soft'. Canted (imperfect)



- | | |
|---|---|
| H – Strength of applied field (T) | SIRM - Max M_r following application of M_s under a constant temperature |
| M – Intensity of magnetization (A/m) | M_{rs} – Saturation remanent magnetization (f) |
| M_s – Saturation magnetization | H_c – Coercive field |
| H_s – Saturating applied field | H_{cr} – Coercivity of remanence |
| M_r – Isothermal remanent magnetization | |

Figure 1.4: M-H plot for ferromagnetic material showing hysteresis parameters (Walden et al. 1999).

antiferromagnetic minerals such as hematite acquire the majority of their remanence at larger field sizes, so they are known as magnetically ‘hard’ (Walden et al. 1999). The hysteresis properties of common iron minerals found in the environment are thought to be a result of ‘imperfections’ such as dislocations, impurities or crystalline anisotropy (Walden et al. 1999). In a material without these types of imperfections, the M-H relationship would be hysteresis free (anhysteretic).

1.2.7 Domains

A domain is a region of parallel atomic magnetic moment in a crystal that is influenced by the size and shape of magnetic grains (Walden et al. 1999). Ferromagnetic particles have various energies which control their magnetization, but the grain seeks the configuration of magnetization which minimizes its total energy (Butler 1992). When all of the magnetic moments (also modelled as pairs of electrical charges) of atoms in a particle are lined up, they cancel each other out inside the particle but overall there is a net magnetic moment (aka the particle is split with one hemisphere having a negative charge while the other has a positive charge). There is energy stored in the charge/moment distribution due to repulsion of adjacent charges or moments which is the magnetostatic energy (e_m). A uniformly magnetized ferromagnetic grain has $M = M_s$, and within each individual domain (relative to itself and not the whole particle if $>SD$) $M = M_s$. Forming magnetic domains decreases e_m because the net magnetization of the particle will be reduced from M_s since the magnetic moments will not be aligned in the same direction (uniform magnetization would maximize e_m) (Butler 1992). The region

separating domains is the domain wall, which has finite energy and width. If more than one domain exists in a grain, then it is called *multi-domain (MD)*.

With decreasing grain size, the number of magnetic domains decreases because the grain becomes so small that the energy required to make a domain wall is larger than the decrease in magnetostatic energy resulting from dividing the grain into two domains. Only one domain exists in grains referred to as *single-domain (SD)* grains because the energy savings from splitting into more domains is less than the energy required to make a domain wall (so it's not worth it!). The single domain threshold grain size depends on grain shape and M_s ; materials with low M_s have less reason to form domains because magnetostatic energy is so low so SDs can exist at larger grain diameters. Hematite ($M_s = 2.5 \text{ G}$) is SD up to grain diameter of 15 μm , while magnetite ($M_s = 480 \text{ G}$) is SD only in very fine grains ($<1 \text{ }\mu\text{m}$) (Butler 1992; Dunlop and Ozdemir 1997). SD grains can be very efficient carriers of remanent magnetization (because they are efficient in acquiring remanent magnetization but resistant to demagnetization). SD grains are magnetically hard and have high coercivities and remanence (Moskowitz 1991).

The particles that exist in the fuzzy boundary between large SD grains and small MD grains where intermediate M_r/M_s and h_c values exist are referred to as *pseudo-single-domain (PSD)* grains. A few domains can exist, with significant coercivity and time stability of remanent magnetism.

Superparamagnetic-domain (SP) grains are SD grains that experience decay in the remanent magnetization to zero shortly after the removal of an applied field since

they have short magnetic relaxation times (Butler 1992). Magnetic relaxation is the effect of thermal activation that causes remanent magnetization of SD grains to decay with time (it is strongly temperature dependent).

1.2.8 Magnetic Parameters

Magnetic Susceptibility (χ or κ)

When a material is exposed to a magnetic field H , it acquires an induced magnetization, M . These quantities are related through the magnetic susceptibility, κ : $M = \kappa H$. Magnetic susceptibility can be regarded as the magnetizability of a substance; i.e. the ratio of the strength of the magnetization divided by the applied magnetic field (Butler 1992; Evans and Heller 2003). The four factors controlling magnetic susceptibility are mineral concentration, composition, crystal size and crystal shape (Thompson and Oldfield 1986). The susceptibility of a sample is most likely controlled by the ferrimagnet component, rather than other minerals present (Walden et al. 1999). This is due to the fact that magnetite (a ferrimagnetic mineral) is about 1000 times more magnetic than the strongest canted antiferromagnetic or paramagnetic mineral, and about 10,000 times stronger than the weakest clay mineral (Walden et al. 1999). Samples of rocks and soils without ferrimagnetic minerals that show purely paramagnetic behaviours rarely show χ (low freq.) values exceeding $0.1 \times 10^{-6} \text{ m}^3 \text{ Kg}^{-1}$, so any sample with values greater than this are assumed controlled by ferrimagnetic minerals (Walden et al. 1999).

Magnetic susceptibility measurements are convenient because they can be made on all materials; they are safe, fast and non-destructive; they can be made in the

laboratory or field; and they complement many other types of environmental analyses (Walden et al. 1999).

% Frequency Dependence of Magnetic Susceptibility ($\chi_{fd\%}$)

$\chi_{fd\%}$ is calculated (see Equation 1.1) from the difference in susceptibilities measured in constant low magnetic fields produced at room temperature at two or more AC frequencies (0.46 and 4.6 kHz) (Walden et al. 1999).

$$\chi_{fd\%} = \frac{\chi_{0.46 \text{ kHz}} - \chi_{4.6 \text{ kHz}}}{\chi_{0.46 \text{ kHz}}} \quad \text{Equation 1.1}$$

The magnetization of very fine grain size (<~ 0.03 μm) materials near the SD-SP boundary is blocked as soon as the operation frequency of the χ meter becomes comparable to the relaxation frequency of grains (i.e. ~5 kHz hf on meter) (Walden et al. 1999; Evans and Heller 2003). $\chi_{fd\%}$ is used to detect the presence of ultrafine (<0.03 μm) superparamagnetic ferrimagnetic minerals occurring as crystals produced by bacteria or chemical processes mainly in soil (Walden et al. 1999; Evans and Heller 2003).

If $\chi_{fd\%}$ values are < 2% then there are virtually no SP grains and non-SP grains have diameters $\geq 0.03\mu\text{m}$ (Walden et al. 1999). Values of $\chi_{fd\%}$ < 5% are typical for samples in which non-SP grains dominate the assemblage or where extremely fine grains (<0.005 μm) dominate the SP fraction. Samples with a significant proportion of SP grains have $\chi_{fd\%}$ values >6%. Values between 2% and 10% could be mixtures of SP and coarser grains or SP grains < 0.005 μm . For samples with $\chi_{fd\%}$ > 10%, SP grains dominate the assemblage and χ_{fd} can be used semi-quantitatively to estimate their total

concentration, BUT $\chi_{fd}\%$ values can be exaggerated by the presence of a significant diamagnetic component.

Natural Remanent Magnetization (NRM)

This is the remanent magnetization present in a sample prior to laboratory treatment, which depends on the geomagnetic field and geologic processes during rock formation and during the history of the rock (Butler 1992). The primary component of NRM can have 3 forms; 1) ***Thermoremanent magnetization (TRM)*** – acquired during cooling from high temperature, 2) ***Chemical remanent magnetization (CRM)*** – formed by growth of ferromagnetic grains below the Curie temperature, or 3) ***Detrital remanent magnetization (DRM)*** – acquired during accumulation of sedimentary rocks containing detrital ferromagnetic minerals (Butler 1992). SD (best) and PSD grains are effective carriers of TRM, while it decays rapidly in larger MD grains that are likely to carry a component of magnetization acquired long after original cooling (Butler 1992). CRM reflects the applied field from when the growth of the grain passes the blocking volume (so it's then SD), or when chemical alteration involves a major change of crystal structure (eg. magnetite to hematite, but not titanomagnetite to titanomaghemite). Initially ferromagnetic particles align with the geomagnetic field at the moment it enters the sediment/water interface, so that initial deposition (and DRM) is probably in this configuration (but gravity may force long axis of grain to lie flat). Post-depositional DRM can occur in water-rich slurry of sediments deposited 10-20 days before because the ferromagnetic minerals are able to reorient themselves relative to the applied field

(even after bioturbation) (Butler 1992). DRM is locked in when dewatering and consolidation restrains motion of sedimentary particles.

Viscous Remanent Magnetization (VRM)

This is a remanent magnetization that is gradually acquired while exposed to weak magnetic fields. For SD grains, acquiring VRM is the inverse of magnetic relaxation; magnetic moments of grains with short relaxation times (τ) are realigned according to the applied field. For MD grains lower coercivities lead to more rapid VRM acquisition (Butler 1992).

Isothermal Remanence Magnetization (IRM)

IRM is the remanent magnetism acquired by a sample after a short-term exposure to an external dc magnetizing field using a pulse magnetizer at constant temperature (Butler 1992). Remanence is measured using a magnetometer (eg. Molspin ring-fluxgate magnetometer) that is sensitive to very small magnetic fields.

IRM work should be done after ARM measurements are made and then the sample must be demagnetized using the Molspin AF demagnetizer, see Walden et al. (1999; p. 76). The Molspin 1T pulse magnetizer should be used to apply progressively larger fields in the same direction (forward fields) to induce IRMs, but after each field is applied the IRM applied field must be measured using the Molspin 1A magnetometer. A typical series of forward fields used includes: 20, 40, [60, 80,] 100, [200,] 300, 500, 600, 800, and 1000 (mT) in order to compare the sample against theoretical IRM acquisition

data. Sometimes a number of IRMs induced with applied fields (20, 40, 100, and 300 mT) in the reverse direction (backfields) are also used.

When low fields (eg. 20 mT) are used to induce IRM, the magnetically hard canted antiferromagnetic minerals such as haematite or goethite are unlikely to contribute to the IRM even at fine grain sizes (Walden and Addison 1995). If higher fields of 300 mT or 1000 mT are used to induce IRM then the majority of magnetically soft ferrimagnetic minerals will already have saturated and any subsequent growth of IRM will be due to a magnetically harder canted antiferromagnetic material in the sample (Walden and Addison 1995).

Remanent Coercive Force (Bcr)

This is the field at which the IRM of a previously saturated sample is reduced to zero in the backfield direction. It is determined by identifying the value of the x-intercept on a plot of applied backfields versus measured remanent magnetization values for a sample that was initially magnetically saturated in the forward direction. Each magnetic mineral species has a specific range of possible Bcr values that are shown in Table 1.1.

1.2.9 Magnetic Bivariate Ratios and Plots

IRM/SIRM

This ratio is often taken as a measure of efficiency in acquiring remanent magnetization – SD particles with long axes lined up should be most efficient (Butler 1992; p. 38). Larger grains with pseudo to multi domain grains have lower h_c and lower M_r/M_s ratios.

IRM/SIRM ratios divide the raw remanence data value of each applied field by the raw remanence data value at the saturation field so that the data for each sample will be normalized to ratios between -1 and 1 . This ratio is relative to the sample's concentration of magnetic minerals and shows what proportion of the sample's remanence was acquired at low or high fields. Different magnetic mineral species acquire the greatest proportions of their remanence at different field sizes. Soft minerals are ferrimagnetic minerals that acquire remanence relatively easy during low fields, while magnetically hard minerals such as haematite that is a canted (imperfect) antiferromagnetic mineral acquires the majority of its remanence at larger field sizes (Walden et al. 1999). Therefore IRM/SIRM ratios can provide information about the amount of soft or hard mineral species in each sample. Note: SIRM influenced by concentration of ferromagnetic minerals, but is also strongly dependant on mineral types and magnetic grain size (Walden et al. 1999). M_r/M_s is ≥ 0.5 for SD particles (Dunlop and Ozdemir 1997) and decreases as particle size increases into the PSD and MD fields (MD behaviour has a M_r/M_s value ≤ 0.05 , and PSD is inbetween SD and MD). This is because domain walls (present in PSD and MD particles) allow particles to acquire a remanence configuration that minimizes its magnetostatic energy (and hc), which leads to lower M_r values (Evans and Heller 2003).

S-Ratio ($IRM_{-100mT}/SIRM$)

Once a sample acquires SIRM in the forward direction, a series of backward direction fields (backfields) are applied from a low field of 10 mT to 300 mT and the

resulting remanent magnetization is measured. The first few low intensity fields remagnetize the low-coercivity component of the sample but any high coercivity components are unchanged. The S-ratio examines the magnetism acquired after application of the 100 mT backfield relative to the magnetism acquired after saturation in the forward direction. Values close to unity indicate that the remanence is dominated by soft ferrimagnetism, while low magnitude values indicate that antiferromagnets such as hard hematite may dominate the signal since high coercivity materials will not acquire much remanent magnetism with a -100mT backfield. This ratio is commonly measured because it equals -1 for samples dominated by magnetite magnetic behaviour because SIRM occurs @ 100mT and IRM-100mT has the same magnitude but opposite sign. Samples that have magnetically harder mineral types (and therefore show a stronger resistance to demagnetization) have higher ratios, and if ferrimagnetic minerals are virtually absent the ratios may be positive (Walden et al. 1999).

S-ratio is not concentration dependant because the IRM-100mT and SIRM values are examined for the same sample, therefore the ratio is normalized against concentration dependence. It does however depend strongly on magnetic mineral composition and to a smaller extent on grain size because the domain states possible due to the grain size(s) will alter the coercivity of the magnetic material (larger grains = lower coercivity for a particular magnetic mineral).

S-Ratio versus χ Plot

Pure magnetite results in an S-ratio value of -1 . Therefore, if higher χ values are associated with S-ratio values that approach -1 , you can infer that the samples are dominated by magnetite. If higher χ values are associated with S-ratio values that are decreasing, then a magnetically harder material is present and influencing the signal of higher χ sediments. The contribution from harder materials increases as the value of the S-ratio increases (i.e. away from -1). S-ratio is strongly magnetic mineral composition dependant, minorly dependant upon grain size, and not dependent on concentration. χ is strongly concentration dependant, composition dependent, and not dependent upon grain size unless SP grains are present.

SIRM/ χ

SIRM is dependant upon (in usual order of importance) magnetic mineral composition, concentration, and grain size. χ is composition and concentration dependant, but is only affected by grain size when superparamagnetic grains are present since the grain relaxation time is faster than a susceptibility meter's ability to measure the induced magnetism. Since SIRM is grain size dependant (decreases with larger sized particles), while χ is not (unless sample has superparamagnetic grains), the SIRM/ χ ratio will be higher if there are a greater number of smaller particles (Evans and Heller 2003). The SIRM/ χ ratio is a grain size indicator for magnetite (Evans and Heller 2003). This ratio is also useful for indicating the presence of greigite when SIRM/ χ values exceed 30 kA/m in the absence of a major hard remanence component that could be due to

haematite or goethite (Reynolds et al. 1999; Walden et al. 1999; p. 105; Evans and Heller 2003 Ch. 3) Roberts et al., 1996.

Both SIRM and χ are usually strongly concentration dependant with mineralogy and grain size (i.e. domain state) imparting smaller influences on the magnetic signal. A plot of SIRM versus χ would evaluate the validity of this assumption because a strong linear correlation with no (or minimal) scatter would indicate that both parameters do depend strongly on concentration (since both parameters are concentration dependant, if concentration is the only factor altering the sediment composition then the data should plot in a straight line), while the degree of scatter indicates the relative influence that mineralogy and/or grain size has on the value of the parameters.

SIRM/ χ versus Bcr Plot

Peters and Dekkers (2003) demonstrated that this plot can differentiate between mineral magnetic species by using field and laboratory samples of each of the minerals from over 16 different studies. This plot identifies the dominant magnetic mineral that contributes to the magnetic signature for the sediment sample. The advantage of employing this plot is that though the SIRM/ χ and Bcr properties are both able to offer information about the possible magnetic mineral species but suffer from non-unique answers due to minor range overlapping, once these parameters are plotted together the overlapping data are separated into distinct magnetic mineral species ranges. The only exception to this is the region for maghaemite that plots within the magnetite region, but

the correct mineral species can be determined by measuring the Curie temperature, which is 590-675°C for maghaemite and 580°C for magnetite (Dunlop and Ozdemir 1997).

χ versus Bcr Plot

Bcr is a strong indicator for the dominant magnetic mineral species, especially once you have used the SIRM/ χ versus Bcr plot to isolate the major contributor. A plot of χ versus Bcr can help identify which magnetic mineral species causes the magnetic enhancement in the sediment by determining how the Bcr values change as χ increases. Positive correlations would indicate that harder magnetic minerals are causing the higher susceptibilities, while negative correlations would indicate that an increase in softer magnetic minerals are leading to the higher magnetic susceptibilities. It is also important to look at relative changes of Bcr in this plot. A negative correlation that moves from a Bcr value of 42 mT to a Bcr value of 25 mT when maximum χ values are measured indicates that magnetic enhancement is due to an increase in the magnetically softer magnetite (avg. 24.4 mT) from the dominantly harder titanomagnetite (avg. 41.4 mT) sediments at lower χ values.

χ versus TOC + CO₃ Plot

This plot is used to determine if variations in χ are due to dilution of a detrital uniform component with diamagnetic organic and carbonate matter. A strong correlation would indicate that variations in χ are strongly influenced by organic and carbonate matter content diluting the magnetic signal, while heavy scatter or a random plot would indicate that the organic and carbonate content has little or no effect. In the latter case

concentration would not be the dominant parameter controlling the signal, but grain size or mineral composition could be.

Gradient of IRM Acquisition Curve

To determine the IRM acquisition behaviour of a sediment sample, a series of forward applied fields of increasing magnitude are applied to the sample, and the resultant remanent magnetization is measured in between each application of an applied field. The gradient of IRM acquisition curve is plotted using the change (a positive increase) in IRM after each higher magnitude applied field is applied to the sample (Robertson and France 1994; Stockhausen 1998; Geiss 1999). This curve is useful because the magnitude of the applied field at the centre of any gaussian curve on the graph identifies the presence of a mineral magnetic species because this median applied field point represents the Bcr' value (which approximates Bcr) (Robertson and France 1994; Stockhausen 1998). This median applied field point can then be compared against known Bcr values to identify the magnetic mineral species. This method is useful because it allows you to identify multiple magnetic species, and small concentrations of magnetically hard or soft material in a sample that may be dominated by the other type of magnetic species.

1.2.10 Environmental Applications of Magnetics

As discussed previously, geological processes such as erosion and weathering, or limnological parameters such as lake status and water chemistry can change the concentration, mineralogy and particle-size distribution of the magnetic minerals present

in sediments. This section will investigate how relative changes in some key parameters and ratios (or a typical suite of indicators) can be used to identify different processes acting on the sediment and/or depositional environments.

Magnetic Mineral Concentration, Mineralogy and Grain Size

Both magnetite and maghemite are actively produced in top soils (Walden et al. 1999). These fine-grained secondary magnetization minerals contain a significant SP component that overprints the magnetization of the original material. These fine grained soil derived ferrimagnets appear to be formed of only SSD or SP grain sizes that gives them χ_{fd} between 8% to 16% and they usually have a steep viscous acquisition or loss of IRM in low fields (Walden et al. 1999).

Surface weathering oxidizes magnetite to hematite or iron-hydroxides and NRM carried by the magnetite can be deteriorated and modern CRM may be formed (Butler 1992).

Magnetite can be degraded by sub-oxic 'dissolution' diagenesis that is driven by organic matter decomposition. Steep declines in concentration indicators point to selective loss of finer grains due to diagenesis (Walden et al., 1999; p. 105). A decreased ratio of soft to hard remanence is another sign of diagenesis because hard remanence survives longer and soft is more quickly lost.

In marine or lake settings authigenic magnetite and/or pyrite may precipitate if neutral or reducing conditions occur during diagenesis (Butler 1992). In strongly reducing environments, detrital magnetite may be totally destroyed.

Products of fossil fuel combustion tend to fall into MD, PSD, and SSD size ranges, while burning, pedogenetic processes and bacterial action tend to produce fine crystals of SSD or SP behaviour (Walden et al. 1999). Fire (in excess of $\sim 400^{\circ}\text{C}$) applied to iron rich soils and substrates in the presence of organic matter or some other reducing agent can generate large quantities of magnetic minerals, as can the ashing of peat (Walden et al. 1999). During burning of top soil and/or surface vegetation cover, heating probably causes finely divided oxides and hydroxides of iron to be converted to magnetite, especially under reducing conditions in the presence of organic matter (Walden et al. 1999). The effect of the burning may be seen over longer distances due to the magnetite-rich dust fallout from the fire. Industrial combustion processes (i.e. coal combustion) provide a larger scale atmospheric flux of magnetic minerals that is generally MD/SSD sized and lacks a major viscous component of magnetization (Walden et al. 1999). Fine grained ferrimagnets can lead to extremely high χ values and extremely low IRM/χ values since SP grains do not hold a remanence, and $\chi_{\text{fd}\%}$ will usually be below peak values associated with normally enhanced soils.

During postglacial conditions the magnetic properties of the lagoon sediment reflects the magnetic composition of the source material. Once primitive grasslands and then forests develop in the watershed/catchment during warm and humid interglacial conditions, the vegetation's added stability results in lower erosion rates and high rates of organic inputs/productivity. Erosion of soil material can lead to lagoon sediments that

are enriched in fine and ultrafine-grained maghemite (Geiss 1999). Subaerial weathering can lead to the formation of secondary antiferromagnetic hematite (Geiss 1999).

Magnetic Susceptibility

Previously examined relationships between magnetic susceptibility and sediment properties were limited to mineral exploration studies of bedrock and ore bodies, which are rich in magnetite or other magnetically-rich minerals (Breiner 1973; King et al. 1982). The application of magnetic susceptibility in environmental studies was pioneered by Beckwith et al. (1986), and further developed by Versteeg (1994), Versteeg et al. (1995), and Morris et al. (1994; 1995). Beckwith et al. (1986) identified a linear relationship between magnetic susceptibility and metal (Cu, Fe, Pb & Zn) concentrations present in urban source sediments. Versteeg et al. (1994) found that the magnetic susceptibility profile evident in the sediment profile strongly reflected the onset of colonization and later industrialization (Figure 1.5). Higher trace metal and contaminant concentrations as well as higher κ in urban and industrial sediments due to magnetite have been correlated to combustion processes involving fossil fuels (Locke and Bertine 1986). It was found that the magnetic particles are associated, directly or indirectly, with contaminants such as PAHs (polyaromatic hydrocarbons) and trace metals because they are all by-products of fossil fuel combustion. The knowledge of these associations can be applied to magnetic mapping of contaminated sediments, provided that magnetite

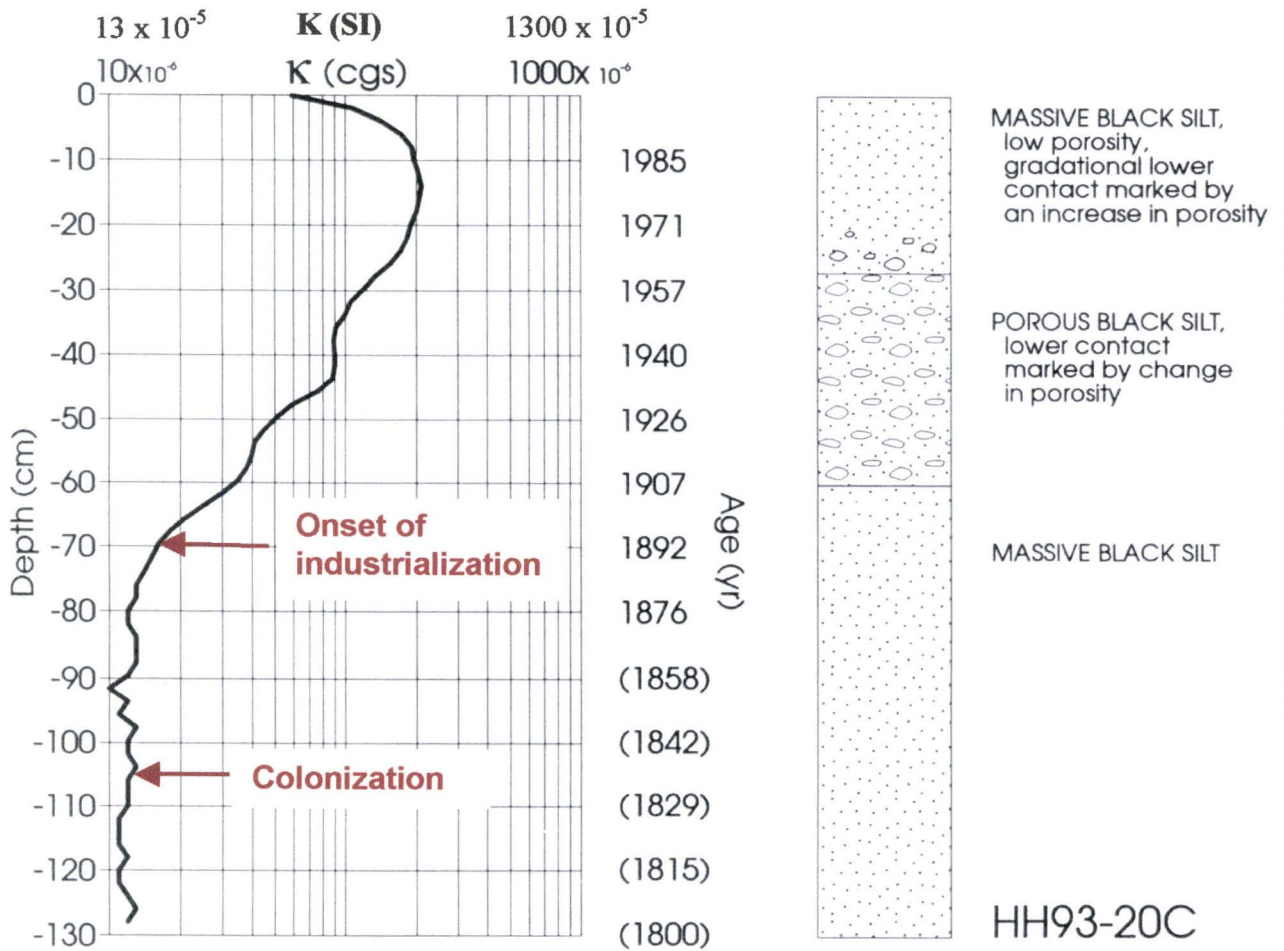


Figure 1.5: Magnetic susceptibility response in the sediment profile of Hamilton Harbour (Versteeg 1994).

concentration from urban sources is at levels high enough to be detected above the normal susceptibility of ‘background’ sediments. Frenchman’s Bay, like many other areas in the lower Great Lakes is characterized by bottom sediments with low magnetic susceptibility, therefore the magnetic susceptibility profiles observed in Frenchman’s Bay can be analyzed for evidence of industrialization and other events.

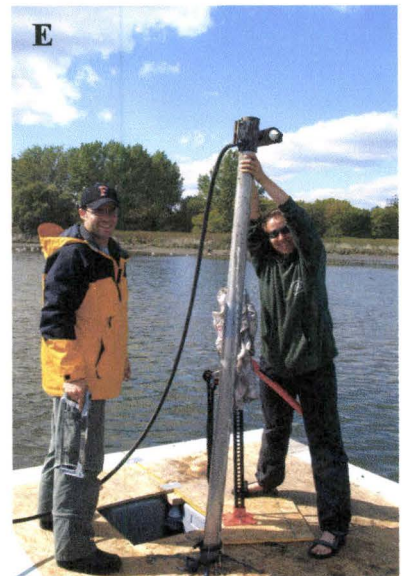
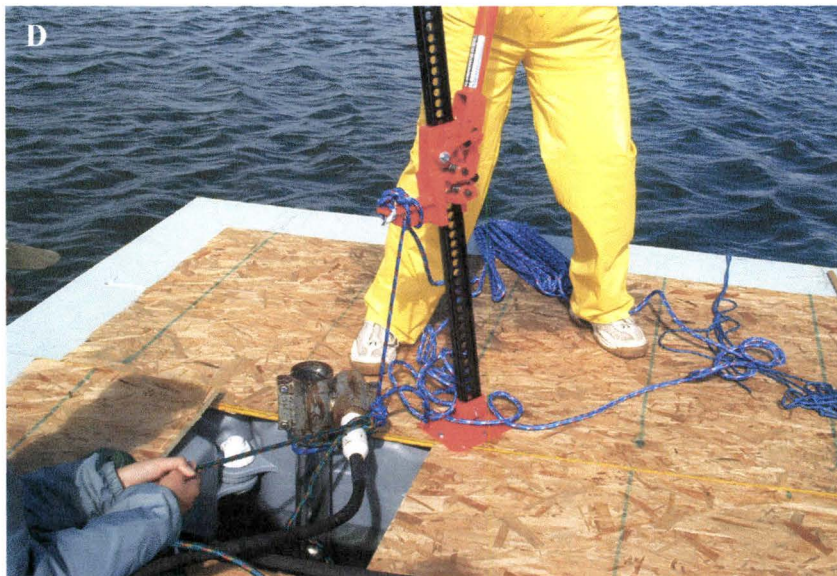
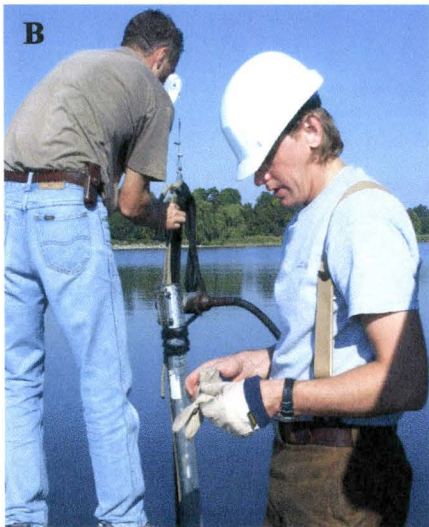
1.3 Methods

1.3.1 Sampling Procedures

Coring

Cores are removed from Frenchman’s Bay using a vibracore. The vibracore operates based on the principle that as the aluminium tube walls are vibrating, they liquefy the sediments in the path of the wall so that the tube can pass into the sediments while disturbing and compacting the sediments only a minimal amount. The vibracoring apparatus is made up of a vibrating head commonly used for agitating concrete, attached to an approximately 20’ long 3” diameter aluminium irrigation tube via a removable reinforced steel coupling, see Figure 1.6 A. Once the coupling is secured, a pliant rope is used to tie the core loosely (using a prussic knot) to the boat-mounted winch so that it can be recovered easily later on (rope shown in Figure 1.6 B). When the desired coring location is reached, the boat must be secured in place using two anchors to prevent drift. If the boat is not anchored well, than once the core is driven into the sediments the boat may drift overtop of the core, making recovery difficult without bending the tube or stressing the winch. After securing the boat position, the vibracore apparatus is placed

Figure 1.6: Lake-based vibracoring. A. Vertical placement of the vibracore (aluminium core with vibrating head) into the lagoon bottom sediments from a boat platform. B. Recovery of the core using a boat-mounted winch and cable system. C. Capping and sealing the bottom of the core for storage. D & E.. Lake-based vibracoring from a floating dock platform for depths too shallow for the passage of the 15 foot boat used in pictures A to C. Note that the core is recovered using a ‘truck-jack’ winching system due to the preferred lower center of gravity on a floating dock system.



into the water maintaining a vertical position as you lower it to the sediment surface. When the base of the tube reaches the sediment surface, the vibracore can be turned on. Once the vibrating head starts, the tube may descend quite rapidly into the sediments if they are unconsolidated and/or fine grained. If there are coarse grained and/or consolidated sediments, then the vibracore may need some 'guidance' in the form of brute force, so that maximum depth penetration is achieved. Since the coring was done over water with depths up to 3m, a boat reaching-pole was found to be very useful to push the core down a few extra feet to maximize the length of core recovered.

The core was recovered using a boat-mounted winch and cable system, as shown above in Figure 1.6 B. Before the core was brought onto the boat, floral foam (the material used in floral arrangements) was pushed into the top and bottom of the core until the sediment surface was reached so that the saturated sediments would not be disturbed during transport. Once the foam was placed, the top section of the tube that was only filled with water was removed using a circular saw. Both ends of the core were then sealed with Ziploc bags and a lot of duct tape so that they would not leak during transport to the lab, see Figure 1.6 C. It is important to note that in order to determine the uncompacted depth and length of the cores obtained, the measurements shown in Figure 1.7 must be recorded for each core. The uncompacted depth is calculated using the equation (see Figure 1.7 for variable definitions):

$$\text{Uncompacted core length} = b + c - a \qquad \text{Equation 1.2}$$

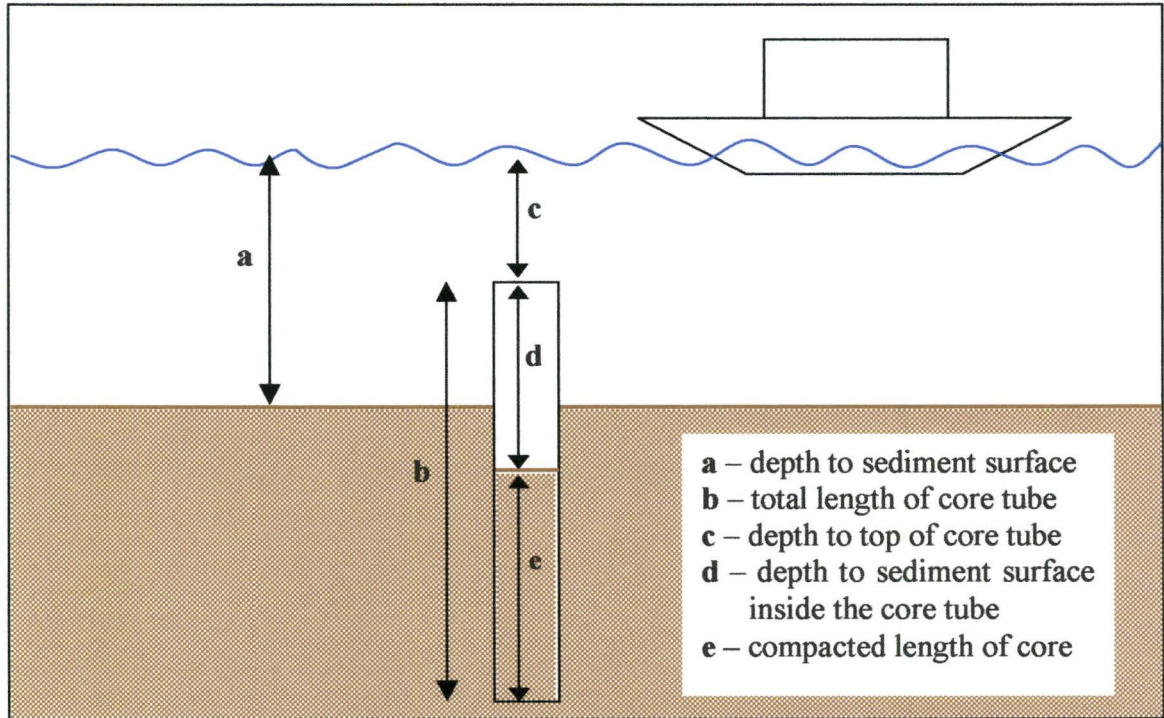


Figure 1.7: Measurements required to determine uncompacted core length and elevation calculations.

Proto-type Probe

An inexpensive proto-type probe was constructed using a Bartington MS2-F sensor mounted in waterproof ABS plastic housing with an extendable 10 m handle (see Figure 1). The probe tip and handle are 3 cm in diameter and can be driven up to 3-4 m into soft unconsolidated muds and clays. The probe housing was designed with a minimum wall thickness (< 4 mm) to maximize the active sensing volume of the MS2-F probe tip. Details regarding effective sensing volume and sensitivity of the probe are discussed in section 2.3.1.

To obtain near continuous in-situ measurements of sediment volume susceptibility (κ), three minutes of air measurements were taken before and after profiles were obtained so that the instrument drift could be removed (linear drift assumed). The proto-type probe was then lowered down to the surface of the lagoon bottom sediments. A volume magnetic susceptibility measurement was obtained, and then the probe was lowered down 2 cm into the sediments using the extendable handle. The κ measurement and lowering of the probe by 2 cm repeated until the proto-type probe could no longer be lowered into the sediments due to coarse-grained sediments or heavy compaction. Elevation of the measurements was monitored by noting the depth of the proto-type probe tip relative to the FMB water surface. Elevation was then calculated by subtracting the depth of the measurement from the water level of Lake Ontario measured for August 2003 (CanadianHydrographicService 2003). The use of the proto-type probe is limited in

choppy waters since the water level is used as a datum, and when coarse or compacted sediments are present since it is difficult to penetrate with the probe.

1.3.2 Geotechnical Analyses

Lithology

When not in use, the cores are stored in a large walk-in refrigerator at a constant temperature of 0 - 3°C to reduce microbial activity. In order to evaluate and subsample the sediments within the cores, the cores obtained from the field must be split and prepared for lab work. The aluminium cores are first cut on either side with a hand held grinder using metal cutoff wheels, as shown in Figure 1.8. A custom wooden core-splitting bench was created specifically for the 3” aluminium cores so that the cores could quickly and easily be cut down either side (also shown in Figure 1.8). The ends of the core that are wrapped in duct tape and Ziploc bags are also cut in the middle. Then a brass wire is placed across the middle of the core and is pulled down the core from the top to bottom so that the core is split in half. The core is then pulled apart so that each half can be cleaned off with a sediment spatula. One half of the core will be set aside for the archive, while the other will be used for sediment sampling.

When storing the core halves, they must first be wrapped in saran wrap to prevent them from drying out. Each half is then placed inside a long plastic bag and is vacuum-sealed to reduce oxidation and contamination. It is very important to ensure that your core is always properly labelled, especially once it is split in half. It is also useful to

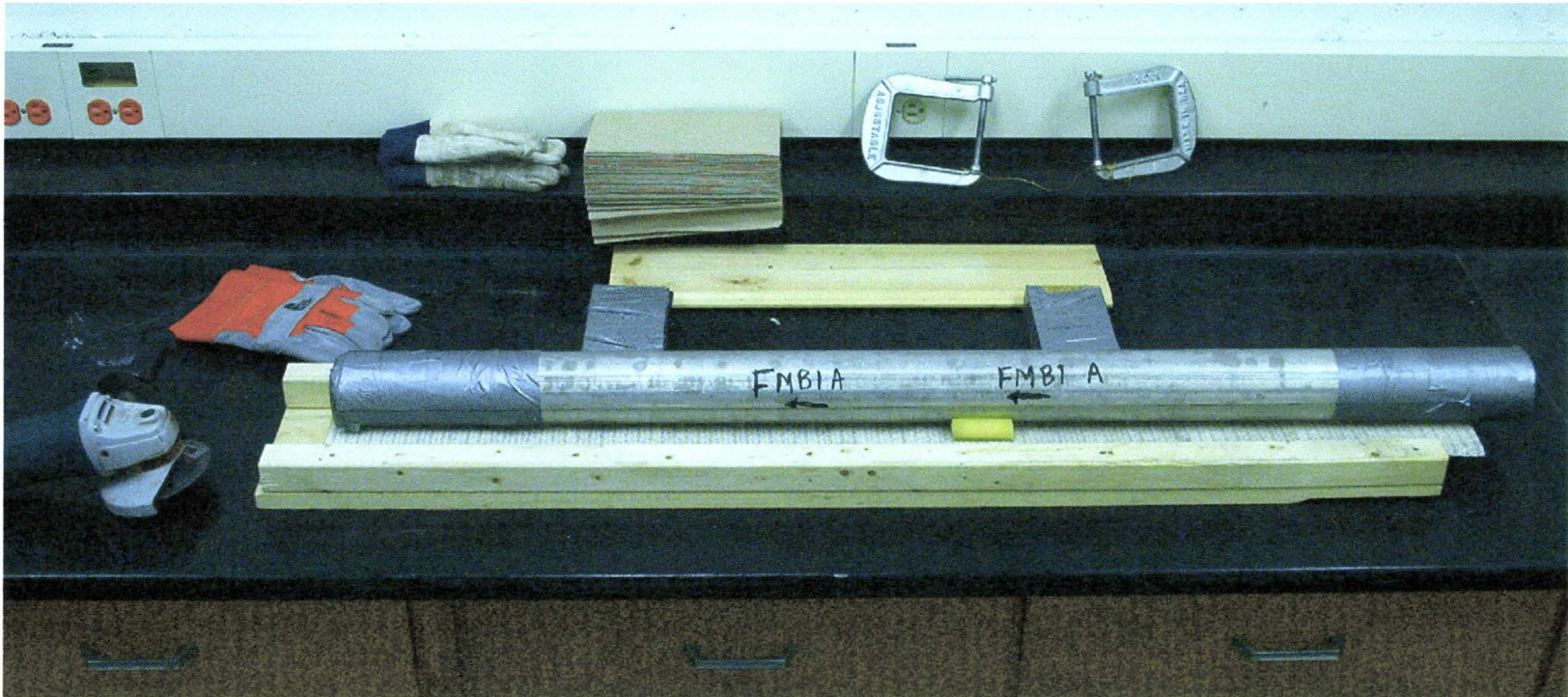


Figure 1.8: Equipment required to split aluminium sediment cores obtained from the field.

The hand held grinder (with metal cutoff wheel) used to split the aluminium core tube is shown in the bottom left. The custom built wooden core-splitting bench is shown under the core in the middle of the picture. The brass wire used to slice the core down the middle was held between two large C-clamps (top right) for ease of use. For safety reasons a dust mask had to be worn while splitting the core due to aluminium particulate matter in the air, as well as safety goggles and leather work gloves.

handle the core sections the same way, such as always holding the top of the core with your left hand, to reduce the chance of sampling or logging core upside down.

The sediments were described visually and relevant features were recorded using the sediment log template modified for lake sediments shown in Appendix A: . Relevant

features noted include:

- Lithology
- Approximate grain size (estimated by feeling and looking at the sediment);
- Sorting
- Frame / matrix supported;
- Colour (using munsell colour chart);
- Approximate % OM (organic matter);
- Sedimentary structures and/or inclusions.

Grain Size

10 cc sediment samples were obtained from strategic points of interest along the study cores. Single points were chosen for each distinct unit, while additional samples were taken if grading or unique features were observed. Care was taken to not sample any of the sediment at the sides of the core tube since those sediments would be disturbed by the action of the vibrocore. The samples were each placed in 50 ml centrifuge tubes for pre-treatment before conducting grain size analysis using the Beckman-Coulter LS 230 laser particle size analyser.

Murray (2002) conducted a comparability and reproducibility study of the various preparation methods currently in use for grain size analysis using the Beckman-Coulter LS 230 laser particle size analyser. Four different preparation methods were compared using carbonate-rich lake sediments during the study:

- No preparation;
- Removal of carbon by loss on ignition;
- Removal of carbon by digestion with hydrogen peroxide; and
- Removal of carbonates with 10% hydrochloric acid followed by removal of organic material by digestion with hydrogen peroxide.

Murray (2002) found that the choice of pre-treatment has a significant effect on the particle size results obtained, and the only method that provided any degree of repeatability was the fourth method (hydrochloric acid then peroxide digestion), which will be applied in this study.

To obtain an accurate measurement of sediment grain size without including large shell fragments, carbonate cement, or pieces of leaves and twigs, all carbonates are removed by adding 10% hydrochloric acid (HCl), and then organic material is removed by adding hydrogen peroxide. Murray (2002) presents two reasons for removing organic matter: it binds the mineral particles together (especially the clay fraction) hindering dispersion, and reported particle size data are limited to the mineral fraction, so the organic component must be removed. Carbonates are removed because they can act as a cement, binding smaller particles together. To speed up the process, the samples can initially be passed through a 2mm sieve to remove large shells, roots, or clasts. Throughout the preparation the samples are placed in a hot water bath and manually agitated every few hours to increase the rate of reaction since the lake sediments are both carbonate and organic rich. Every 8 - 12 hours the samples are centrifuged for 8 minutes and excess fluid is decanted from the top. Fresh 10% HCl or peroxide is added (depending on the stage in the process) until any sign of reaction (bubbles, gas evolving) is removed.

Once the reaction with peroxide is complete, a representative section of each prepared sample is then mixed with ~3 ml distilled water and a dispersion agent (5 drops of a 5% Calgon solution) in 5 ml test tubes. These samples are then analysed using the automated Beckman-Coulter LS 230 laser particle size analyser to obtain grain size fractions using laser diffraction.

The Beckman-Coulter LS 230 laser particle size analyser (see Figure 1.9) has a 5 mW, 750 nm laser beam and 126 detectors placed at angles up to 35° to the laser beam (Coulter 2001). The LS 230 measures particle sizes from 2 mm to 0.4 µm using the Fraunhofer theory of light scatter. When light from a laser is shone at a particle, a portion of the light is diffracted, depending upon the size of the particle (Murray, 2002). Smaller particles result in larger maximum angles of diffraction, so particles of different sizes produce a characteristic diffraction pattern. A second unit measures particle size down to 0.04 µm using a technique that Coulter refers to as PIDS (Polarisation Intensity Differential Scatter). This method is also based on laser diffraction, but it measures light flux only at high angles to the beam. Six detectors and a tungsten light source are used by the PIDS unit to compare the intensity of light scatter at two polarisation angles using three different wavelengths (450 nm, 600 nm and 900 nm) (Murray, 2002). Sediment properties such as the mean, median and mode grain size, standard deviation, variance, coefficient of variation, skewness and kurtosis are reported for each sample. An example of the results obtained for a silty clay sample is available in Appendix B: as a sample

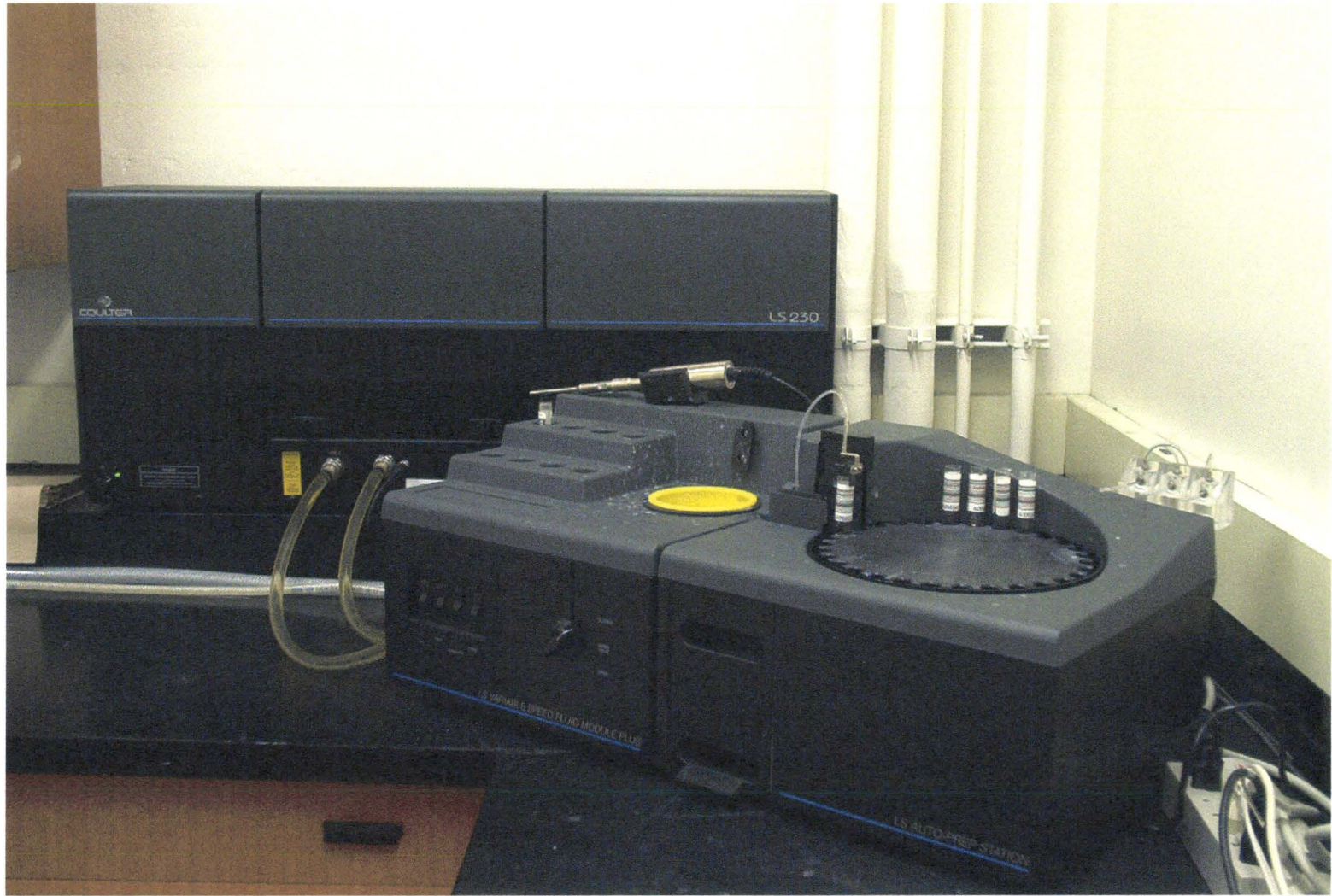


Figure 1.9: The automated Beckman-Coulter LS 230 laser particle size analyzer. An example grain size analysis print out is available in Appendix B: .

coulter counter printout. An adequate amount of sample for your mixture of sediments must be added to the test tube for analysis, otherwise you will not achieve a statistically significant measurement (PIDS ideal between 8% to 13%).

Applications and Limitations

Grain size statistics offer information about possible depositional environments, sediment sources, etc. Larger grain sizes are transported with larger energy events, since more energy is required to transport the sediment. Therefore storm events can be detected via sand lenses and/or erosional surfaces. The presence of coarse sands and gravel in the lagoon may suggest higher energy streams in the past according to McCarthy (1986), while angular coarse sands deposited at river mouths have been associated with the sanding of winter roads since the sand used to de-ice roads is mechanically crushed and not exposed to weathering processes that typically smooth grains. Other coarse sand grains that are subrounded could have been transported during high-energy storm events or by longshore drift. Larger cobble or pebble grain sizes supported by a clay matrix may be evidence of dropstones from ice rafts. The degree of sorting is a function of the origin and transport history of the sediment. With increased transport distance or repeated agitation of the sediment, the different sizes tend to become separated so that a smaller range of grain sizes is present (Nichols 1999). For example, sediments eroded from a nearby (autochthonous) upland area would be poorly sorted, whereas sediments from a far-away (allochthonous) area or those reworked along the shoreline due to increased energy would be better sorted.

A major limitation for this method is time. Lake based sediments, especially those from FMB contain a lot of carbonates and organic material which require a long time to react with the HCl and peroxide. Regular immersion in a hot water bath and replacement of the reactive agent is required to process samples at a reasonable rate. The coulter counter can be used to measure from 0.04 μ m to 2000 μ m (full grain size scale), but experience with your sediment type is required when trying to achieve correct PIDS values for a statistically significant measurement.

Loss on Ignition (LOI)

Weight percent organic matter and carbonate content in sediments is determined using a loss on ignition (LOI) analysis that is based on sequential heating of the samples in a muffle furnace. Heiri et al. (2001) conducted a comparability and reproducibility study of the various methods currently in use for LOI analysis of organic and carbonate content. Three types of temperate lake sediments were used during the study: 1) high organic content, low carbonate content, 2) low organic matter and intermediate carbonate content, and 3) low organic content, high carbonate content. After evaluating the reproducibility of the results under a variety of ignition temperatures, exposure times and sample sizes, Heiri et al. (2001) recommend the following for lake sediments:

- Sample size must remain consistent;
- Samples should be initially dried in the furnace @ 105°C for 12 to 24 hours;
- 4 hours of exposure @ 550°C is required for combustion of organic matter;
- 2 hours of exposure @ 950°C is sufficient to evolve the carbon dioxide from the carbonates.

Weight percent organic matter is determined using the difference in mass once the organic matter is combusted to ash and carbon dioxide. The LOI, and weight percent organic matter, is calculated by:

$$\text{LOI}_{550} = ((\text{DW}_{105} - \text{DW}_{550})/\text{DW}_{105}) * 100 \quad \text{Equation 1.3}$$

Where: LOI₅₅₀ - LOI at 550°C, or weight percent organic matter

DW₁₀₅ - dry weight of the sample before combustion (g)

DW₅₅₀ - dry weight of the sample after heating to 550°C (g)

The carbonate content is determined using the difference in mass once the carbon dioxide is evolved from the carbonate at 950°C, leaving oxide behind. The LOI, and weight percent carbonate content, is calculated by:

$$\text{LOI}_{950} = ((\text{DW}_{550} - \text{DW}_{950})/\text{DW}_{105}) * 100 \quad \text{Equation 1.4}$$

Where: LOI₉₅₀ - LOI at 950°C, or weight percent carbonate content

DW₁₀₅ - dry weight of the sample before combustion (g)

DW₅₅₀ - dry weight of the sample after heating to 550°C (g)

DW₉₅₀ - dry weight of the sample after heating to 950°C (g)

Heiri et al. (2001) also cautions that organic rich sediment seemed more prone to inconsistencies, even under the above ideal conditions. They suggest that this may be because other reactions than burning of organic matter can occur at 550°C, such as dehydration of clay minerals or metal oxides, loss of volatile salts, or loss of inorganic carbon in minerals such as siderite, magnesite or rhodochrosite.

Applications

The organic and carbonate content values can help differentiate units and determine depositional environments. The proportion of marl in each unit depends on water depth. The rate of marl production is highest at intermediate water depths in the littoral zone, where marl-producing genera such as *Chara globularis* (fragile stonewort)

are most abundant (McCarthy 1986). The fragile stonewort are reported to be most frequent between 1 and 2m, dropping sharply below 4m. Carbonate content can therefore indicate the depositional environment since Dean (1981) determined that for north temperate lakes, littoral sediments in marl lakes usually contain more than 60% carbonate, whereas profundal sediments rarely contain more than 50% carbonate. It was also determined that the profundal sediments commonly contained more than 20% organic matter.

²¹⁰Pb Dating

²¹⁰Pb is an isotope in the uranium-238 decay series. It occurs naturally throughout the biosphere. Although it can occur in secular equilibrium with its grandparent, ²¹⁰Pb concentrations are not constant because geo-chemical processes separate ²¹⁰Pb from the longer lived parent isotopes in many systems. This separation and subsequent decay provides the opportunity for the use of ²¹⁰Pb as a dating tool (Cornett and Lardner 2004). Sediment systems provide a natural storage system because Pb, Bi and Po are immobile or only mobilized together in these systems. In all but the top few cm of most sediment cores the sediment is old enough to ensure that the concentration of ²¹⁰Pb will be equivalent to that of the shorter-lived daughter isotopes. Tests of the top few cm and of surficial sediment indicate that the Po and Pb concentrations are quite similar. Therefore for ²¹⁰Pb dating of sediments the analysis of the concentration of ²¹⁰Po is equivalent to the measurement of ²¹⁰Pb until the shorter lived isotope is radiochemically separated from the

^{210}Pb . ^{210}Po measurement by Alpha Spectroscopy is the method employed by the dating laboratory used in this study (MyCore Scientific Inc.) (Cornett and Lardner 2004).

^{210}Pb dating requires information from the entire concentration-depth profile as well as from a background sample since the decrease in ^{210}Po activity is used to date the sediment. Therefore the surface sample and a deep sample from near the bottom of the core must be analyzed. 12 to 20 sections of a sediment core must be analyzed before the core can be dated, therefore a number of samples were taken from throughout the core. The wet weight as well as the dry sediment weight for the sampled sediment was measured and supplied as required by the dating laboratory. The Pb and Po isotopes can be volatilized from the samples at temperatures in excess of 150°C (Cornett and Lardner 2004), therefore the wet samples were dried at a maximum temperature of 105°C . Each dried sample was ground to pass through a screen with about 100 mesh size and 1 g sub-samples from a homogenized section of the core were obtained and sent away to MyCore Scientific Inc. for ^{210}Pb dating analysis.

ESEM and XRD

Approximately 2 cm^3 of sediment was sampled at strategic points of interest along the core. Since the organic and carbonate matter was not to be investigated at a microscopic level, it was removed from the sample by first treating it with 10% HCl and then peroxide in a warm water bath as described in section 1.3.2 for grain size analysis. For each sample the grains were separated into two grain size fractions ($> 63\ \mu\text{m}$ and $\leq 63\ \mu\text{m}$) using wet sieves. This was done for two reasons; to produce a better ESEM

image by reducing the potential size variation so that the focus of the image would not be limited to either the larger or smaller grains (since the magnification would be so great), and second to separate the expected 60 μm and smaller atmospheric magnetic spherules from the larger angular detrital magnetic grains so that they could be located more easily.

The samples were then left to air dry inside enclosed (to prevent contamination) plastic sample Petri-dishes so that magnetic particles could be separated using a natural earth magnet. Magnetic grains larger than 63 μm could be separated using a hand magnet held within Kim Wipe non-static paper (so that the grains could be recovered after separation), but the fraction of grains smaller than 63 μm could not be separated from the rest of the sample possibly due to static and/or cohesive forces. Therefore individual magnetic grains were identified and selected that were $> 63 \mu\text{m}$, but a homogenous representative sample had to be used from the $\leq 63 \mu\text{m}$ fraction.

The samples were mounted on aluminium scanning electron microscope stubs that were coated with a 1:1 colloidal graphite and craft glue solution. The sample stage (aluminium stub with mounted sample) was then placed in the environmental scanning electron microscope (ESEM) to acquire grain specific images and for elemental analysis according to the methods described by Schultes (2004). The elemental composition of the grains or areas of interest was determined using X-ray diffraction in conjunction with the ESEM.

Locke and Bertine (1986) present a method for separating small magnetic grains that may work for the $\leq 63 \mu\text{m}$ grain size fraction that could not be separated in this

study. Approximately 0.2 g of the sample of interest is mixed with reagent grade acetone and placed in an ultrasonic generator for 15 minutes. Then a hand magnet wrapped in a plastic bag is swirled in the solution to attract the small magnetic grains.

1.3.3 Magnetic Property Analyses

Bulk Magnetic Susceptibility (χ)

In order to determine the magnetic signature of the sediments along the profile, each core was first subsampled using 8 cm³ cubets placed side by side along the core. Once the cubets were positioned upside down on the core, a board was placed above the row of cubets and pressed down so that each cubet would be sampled in the same way (and quickly). Bulk magnetic susceptibility (χ) was determined by measuring the volume magnetic susceptibility (κ) and mass of each cubet, then using the equation:

$$\chi (10^{-8} \text{ m}^3/\text{Kg}) = \frac{\kappa (10^{-5} \text{ SI}) * \text{cubet volume (m}^3\text{)}}{\text{sample mass (Kg)}} \quad \text{Equation 1.5}$$

The cubet sample volume magnetic susceptibility (κ) was measured using a Bartington Instruments MS2 meter with a type MS2C sensor, after the cubets had equilibrated with room temperature. An air measurement was made prior to and following each sample measurement to correct for instrumental drift. The mass of each cubet was measured on a Denver Instrument M220D analytical balance to 6 significant digits.

Volume Magnetic Susceptibility (κ)

The laboratory-based volume magnetic susceptibility (κ) profiles were measured at 1 cm intervals from the archive half of the cores using the Bartington Instruments MS2 meter with the type MS2F sensor in the proto-type probe, after the cores had equilibrated

with room temperature. Three minutes of air measurements were taken before and after the sediments of the archive half of the core were measured so that instrument drift corrections could be made base on the trend of the drift from the air measurements.

Natural Remanence Magnetization (NRM)

The remanence of the natural sample (i.e. fresh sediment removed from area of interest) is measured using the Molspin 1A Magnetometer that is sensitive to very small magnetic fields. If a sample is placed in the centre of a coil & is spun, and has a remanent magnetization, the magnetic field it generates induces an electrical current within the coil as defined by Faraday's Law (Walden et al., 1999). The size of the current is proportional to the size of the remanence in the sample, but only the component of the remanence that is perpendicular to the axis of the coil contributes to the signal generated, so all 3 axes must be examined to determine the direction of magnetization of the sample. The magnetic vector of the NRM is reported in terms of remanence intensity (mA/m), declination (degrees from magnetic north) and inclination (degrees from the horizontal). Walden et al. (1999; p. 68) offer a detailed description of how to use the magnetometer.

Isothermal Remenence Magnetization (IRM)

Isothermal Remenence Magnetization (IRM) is the magnetic remanence acquired by a sample after being exposed to an external dc magnetic field using a Molspin 1T pulse magnetizer at a constant temperature. The resulting remanence vector is measured using the Molspin 1A Magnetometer described in the previous section. The Molspin 1T

pulse magnetizer should be used to apply progressively larger fields in the same direction (forward fields) to induce IRMs, but after each field is applied the $IRM_{\text{applied field}}$ must be measured using the Molspin 1A magnetometer. A typical series of forward fields used includes: 20, 40, [60, 80,] 100, [200,] 300, 500, 600, 800, and 1000 (mT) in order to compare the sample against theoretical IRM acquisition data. In this study after a forward field of 1000 mT was used to determine SIRM, a number of IRMs were induced with applied fields (10, 20, 30, 50, 100, 200 and 300 mT) in the reverse direction (backfields). These IRM acquisition data using backfields rather than forward fields was done to maximize the information that would be obtained since the S-ratio values are calculated using SIRM and $IRM_{-100 \text{ mT}}$ and the usual series of forward fields would not add enough information to justify the time required to take the measurements on top of all of the other IRM measurements.

Field sizes between 0 and 1 Tesla (1000 mT) can be generated using the Molspin 1T Pulse Magnetizer by using electromagnets to induce isothermal remanence in a sample. The Molspin 1T pulse magnetizer uses a capacitor system in which electrical charge is built up to the necessary level and the required magnetic field is generated as a short duration pulse (Walden et al., 1999). The magnetic remanence acquired at a particular applied field is referred to as $IRM_{\text{applied field}}$ or $IRM_{20\text{mT}}$ for example. To differentiate between haematite and goethite field sizes of $\sim 3\text{T}$ are needed, therefore this separation is not possible for this study. Walden et al. (1999; p. 77) offer a detailed description of how to use the pulse magnetizer.

Chapter 2: RAPID IN-SITU MEASUREMENT OF MAGNETIC SUSCEPTIBILITY IN LAKE SEDIMENTS: A CASE STUDY FROM FRENCHMAN’S BAY, LAKE ONTARIO, CANADA

Christina T. Clark and Joseph I. Boyce

School of Geography and Geology,

McMaster University, Hamilton Ontario, Canada

2.1 Abstract

Magnetic susceptibility measurements can provide a useful indicator of anthropogenic effects in lake basins, including the onset of land clearance, forest fires, soil erosion and as a proxy for estimating contaminant levels in sediment. Susceptibility is commonly measured on whole or split cores, or on core sub-samples, but coring can be expensive and time consuming where a large number of profiles are required to correlate and map sediment volumes. Post-sampling mineralogic changes in cores are also a potential concern. An alternate approach investigated in this study is to obtain near continuous in-situ measurements of sediment volume magnetic susceptibility (κ) using a probe driven into the lake bottom. An inexpensive proto-type probe was constructed using a Bartington MS2-F sensor mounted in waterproof housing with an extendable 10 m handle. Several calibration runs were made in a laboratory test column to determine the probe response characteristics and reproducibility. Testing showed that the effective

sensing volume is a 2.2 cm radius around the probe tip and that edge effects from sensor shoulders are negligible.

The probe was then used to measure the thickness and distribution of a post-colonial sediment layer in a shallow coastal lagoon (Frenchman's Bay) in western Lake Ontario. Volume susceptibility profiles were collected at 35 locations by driving the probe up to 2.5 m into the lagoon bottom sediments at 2 cm measurement intervals. The in-situ volume susceptibility profiles were then compared with volume and bulk susceptibility measurements obtained on 4 of the vibracores extracted from the lagoon. The probe measurements showed comparable resolution to the core-derived data and closely paralleled the core susceptibility curves. The base of the post-colonial sediment layer present in the lagoon was identified by an abrupt increase in magnetic susceptibility at 0.5-1.2 m depth. The marker horizon was correlated across the lagoon and the thickness and volume of the anthropogenic layer was estimated. The results demonstrate that in-situ susceptibility measurements using a sediment probe can provide a rapid and highly repeatable method for correlating shallow stratigraphic boundaries within unconsolidated lake bottom sediments.

2.2 *Introduction*

Lake sediments can provide a continuous record of paleoenvironmental conditions on continents, and their study is fundamental to understanding past climates and the environmental impact of human activities (Reynolds and King 1995; Verosub and Roberts 1995). Magnetic minerals are ubiquitous in lake sediment and their composition

and abundance are controlled by processes that are strongly influenced by changes in climate. For example, shifts in temperature and precipitation directly affect rates of continental erosion and weathering and also many diagenetic and biological processes that can alter sediment magnetic characteristics (e.g. oxidation, reductive dissolution, biogenic magnetism) (Snowball 1994). All of these effects contribute to the mineralogy and magnetic particle-size distribution in lake sediment and can be measured by analysis of the rock magnetic properties (Walden et al. 1999).

Magnetic susceptibility measurements can also provide a useful indicator of anthropogenic effects in lake basins, including the onset of land clearance (Boar and Harper 2002), roadside pollution (Hoffmann et al. 1999; Petrovsky et al. 2000), forest fires (Rummery 1983), and soil enhancement & erosion (Shenggao 2000). Beckwith et al. (1986) pioneered the application of magnetic susceptibility as a contaminant proxy when they identified a linear relationship between χ and trace metal (Cu, Fe, Pb & Zn) concentrations present in urban source sediments, which has been confirmed for Pb, Cu, Zn, Cd and Cr during later studies (Chan et al. 1998; Heller et al. 1998; Desenfant et al. 2004). Further confidence in employing χ as a contaminant proxy was gained when atmospheric inputs of magnetic particles (as magnetite-rich spherules) were identified as being associated indirectly with contaminants such as polyaromatic hydrocarbons, PAHs (Morris et al. 1994), and trace metals Cr, Zn, Ti & Fe (Locke and Bertine 1986) since they are formed by the oxidation of pyrite to magnetite during combustion of the trace metal and PAH-rich coal.

Susceptibility is commonly measured on whole or split cores, or on core subsamples, but coring can be expensive and time consuming where a large number of profiles are required to correlate and map sediment volumes. Post-sampling mineralogical changes in cores are also a potential concern. An alternate approach investigated in this study is to obtain near continuous in-situ measurements of sediment volume susceptibility (κ) using a probe driven into the lake bottom. Here we describe a method of constructing a waterproof probe case for the Bartington MS2F sensor that is suitable for lake settings, which was first tested in the laboratory to determine the probe response characteristics and reproducibility. The success of the proto-type probe was then evaluated by comparing in-situ volume magnetic susceptibility values measured at depth within Frenchman's Bay lagoon against ex-situ laboratory-based volume magnetic susceptibility measurements of cores obtained in comparable locations. This technique can be employed in other lake-based settings with unconsolidated late Holocene sediments that have been impacted by urban inputs, as a means of mapping contaminated sediment thickness for site remediation studies or mapping of effluent outfalls.

2.3 *Methods*

2.3.1 Probe Construction

An inexpensive proto-type probe was constructed using a Bartington MS2-F sensor mounted in waterproof nylon housing with an extendable 10 m ABS plastic handle (see Figure 2.1). The probe tip and handle are 3 cm in diameter and can be driven up to 3-4 m into soft unconsolidated muds and clays. The probe housing was designed with a

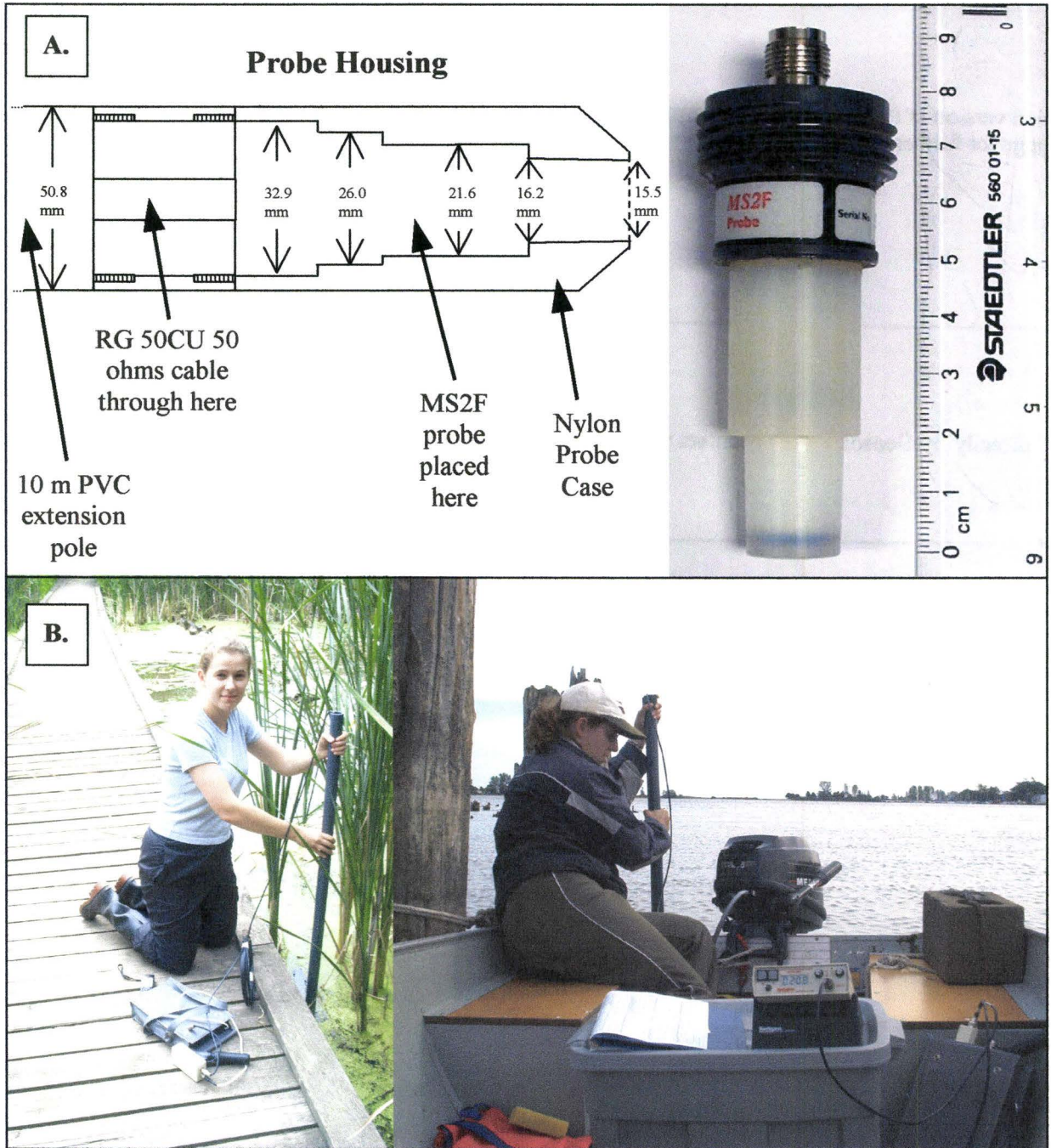


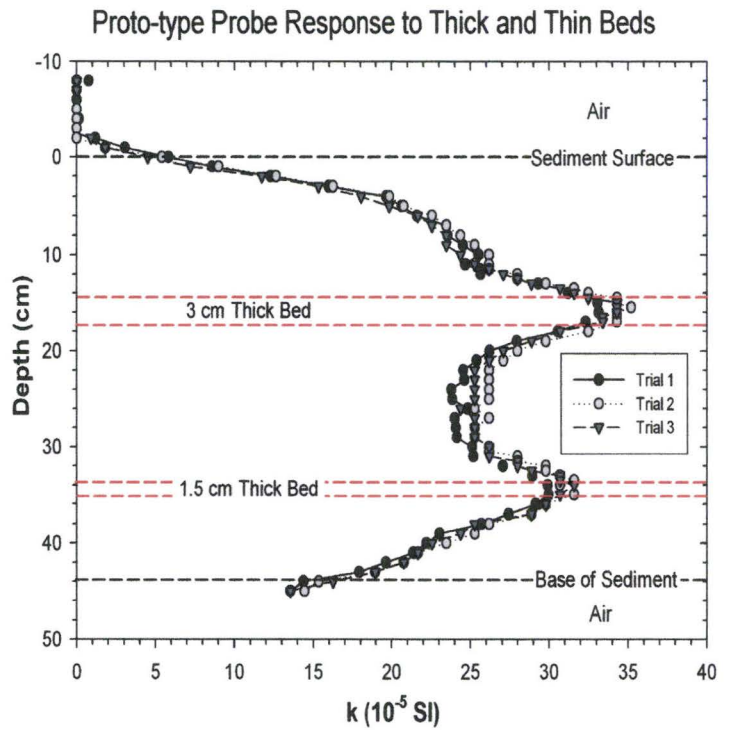
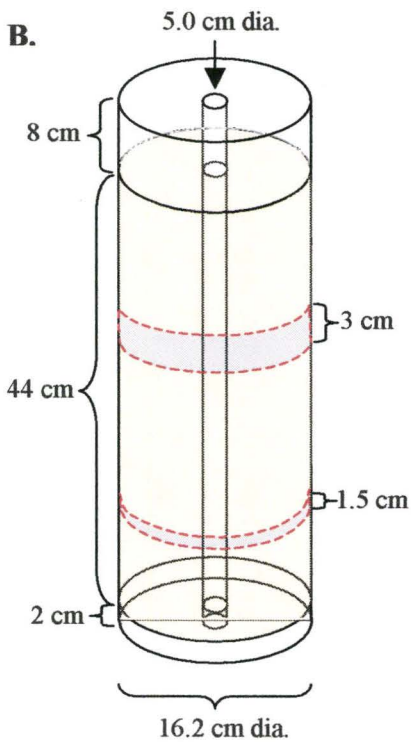
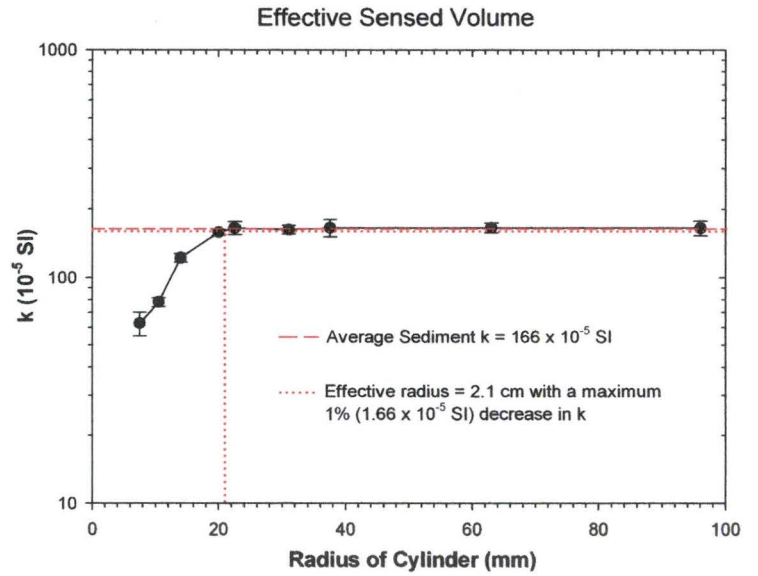
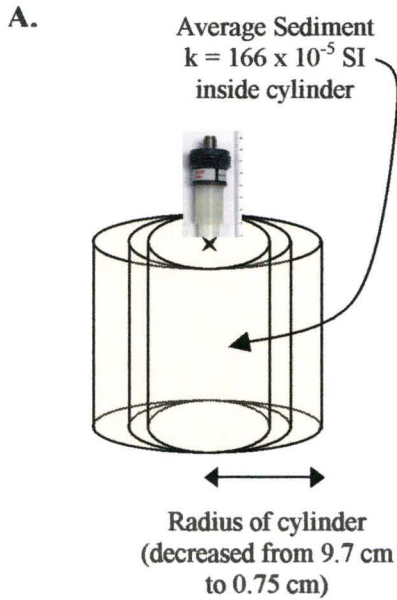
Figure 2.1: A. Probe housing for the MS2-F probe shown on the right. Probe tip is attached to 5 m long PVC and ABS pole. B. Probe in use in the field for in-situ measurements of sediment volume magnetic susceptibility (κ). Probe is advanced into sediment at 2 cm intervals.

minimum wall thickness (< 4 mm) to maximize the active sensing volume of the MS2-F probe tip. Several laboratory tests were conducted using an experimental silica sand column to determine the probe sensing volume and response to thin sediment layers.

Effective Sensing Volume

When a magnetic susceptibility meter is employed, the κ of target sediments is determined by measuring the loss of induced magnetic field after a 1 second low intensity (80 A/m) magnetic field is applied to the sediments. A measure of how easily the sediments can be magnetized (κ) will be determined from the amount of magnetism that was temporarily induced versus the applied field used to induce the magnetism. The spontaneous/one second induction field generated from the sensor tip and the field induced in the target sediments decays exponentially with distance since the strength of all magnetic fields decay exponentially with increased distance from the source. Therefore the Bartington MS2F probe has a maximum volume of sediment around the probe tip that is sensed in order to provide κ measurements. In order to determine this effective sensing volume, the probe was inserted sequentially into nine test cylinders (Figure 2.2 A) filled with uniform medium sand with a mean κ of 166×10^{-5} SI. The cylinder radii varied from the largest value of 9.75 cm down to 0.75 cm. The radius that first caused the measured κ values to decrease by 1% (1.66×10^{-5} SI) was used as an indication of the effective hemispheric sensed volume ($\frac{2}{3}\pi r^3$), since any radius decrease below what was required for the probe's sensed volume would result in a measured κ

Figure 2.2: Diagram showing sand columns used to test probe response. A. Probe response and effective sensing volume determined using sand-filled cylinders of decreasing diameters. Effective probe sensing volume is a hemisphere with a 2.1 cm radius. B. Response of the probe to thin sand beds (1.5, 3 cm thickness, $\chi = 39.7 \times 10^{-8}$ SI) within low susceptibility ($\chi = 23.5 \times 10^{-8}$ SI) sand.



value below the κ mean of 166×10^{-5} SI. The effective sensing volume test design is shown in Figure 2.2 A.

Response to Thick and Thin Beds

The sensitivity of the probe may be limited by its effective sensing volume, therefore the next test evaluated the probe's ability to identify thin horizontal layers of slightly higher κ sediments within uniform lower κ sediments, which is common in sedimentary environments. The probe response was tested using a 16.2 cm diameter sand column (Figure 2.2 B) with a height of 54 cm. It was filled from 4 cm above the base to 8 cm from the top of the column with uniform medium sand sediments (mean = 238 μm) with a bulk magnetic susceptibility value of (23.5×10^{-8} SI, $\sigma = 1.1 \times 10^{-8}$ SI) that was obtained by adding pure fine silt grain-size (mean = 22.7 μm) magnetite. Layers of sand (1.5 cm and 3 cm thick) with added magnetite grains to elevate the bulk susceptibility value to 39.7×10^{-8} SI, $\sigma = 1.3 \times 10^{-8}$ SI were placed at different locations within the otherwise lower κ sediments in the test column. A 5.0 cm outside-diameter tube was placed in the center of the test column so that the proto-type probe could be lowered through the sediments inside the hollow tube. The volume magnetic susceptibility values were then recorded from a height of 8 cm above the test column down through the 44 cm column to 4 cm below the column so that edge effects could also be noted if they were present. Figure 2.2 B illustrates the test column design used to determine the proto-type probe's response to thick or thin beds of elevated κ within otherwise uniform lower κ sediments.

2.3.2 Study Area

The field application of the proto-type probe was tested in Frenchman's Bay (FMB), a shallow coastal lagoon on the northwestern shore of Lake Ontario (Figure 2.3). Frenchman's Bay is separated by a natural sand and gravel beach barrier with a maintained navigational channel connecting it to the lake. The lagoon itself extends over 0.84 km² and about 0.55 km² of open water (Eyles et al. 2002). Amberlea, Dunbarton, Pine and Krosno creeks are the four main tributaries in the 2200 km² Frenchman's Bay watershed that is heavily urbanized (80%) with a current population of 47,000 people (TRCA 1999). The lagoon reaches a maximum depth of 3.8 m within a central basin and is less than 2 m over the remainder of the lagoon.

Previous work in Frenchman's Bay indicates that the upper sediment layer is heavily impacted by urban contaminants (Eyles et al. 2002). Remediation of the sediment is dependent upon a detailed understanding the thickness and volume of this upper layer. The probe was employed to map thickness and distribution of post-colonial sediments across the lagoon using the association of post-colonial plus urban source sediments and elevated κ established earlier by Beckwith et al. (1986) and later employed by Versteeg et al. (1995). The latter study measured κ from sediment cores, which is time consuming and costly when compared to in-situ κ measurements. For this study, volume susceptibility profiles were collected at 35 locations by driving the probe up to 2.5 m into the lagoon bottom sediments and taking measurements at 2 cm intervals.

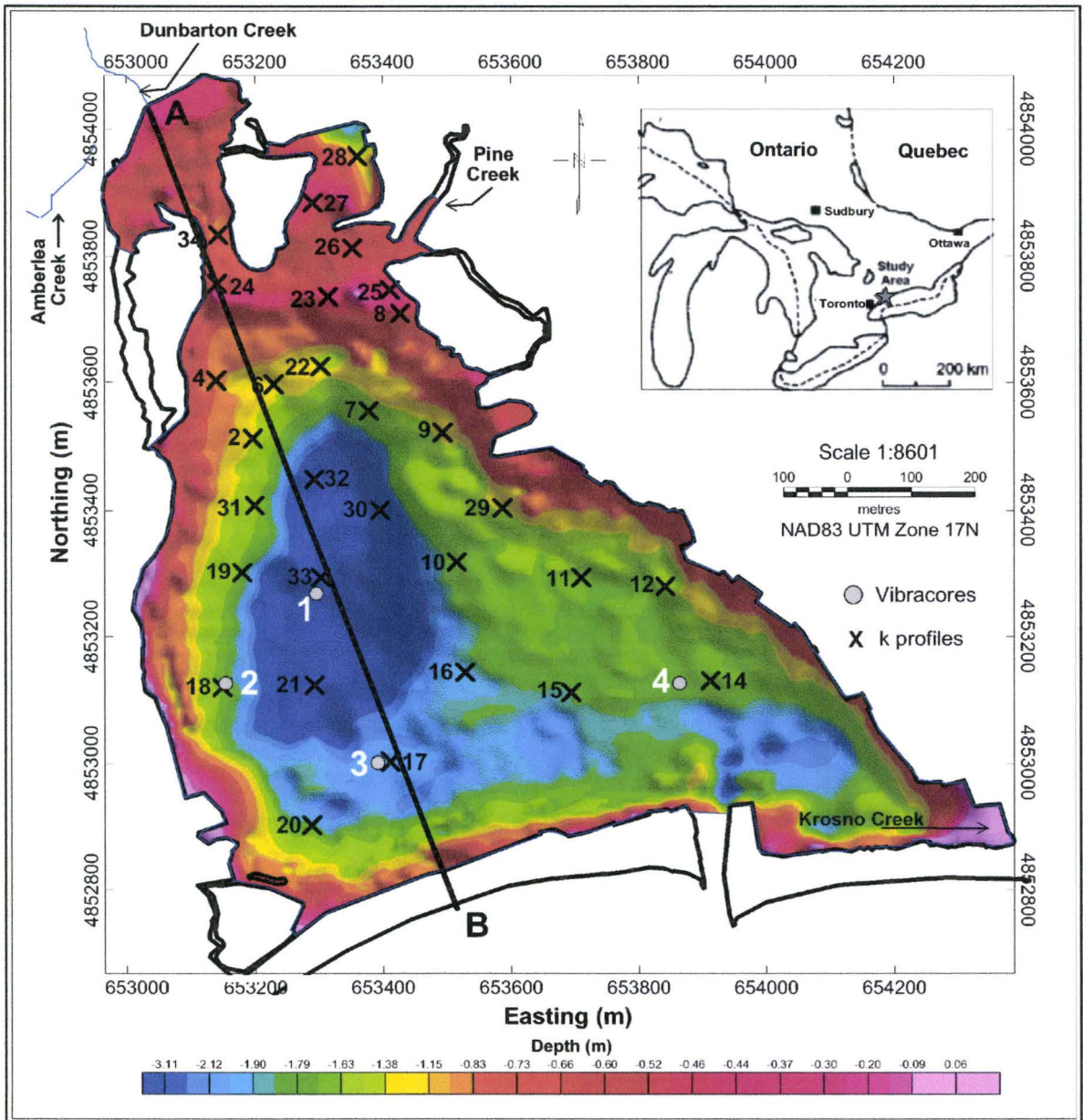


Figure 2.3: Map showing the location of Frenchman's Bay, coring and sediment probe locations and lagoon bathymetry.

Cores were also collected at four locations in the lagoon so that the bulk and volume susceptibility values could be compared. The cores were collected using a vibracorer and 8 cm diameter aluminum tubes. The uncompacted lengths of each core were determined based on field measurements of aluminium tube length, depth to sediment surface, and total recovered core length. The locations of the core sites are also indicated in Figure 2.3 A. The cores were split and one half was set aside as an archive while the other was used for logging and analyses. When not in use, the cores are stored at a constant temperature of 0 – 3 °C to reduce microbial activity. The sediments were described visually and relevant features were recorded which include lithology, approximate grain size, sorting, framework, colour, approximate % organic matter, and sedimentary structures and/or inclusions.

In order to determine the magnetic signature of the core sediments, each was subsampled using 8 cm³ cubets placed side by side along the core. Bulk magnetic susceptibility (χ) was determined by measuring the volume magnetic susceptibility (κ) and mass of each cubet, then using the equation: χ (10⁻⁸ m³/Kg) = κ (10⁻⁵ SI) * cubet volume (m³) / sample mass (Kg). The cubet sample volume magnetic susceptibility (κ) was measured using a Bartington Instruments MS2 meter with a type MS2C sensor, after the cubets had equilibrated with room temperature. The mass of each cubet was measured on a Denver Instrument M220D analytical balance to 6 significant digits. The laboratory-based volume magnetic susceptibility (κ) profiles were measured from the archive half of the cores using the Bartington Instruments MS2 meter with the type MS2F

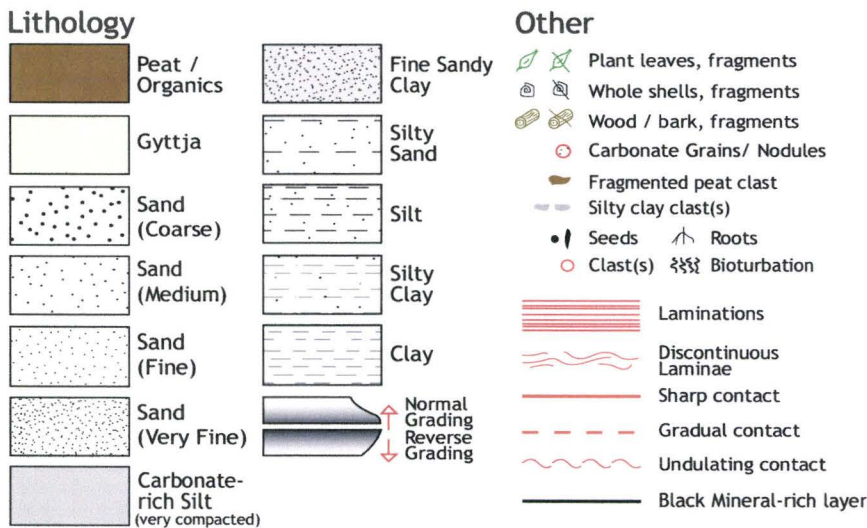
sensor in the proto-type probe, after the cores had equilibrated with room temperature. The laboratory and field measurements obtained for the FMB4 core and κ profile #14 are shown in Figure 2.4 along with the lithologic log to demonstrate the comparable resolution and the similar magnetic susceptibility curves obtained.

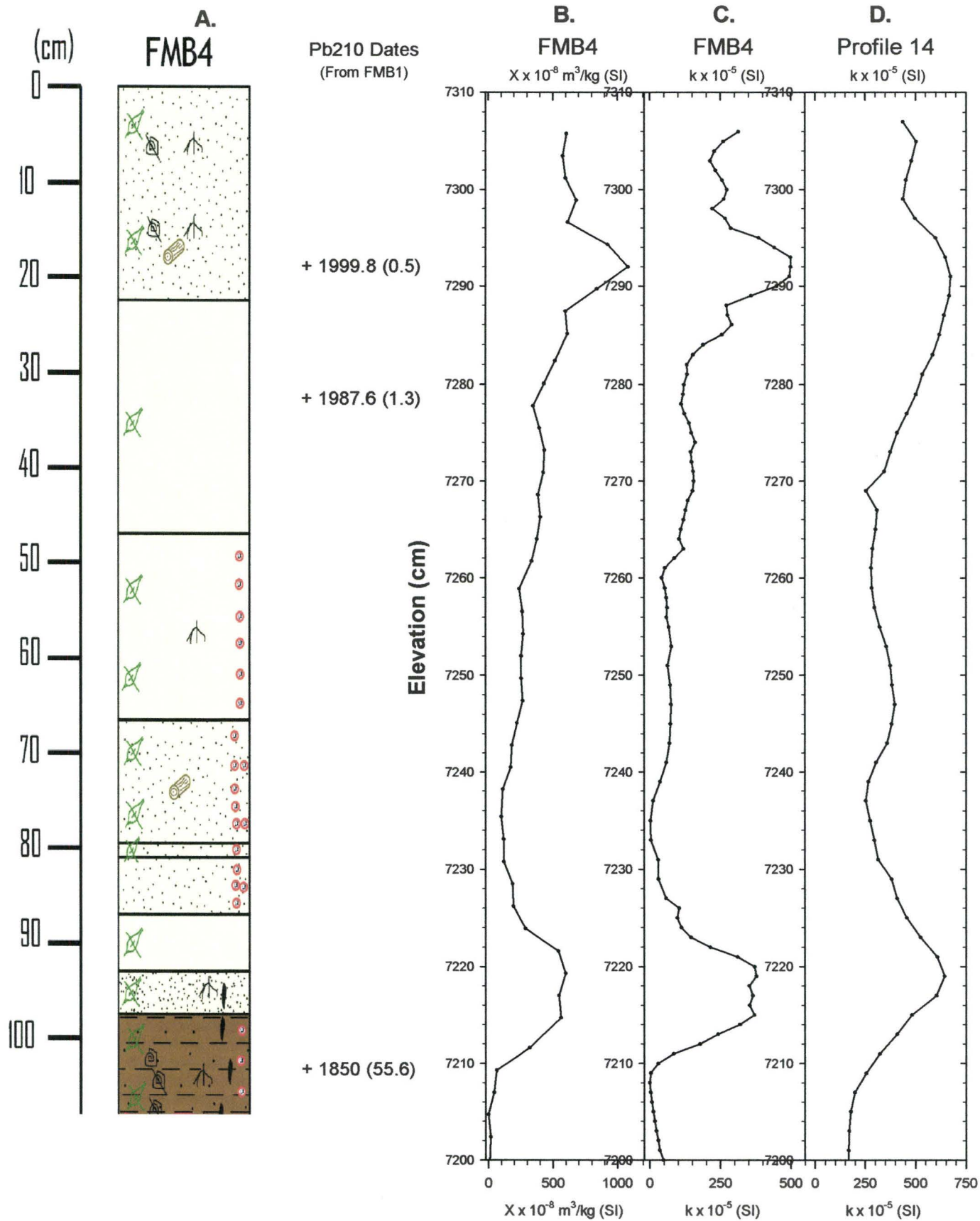
2.4 Results

2.4.1 Probe Response

Testing of the proto-type probe depicted in Figure 2.2 A showed that the effective sensing volume is a 2.1 cm radius around the probe tip since at this radius a 1 % decrease (1.66×10^{-5} SI) below the mean κ of 166×10^{-5} SI for the sediments was measured. The total zone of influence was determined to be 10 cm when the final 1% of the sensing volume is included. It was also determined that edge effects from sensor shoulders are negligible once the sensor is placed inside the proto-type probe waterproof case. While measuring the response in uniform sediments, edge effects over a range of 5 cm were observed at the top and bottom of the test column when the probe moved between air and the test column of uniform sediments (see Figure 2.2 B). Once contrasting beds with a higher χ of 39.7×10^{-8} SI, $\sigma = 1.3 \times 10^{-8}$ SI were added at different locations and with different thicknesses, it was determined that the proto-type probe was able to identify beds that were 1.5 cm and greater.

Figure 2.4: A. Detailed lithologic log for borehole FMB4 with approximate sediment ages based on ^{210}Pb dating. B. The bulk (laboratory) magnetic susceptibility (χ) measured at ca. 2 cm intervals down the core. C. Laboratory volume magnetic susceptibility (κ) profile. D. In-situ volume susceptibility profile measured with probe at location #14.





2.4.2 Frenchman's Bay

The general stratigraphic succession in the lagoon which is typical of lake and lagoon sediments around Lake Ontario (Anderson and Lewis 1985) consists of a thick upper sequence of marly gyttja and organic-rich silty muds overlying Holocene organic-rich laminated marls above [post-glacial] deeper sandy clays with moderate carbonate content and elevated mineral and magnetic susceptibility values. The probe was generally able to penetrate ~2 m into the thick upper layer of gyttja and silty muds.

The in-situ volume susceptibility profiles all reflect the general shape observed for cores collected by Versteeg et al. (1995) from Hamilton Harbour. After fluctuating low ($10\text{-}50 \times 10^{-5}$ SI) background levels a sharp increase in κ of $50\text{-}100 \times 10^{-5}$ SI is observed that continues to rise towards the surface until a drop of $50\text{-}150 \times 10^{-5}$ SI is observed near the sediment-water interface. Comparison of the in-situ κ profiles with κ measurements obtained on 4 vibracores extracted from the lagoon indicates that the probe measurements offer comparable resolution to the core-derived data and similar magnetic susceptibility curves (see Figure 2.4). These laboratory versus in-situ volume susceptibility values were then compared using linear regression (Figure 2.5) to determine if there was a consistent shift in the data that could be corrected for during future use of the proto-type probe. A correction factor for field measurements was determined from linear regression analysis of core FMB4 lab-based κ measurements versus κ profile #14 field-based κ measurements (see Figure 2.5) for a vertical profile at the similar (within 0.5 m) location using a 95% confidence level. The linear regression

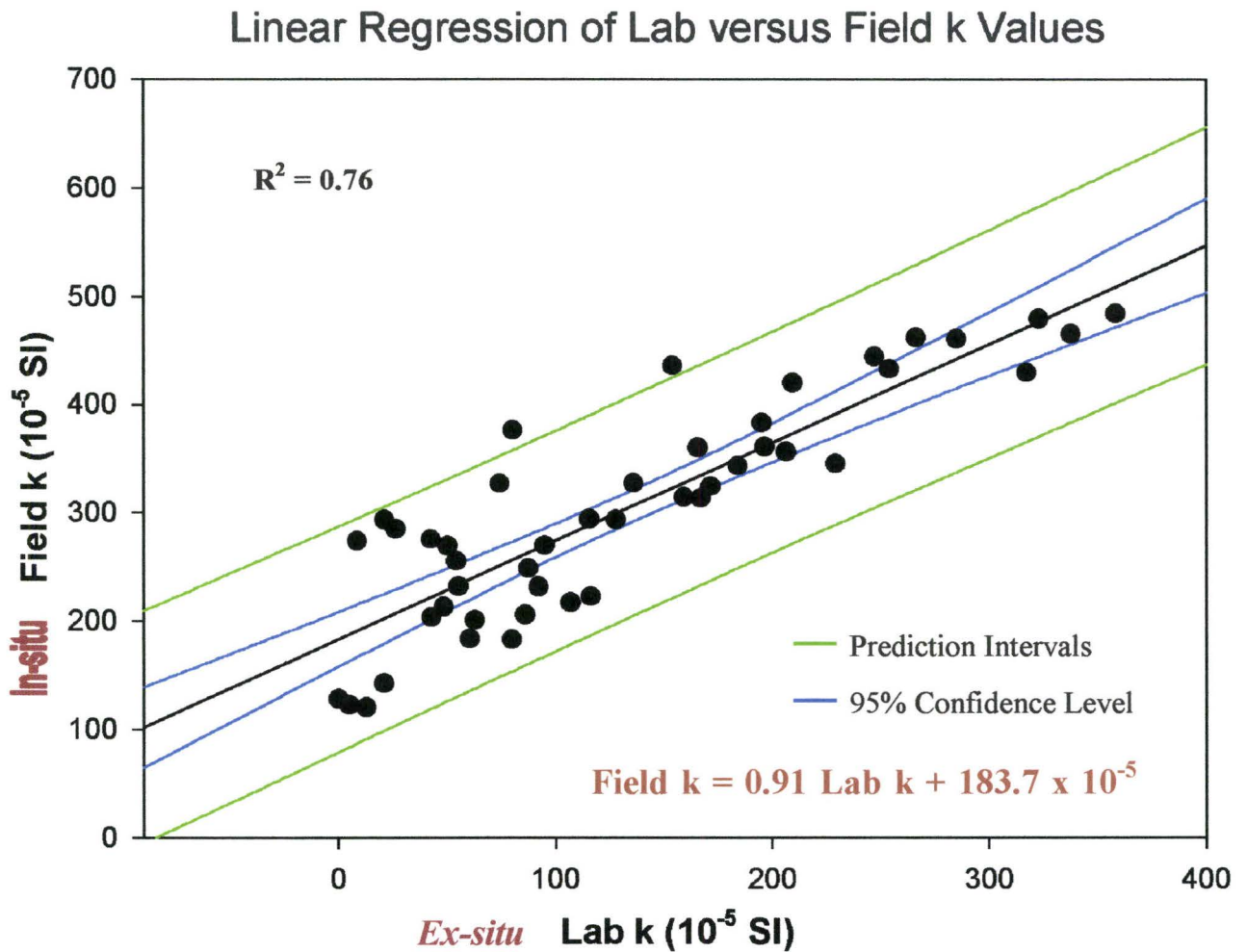
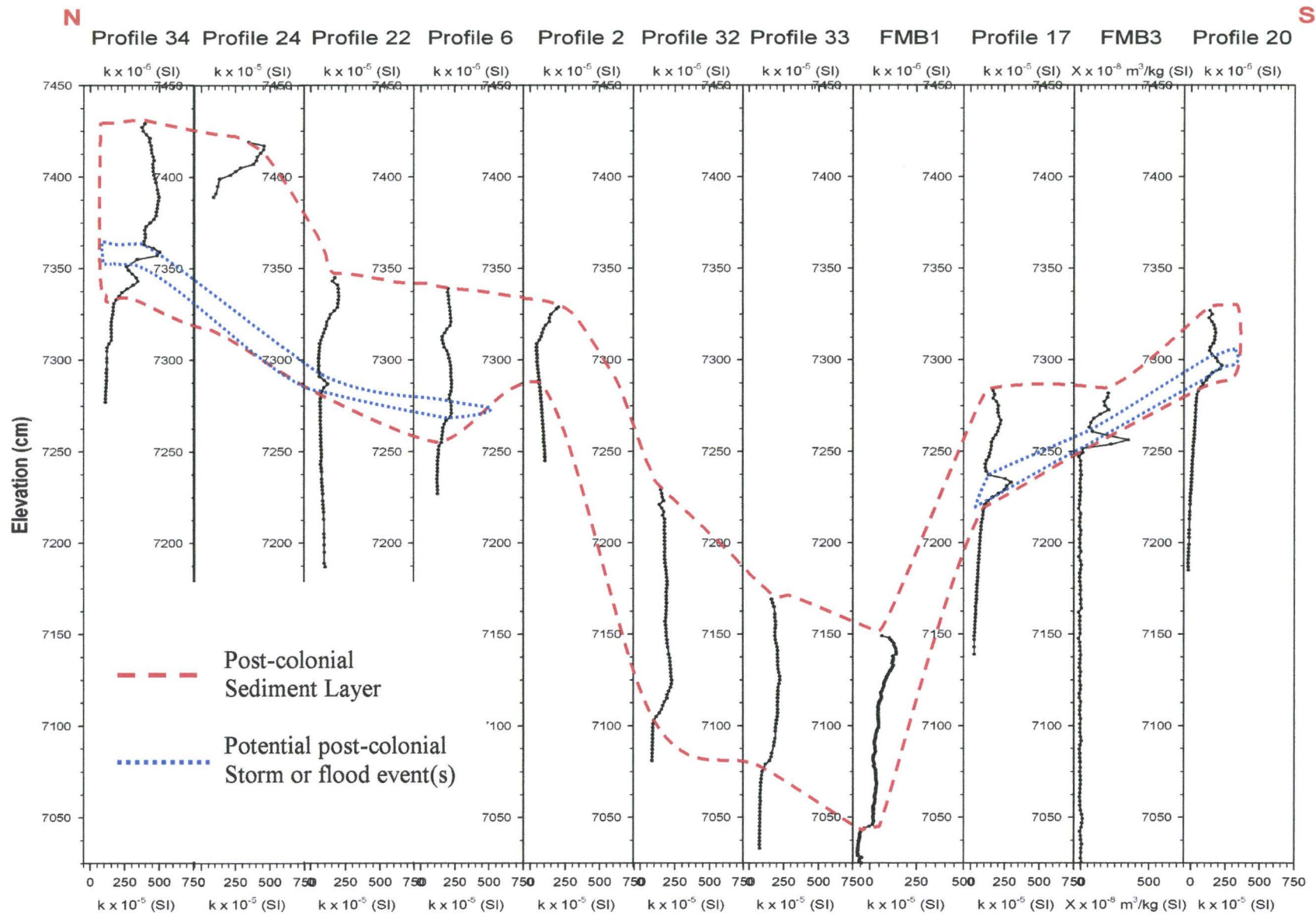


Figure 2.5: Linear regression of laboratory versus in-situ field magnetic susceptibility from FMB-4 and probe #14. Linear equation is used to calibrate in-situ volume magnetic susceptibility measurements against laboratory values.

results ($R^2 = 0.76$) indicated that a consistent shift from laboratory to field derived data could be corrected for using a calibration value of 0.91 along with a bulk shift of 183.7×10^{-5} SI.

To evaluate the use of κ profiles as a correlation tool, the profiles along a North-South transect in Frenchman's Bay are shown in Figure 2.6 with κ correlated units in the subsurface lithology outlined. The base of the post-colonial sediment layer in Frenchman's Bay was identified by an abrupt κ increase of $50-100 \times 10^{-5}$ SI at a sediment depth of 0.5-1.2 m. The marker horizon was correlated across the lagoon as shown in the north-south transect of κ profiles along the line AB (Figure 2.6). The maximum 1.2 m thickness of the anthropogenic layer was identified in each κ profile by noting the depth at which the $50-100 \times 10^{-5}$ SI increase in κ occurred. These anthropogenic layer thickness data were then plotted as an isopach map in Figure 2.7 A to further identify its geometry. The anthropogenic layer existed as a plume of sediment that was thickest at the base of Amberlea and Dunbarton creeks and thinned out into a bird's-foot lobed shape towards the centrally deep area of the lagoon. It was also noted that there was another shorter wavelength (8-20 cm) high intensity ($100-500 \times 10^{-5}$ SI) κ peak at depths below the post-colonial layer of ~ 25 cm in the north and ~ 5 cm to the south, but these peaks were not continuous across the lagoon. Investigation of the geometry of the signal from the isopach map (Figure 2.7 B) and the core sediments at the shorter wavelength high κ peak positions revealed that these peaks correspond to sandy layers in core and may represent a relict beach barrier deposit to the north, while the other signal correlates with the

Figure 2.6: A North-south magnetostratigraphic section showing correlated volume magnetic susceptibility profiles (κ). The post-colonial sediment layer is identified by a κ increase of $50-100 \times 10^{-5}$ SI in the upper 50-120 cm of the profiles. Another feature that had a shorter wavelength (8-20 cm) and higher intensity ($100-500 \times 10^{-5}$ SI) was identified as a sand and sandy silt layer. The location of the transect is shown in Figure 2.3A.



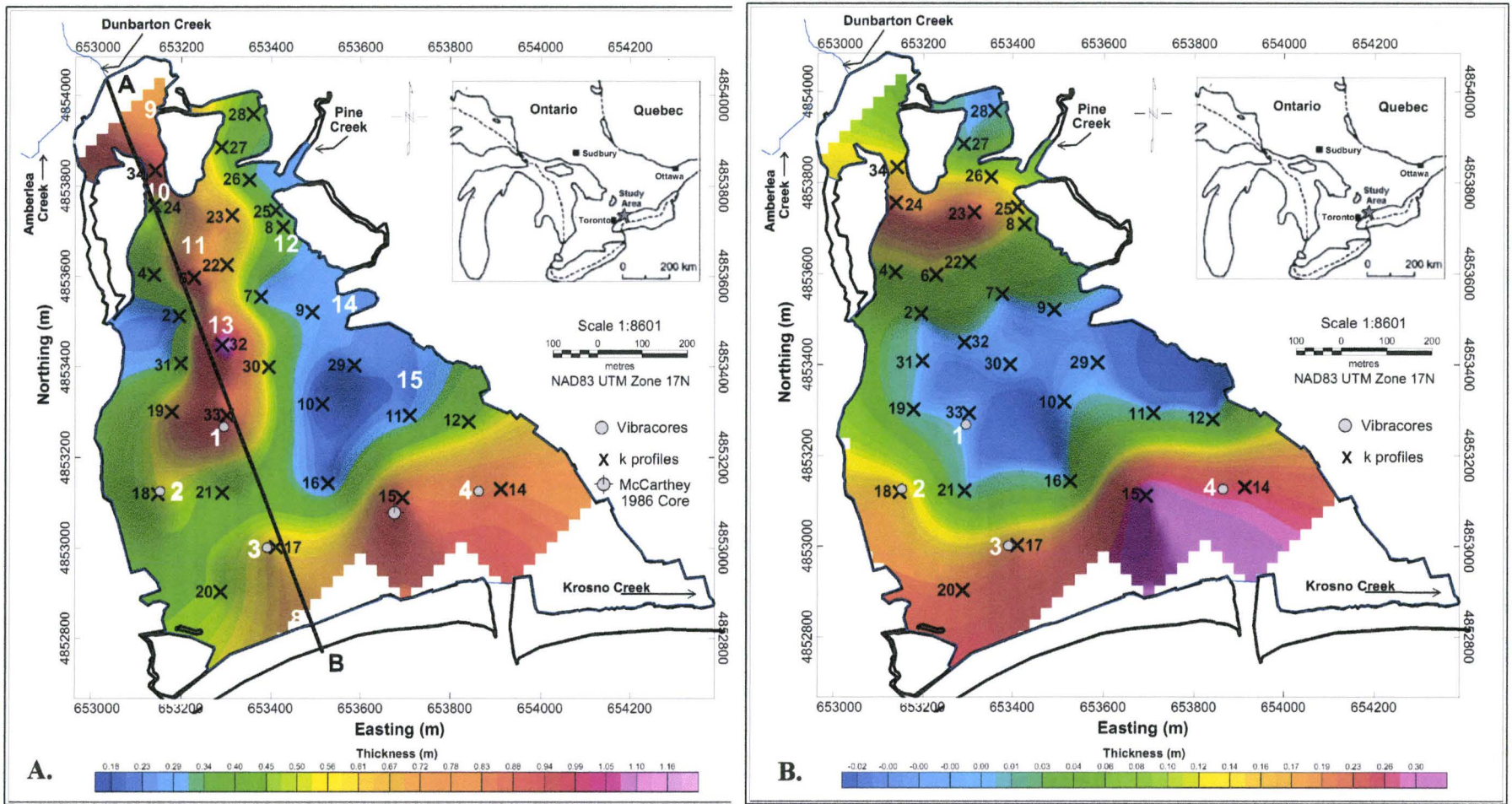


Figure 2.7: Isopach maps showing A. the post-colonial sediment layer in Frenchman's Bay, and B. the location of sandy overwash deposits from the modern and possibly relict beach barriers.

modern beach barrier to the south indicating that these higher κ sediments may be from storm overwash or drift from the open channel. Further evidence for a relict beach barrier and sandy storm overwash is present in the bathymetric map for the lagoon since the shape of an elongate bar parallel to the modern beach barrier is seen in the north at a water depth of 2 m, while fan shape sediments originating from potential overwash channels can be seen in the south on the leeward side of the beach barrier. The shapes of both structures are reflected in the geometry indicated in the isopach maps.

2.5 Conclusions

The inexpensive proto-type probe was able to identify sediment layers as thin as 1.5 cm in the presence of a moderate κ contrast, while edge effects were noted over a range of 5 cm. The effective semi-hemispheric sensing volume was determined to have a radius of 2.1 cm, therefore the proto-type probe is capable of collecting high-resolution data in areas of moderately variable lithology.

The shapes of the field versus laboratory measured κ profiles were directly comparable for similar locations, which can be further emphasized using wiggle trace matching. Linear regression of the laboratory versus in-situ volume susceptibility values demonstrated a consistent 0.91 linear and a 183.7×10^{-5} SI bulk shift, which can be applied as a calibration constant to any future κ profiles obtained in the field.

The probe was successfully used to quickly measure the thickness and distribution of a post-colonial sediment layer and overwash in a shallow coastal lagoon (Frenchman's Bay) in western Lake Ontario. The results demonstrate that in-situ susceptibility

measurements using a sediment probe can provide a rapid and highly reproducible method for correlating shallow stratigraphic boundaries within unconsolidated lake bottom sediments. Potential environmental applications include the mapping of contaminated sediment thickness for sediment remediation studies and mapping of effluent outfalls.

**Chapter 3: A MULTI-PROXY RECORD OF POST-COLONIAL AND LATE
HOLOCENE ENVIRONMENTAL CHANGE IN FRENCHMAN’S BAY, LAKE
ONTARIO, CANADA**

Christina T. Clark, Joseph I. Boyce and Eduard G. Reinhardt

School of Geography and Geology,

McMaster University, Hamilton Ontario, Canada

3.1 Abstract

Coastal environments in the lower Great Lakes have been modified significantly by post-colonial land use changes and the growth of industry. The sediment magnetic record of these changes was investigated in a small coastal lagoon (Frenchman’s Bay, 0.84 km²) lying at the eastern limits of the Greater Toronto Area in western Lake Ontario. A total of 11 vibracores (2 - 4.5 m length) were retrieved from the lagoon and the lithofacies were logged in detail and magnetic property, micropaleontologic and textural analyses were performed on core samples. Magnetic analyses included measurements of volume and bulk magnetic susceptibility (κ , χ) and remanence parameters (NRM, SIRM, B_{cr}) on 8 cm³ sub-samples.

The stratigraphic succession in the lagoon consists of a sequence of gyttja and peat-rich marls overlying Holocene laminated clays. Four distinct magnetostratigraphic units are recognized: an uppermost high magnetic susceptibility ($\chi = \sim 200-300 \times 10^{-8}$

m³/Kg) gyttja layer (Unit 1) extends to 1-1.2 m depth and represents the post-colonial layer. The base of the unit has a ²¹⁰Pb age of 1850 (±55.6), corresponding with the main phase of land clearance and onset of industrialization of the harbour. The ²¹⁰Pb analysis also determined that there was an order of magnitude increase in sediment accumulation rates since the onset of industrialization. Titanomagnetite, maghemite and magnetite spherules indicate soil erosion and coal burning as the predominant sources of magnetic particles. The underlying Unit 2 consists of peaty marls with abundant plant fragments recording a more extensive marsh. Unit 3 consists of more carbonate-rich laminated silty sands (magnetic susceptibility $\chi \approx 6000 \times 10^{-8} \text{ m}^3/\text{Kg}$) deposited in a low energy oligotrophic lagoon. The basal layer (Unit 4) consists of high magnetic susceptibility massive pebbly muds, which record a pre-lagoon phase of higher water levels in post-glacial Lake Iroquois (ca. 13,500 Ka).

The reconstructed depositional model for the lagoon includes four major phases:

1. The formation of a shallow coastal embayment following water level rise from a mid-Holocene low-stand in Lake Ontario (Unit 4);
2. Development of a spit and beach barrier by eastward longshore transport (Unit 3);
3. Closure of the lagoon and development of a stabilized marsh habitat with low sedimentation levels (Unit 2);
4. Destruction of marsh habitats and eutrophication of the lagoon coinciding with land clearance (post-1850's) and an increased in the influx of sediments eroded from the catchment area.

These results demonstrate the utility of magnetic property measurements as a tool in

paleoenvironmental reconstruction of lake basins and for assessing anthropogenic impacts on coastlines.

3.2 Introduction

The colonization of the lower Great Lakes was associated with widespread deforestation, soil erosion and a rapid decline in water and sediment quality following the onset of industrialization in the late 1800's (Skibicki 1991). The impacts of these changes on nearshore and coastal environments have been significant but are poorly documented, particularly with regard to the impacts on wetlands. The effective management and restoration of aquatic habitats requires knowledge of the both the 'background' pre-colonial conditions and the natural variability in these systems in order to understand the effects of human-induced change (Smol 1992). Paleolimnological methods are being directed increasingly at understanding the recent record of anthropogenic changes on lakes, as they can provide insights into long-term changes in water quality and changes in basin physical and hydrologic processes (e.g. sedimentation, water level changes). A wide range of proxy environmental indicators are now employed in such studies, including analysis of microfossils, pollen, sediment geochemistry, stable isotopes and sediment magnetic properties (Last and Smol 2001)

A number of recent studies have demonstrated the advantages of paleolimnologic methods for documenting human-induced environmental changes in lake basins. Hillfinger et al. (2001) examined the oxygen isotope record of Green Lake, a small meromictic lake in northern New York state and recognized a basin-wide shift in $\delta^{18}\text{O}$

and a 7-fold increase in sedimentation rates associated with European land clearance in the 1800's. Patterson et al. (2002) employed freshwater protozoans as indicators of water quality and eutrophication caused by pre-European and European settlement in Swan Lake, in southwestern Ontario. In a more recent study Ekdahl et al. (2004) used microfossils and carbon isotopic data to demonstrate pre-historic and historical anthropogenic impacts on Crawford Lake, a small marl lake northwest of Lake Ontario. Their data shows two major shifts in diatom productivity associated with eutrophication of the lake during aboriginal (Iroquoian) settlement (1268-1486 AD) and later European colonization (post-1867).

Sediment magnetic property analyses can provide further insights into past environmental changes in lake basins and are also direct indicators of anthropogenic impacts and the presence of pollutants in lake sediment (Evans and Heller 2003). Several studies have documented increased magnetic susceptibility in recent lake sediments as a result of the fall-out airborne magnetic particles (Oldfield 1990; Oldfield and Richardson 1990; Morris et al. 1994; Versteeg 1994; Versteeg et al. 1995; Kodama et al. 1997). Morris et al. (1994) employed magnetic property measurements to identify and map a contaminated sediment layer within heavily industrialized Hamilton Harbour, in western Lake Ontario. Their data shows that an uppermost anthropogenic sediment layer (ca. 1-1.5 m thickness) has a magnetic susceptibility more 2 orders of magnitude greater than the underlying pre-colonial sediments. They attributed the increase in magnetization to the presence of airborne magnetite spherules produced by coal burning and steel plant

coking operations in the harbour. Chan et al. (1998) adopted a similar approach in their study of contaminated sediments in Hong Kong harbour and found that heavy metal concentrations in sediments were directly correlated with sediment magnetic susceptibility. They advocated the use of magnetic properties as a rapid and inexpensive method for mapping contaminated sediments. A number of other studies have employed magnetic property measurements to document fire histories (Rummery 1983) and to identify soil erosion events associated with colonization and urban development of watersheds (Hoffmann et al. 1999; Petrovsky et al. 2000; Shenggao 2000; Boar and Harper 2002).

In this paper, a multi-proxy approach is employed to investigate the impact of land use changes associated with colonization and urbanization of Frenchman's Bay, in western Lake Ontario. Frenchman's Bay was one of the first sites settled by Europeans in Lake Ontario (1669) and underwent major land use changes following colonization in mid-1850's, when large tracts of the area north of Lake Ontario were clear cut of forests or burned for agricultural use. The lagoon sediment and water quality are now heavily impacted and have been slated for remediation and habitat restoration (Eyles et al., 2002). A major focus of the present study was to determine the environmental conditions prior to colonization and to document the changes in aquatic habitats, sedimentation and water quality stemming from colonization and urbanization of the watershed. This was accomplished through an detailed multi-proxy study that combined sediment magnetic and geochemical property measurements with sedimentary facies analysis and ^{210}Pb

dating of core samples. The results provide important insights into the Late Holocene evolution of the lagoon as well as the post-colonial changes, including the timing of wetland destruction, changes in sedimentation rates and degradation of water quality. The results reported here have broader implications for understanding water the Late Holocene water level history and anthropogenic impacts in other coastal areas of Lake Ontario.

3.2.1 Study Area and Geologic Setting

Physical Setting

Frenchman's Bay is a shallow coastal lagoon located on the northwestern shore of Lake Ontario (Figure 3.1). The lagoon and wetlands cover 0.84 km² with about 0.55 km² of open water area (Eyles et al. 2002) and has a maximum water depth of about 3.5 m. The lagoon is separated from Lake Ontario by a narrow sand and gravel beach barrier and communicates with the lake via maintained navigational channel. The bay receives the discharge from four streams (Amberlea, Dunbarton, Pine and Krosno creeks) draining a heavily urbanized (> 80%) watershed with a current population of about 47,000 people (Figure 3.2) (Pickering 2001; Eyles et al. 2002).

Settlement History

European settlement, agriculture and urbanization have all had a dramatic effect on the lagoon and watershed. European settlement (first in 1800 and another major migration in 1825; (Skibicki 1991)) in the FMB area was associated with large-scale forest clearance and widespread erosion of soil cover leading to increased runoff and

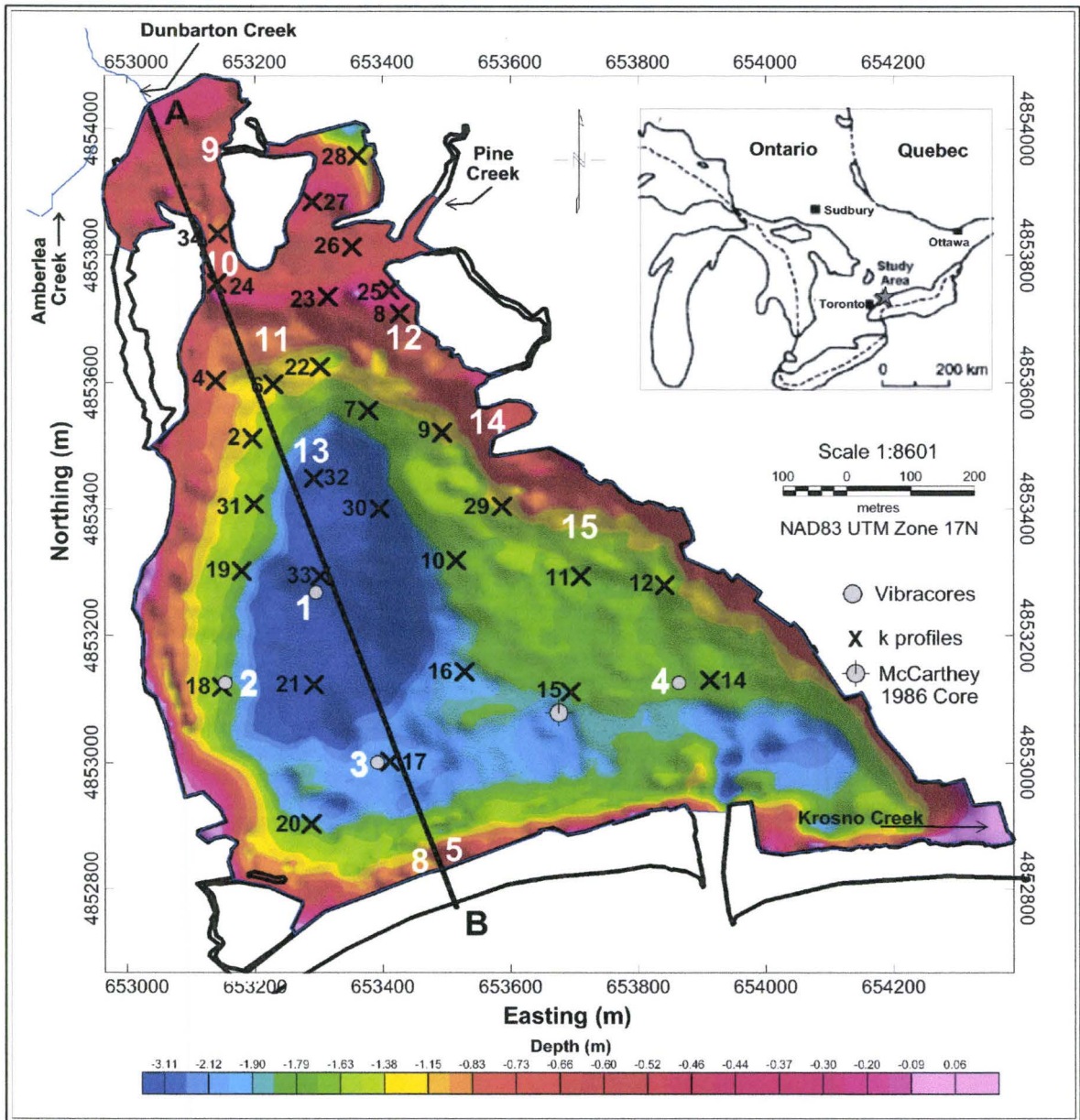


Figure 3.1: Frenchman's Bay (0.84 km²) is a shallow coastal lagoon located on the northwest shores of Lake Ontario on the eastern limits of the Greater Toronto Area. The locations of cores, magnetic susceptibility (κ) profiles and transects obtained for study are also indicated in the figure.

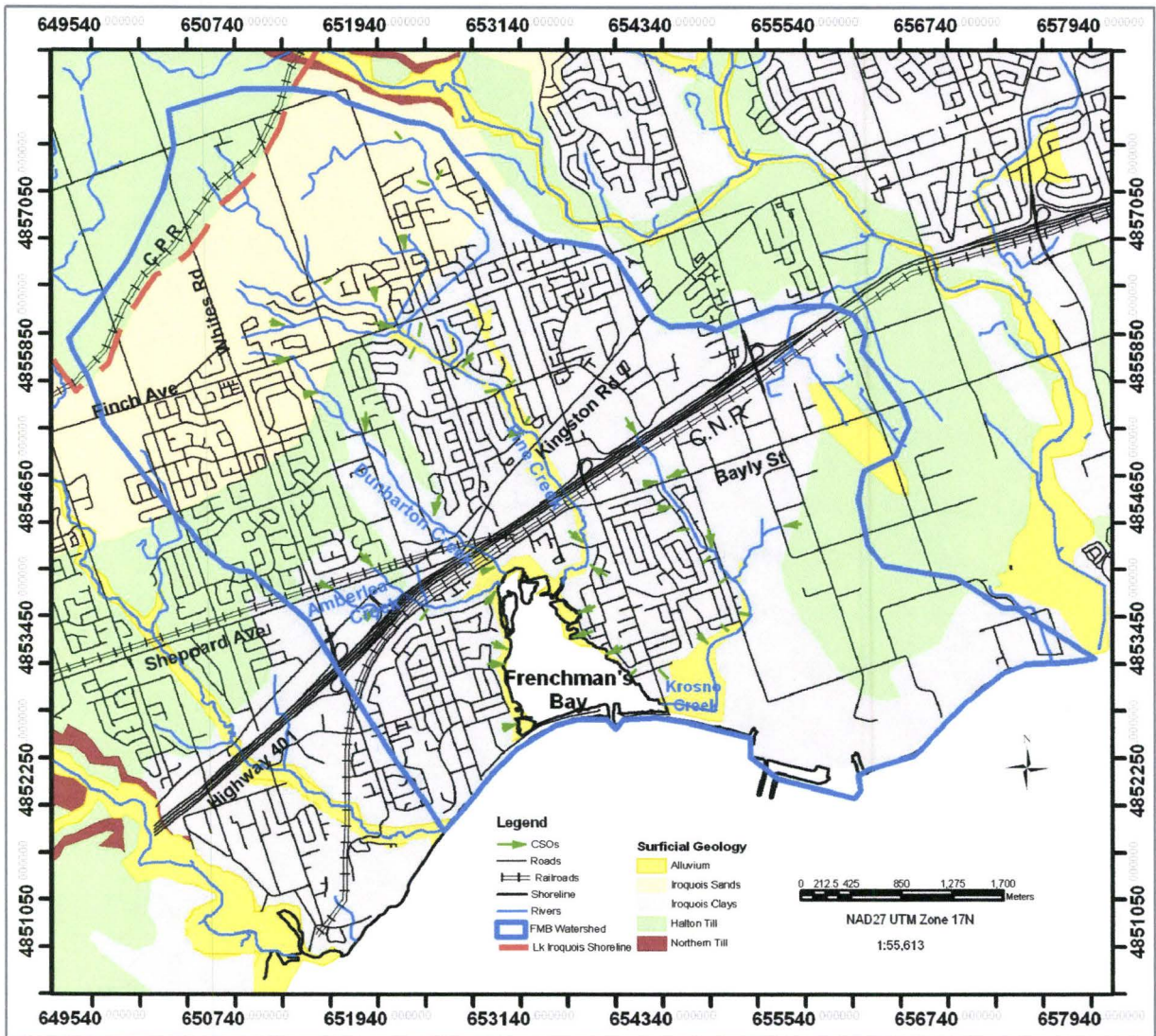


Figure 3.2: Frenchman's Bay watershed showing the extent of urban cover and main sources of urban effluents. Source data obtained from (PlantownConsultantsLtd. 1975; Eyles et al. 2002; Gerrie et al. 2003)

sedimentation rates in the lagoon (Eyles et al. 2002). Historically, Frenchman's Bay was surrounded by extensive wetlands and the once forested landscape that provided habitat and natural wildlife corridors became fragmented as settlers cleared the land for agriculture and provided opportunities for mills, inns and businesses. By 1840 50 steam ships were operating on the lake and FMB became a bustling shipping port; Docks were first built at the north end of the bay but moved one year later to the southeast side of the bay due to heavy silting (Skibicki 1991). A drop in wheat and lumber prices and the building of the Grand Trunk Railway in 1855 resulted in the decline of commercial shipping and the export trade in FMB (Skibicki 1991). It was not until the 1940s, when summer cottages were built, that more communities began to establish.

The construction of highway 401 in the late 1940's led to a rapid rise in residential development that began in 1954, which increased the area of the developed catchment from 10% to over 70% in 1978 (see inset in Figure 3.3) (Hunting 1954; Skibicki 1991). Since 1972, channelization or culverts have modified more than 50 percent of the creeks within the Frenchman's Bay watershed (Pickering 2001). Wetlands have retreated substantially during the past 100 years due to declining water quality and rising water levels (~ 20 cm / 100 years at present) (Eyles and Chow-Fraser 2003). By 1990 only 38% of the wetland area present in 1954 remained, and has continued to decrease as shown in Figure 3.3 (Nelson et al. 1991). In 1968 half of the wetland next to the Pickering Nuclear Generating Station was infilled to create open park space (Skibicki 1991). With a reduction of wetlands, incoming suspended sediment and bedload from

the creeks was able to travel farther into the lagoon. This change in the basin hydrology was an important factor in elevating sedimentation rates within the lagoon.

Geology

Frenchman's Bay was formed between 3000 to 4000 ybp during a period of more rapid lake level rise associated with a phase of the cooler, wetter Neoglacial climate in Southern Ontario (Eyles et al. 2002). The bay was created as the lower reaches of a paleoriver valley were flooded, and was later transformed into a lagoon when a barrier beach formed across the mouth due to longshore drift. Longshore drift from the east continues to deliver sediment to the beach barrier and mouth of the harbour today (Greenwood, 1987).

The sediments within the bay consist of succession of Late Holocene muds and organic deposits overlying post-glacial lake sediments of Lake Iroquois (Eyles 2002). The Lake Iroquois deposits in turn rest on Late Wisconsin glacial sediments (Halton till) and underlying Paleozoic shale bedrock (Whitby Formation). Radiocarbon dating of peats from the base of the lagoon sequence yielded an age of 2750 YBP, indicating a Late Holocene age for the initial formation of the lagoon McCarthy (1986).

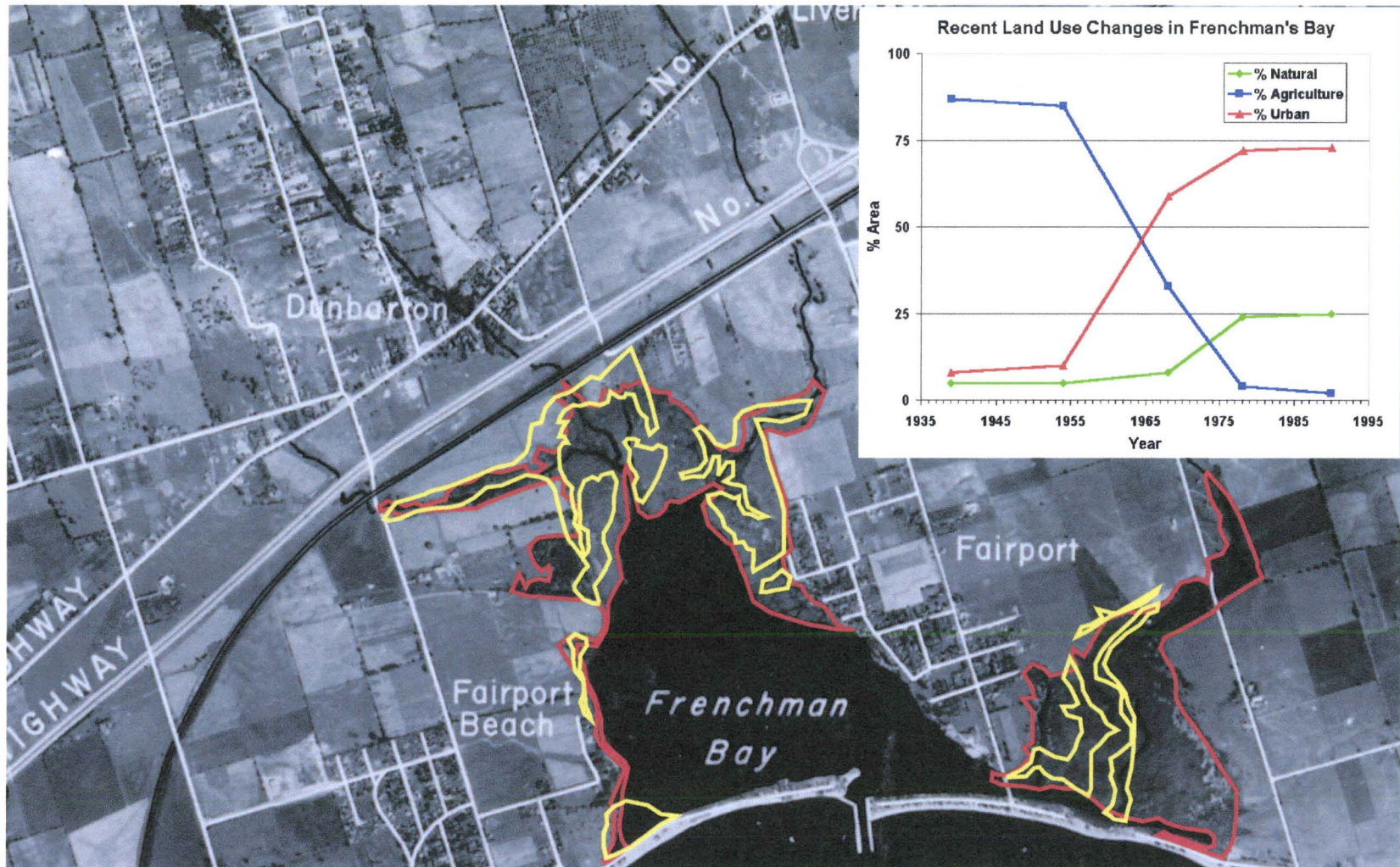


Figure 3.3: A number of transgressive shoreline positions and changes in wetland extent and land use (see inset) in the Frenchman's Bay area are shown on the earlier 1954 aerial photograph (Photo from (Hunting 1954)). Red = 1954 wetland and shoreline position, Yellow = 1995 wetland and shoreline position.

3.3 Methods

3.3.1 Coring

Eleven cores were obtained from Frenchman's Bay in September 2002 using a vibracoring apparatus that employed approximately 20' long 3" diameter aluminium irrigation tubes. The uncompacted lengths of each core were determined based on field measurements of aluminium tube length, depth to sediment surface, and total recovered core length. The locations of the core sites are indicated in Figure 3.1. The cores were split and one half was set aside as an archive while the other was used for logging and sediment analyses. When not in use, the cores are stored at a constant temperature of 0 – 3 °C to reduce microbial activity. The sediments were described visually and relevant features were recorded which include lithology, approximate grain size, sorting, framework, colour, approximate % organic matter, and sedimentary structures and/or inclusions. Weight % water, organic, carbonate and mineral content of selected sediment sub samples were determined using the method of Dean (1981).

3.3.2 Magnetic Properties

For magnetic property analysis, each core was sub-sampled using 8 cm³ cubets placed at 2 cm along the core. Bulk magnetic susceptibility (χ) was determined by measuring the volume magnetic susceptibility (κ) and mass of each cubet, then using the equation: χ (10⁻⁸ m³/Kg) = κ (10⁻⁵ SI) * cubet volume (10⁻³ m³) / sample mass (Kg). The sample volume magnetic susceptibility (κ) was measured using a Bartington Instruments MS2 meter with a type MS2C sensor, after the cubets had equilibrated with room

temperature. An air measurement was made prior to and following each sample measurement to correct for instrumental drift. The mass of each cubet was measured on an analytical balance to 6 significant digits.

The intensity, inclination and declination of the natural remanent magnetism (NRM) for each cubet sediment sample was measured using a Molspin 1A magnetometer. The saturation isothermal remanence (SIRM) was measured for each sediment sample with the Molspin 1A magnetometer after a forward field of 1 Telsa was applied using a Molspin 1T pulse magnetizer. After SIRM was induced, the remanence of coercivity (Bcr) value was determined for each cubet sample as the x-intercept in a plot of applied backfields (10, 20, 30, 50, 100, 200, and 300 mT) versus IRM values obtained after each backfield application. The SIRM/ χ ratio was calculated using density corrected SIRM values and bulk magnetic susceptibility values. The S-ratio (SIRM/IRM_{100 mT}) was calculated using the SIRM and IRM_{100 mT} values for each cubet sample. Percent frequency dependence of magnetic susceptibility ($\chi_{fd\%}$) was determined by measuring volume susceptibility of each cubet sample at both low (0.46 kHz) and high (4.6 kHz) frequency, then employing the equation: $\chi_{fd\%} = ((\chi_{lf} - \chi_{hf}) / \chi_{lf}) \times 100$. At least 15 measurements at both the high and low frequencies were taken for each sediment sample since for the lower magnetic susceptibility values observed in the middle of the core the instrument drift can be a significant contributor to the signal.

An inexpensive proto-type probe was constructed using a Bartington MS2-F sensor mounted in waterproof housing with an extendable 10 m handle to obtain near

continuous in-situ measurements of sediment volume susceptibility (κ). The probe was employed in Frenchman's Bay to aid in lithologic correlations and to quickly measure the thickness and distribution of a post-colonial sediment layer that is heavily impacted by urban contaminants (Eyles et al. 2002). Volume susceptibility profiles were collected at 35 locations by driving the probe up to 2.5 m into the lagoon bottom sediments at 2 cm measurement intervals. Three minutes of air measurements were taken before and after the profiles were measured so that instrument drift corrections could be made base on the trend of the drift from the air measurements. The location of Frenchman's Bay and magnetic susceptibility profiles are shown in Figure 3.1.

3.3.3 Chronology

^{210}Pb dating was performed on a single core (FMB1) to provide estimates of sedimentation rates and ages in the upper 1 m of the core. ^{210}Pb methods can typically provide dates for the last 100-150 years and was employed in this study to provide age constraints on distinctive stratigraphic and magnetic property horizons in the core to the historical record of colonization in Frenchman's Bay. ^{210}Pb dates were obtained on 1 g dried samples of sediment over the 1 m upper portion of FMB1 according to the methods of Cornett and Lardner (2004) (see Section 1.3.2).

3.3.4 ESEM and XRD

Approximately 2 cm³ of sediment was sampled at strategic points of interest along the core for ESEM and XRD analyses. The samples were first treated with 10% HCl and then peroxide in warm water to remove organic matter and carbon (section 1.3.2). For

each sample the grains were separated into two grain size fractions ($> 63 \mu\text{m}$ and $\leq 63 \mu\text{m}$) using wet sieves. The samples were then left to air dry inside enclosed (to prevent contamination) plastic sample Petri-dishes so that magnetic particles could be separated using a hand magnet. Magnetic grains larger than $63 \mu\text{m}$ could be separated using a hand magnet, but the fraction of grains smaller than $63 \mu\text{m}$ could not be separated possibly due to static and/or cohesive forces. Therefore individual magnetic grains were identified and selected that were $> 63 \mu\text{m}$, but a homogenous representative sample had to be used from the $\leq 63 \mu\text{m}$ fraction.

The samples were mounted on aluminium scanning electron microscope stubs coated with a 1:1 colloidal graphite and glue solution and were placed in the environmental scanning electron microscope (ESEM) to acquire grain specific images and for elemental analysis according to the methods described by Schultes (2004). The elemental composition of the grains or areas of interest was determined using X-ray diffraction (XRD) in conjunction with the ESEM.

3.4 Results

The logs were subdivided into four magnetostratigraphic units on the basis of lithology, magnetic parameters, and carbon content. Figure 3.4 to Figure 3.7 display the sediment logs for cores FMB1, FMB2, FMB3 and FMB4 along with their accompanying graphs of χ , κ , NRM, SIRM, Bcr, SIRM/ χ , S-ratio, $\chi_{fd}\%$, weight percent organic carbon, calcium carbonate and mineral content. The stratigraphic succession in the lagoon consists of a thick upper sequence of marly gyttja and organic-rich silty muds overlying Holocene

organic-rich discontinuously laminated marls above sandy clays with moderate carbonate content and elevated mineral and magnetic susceptibility values and is interpreted as pre-colonial late Holocene muds.

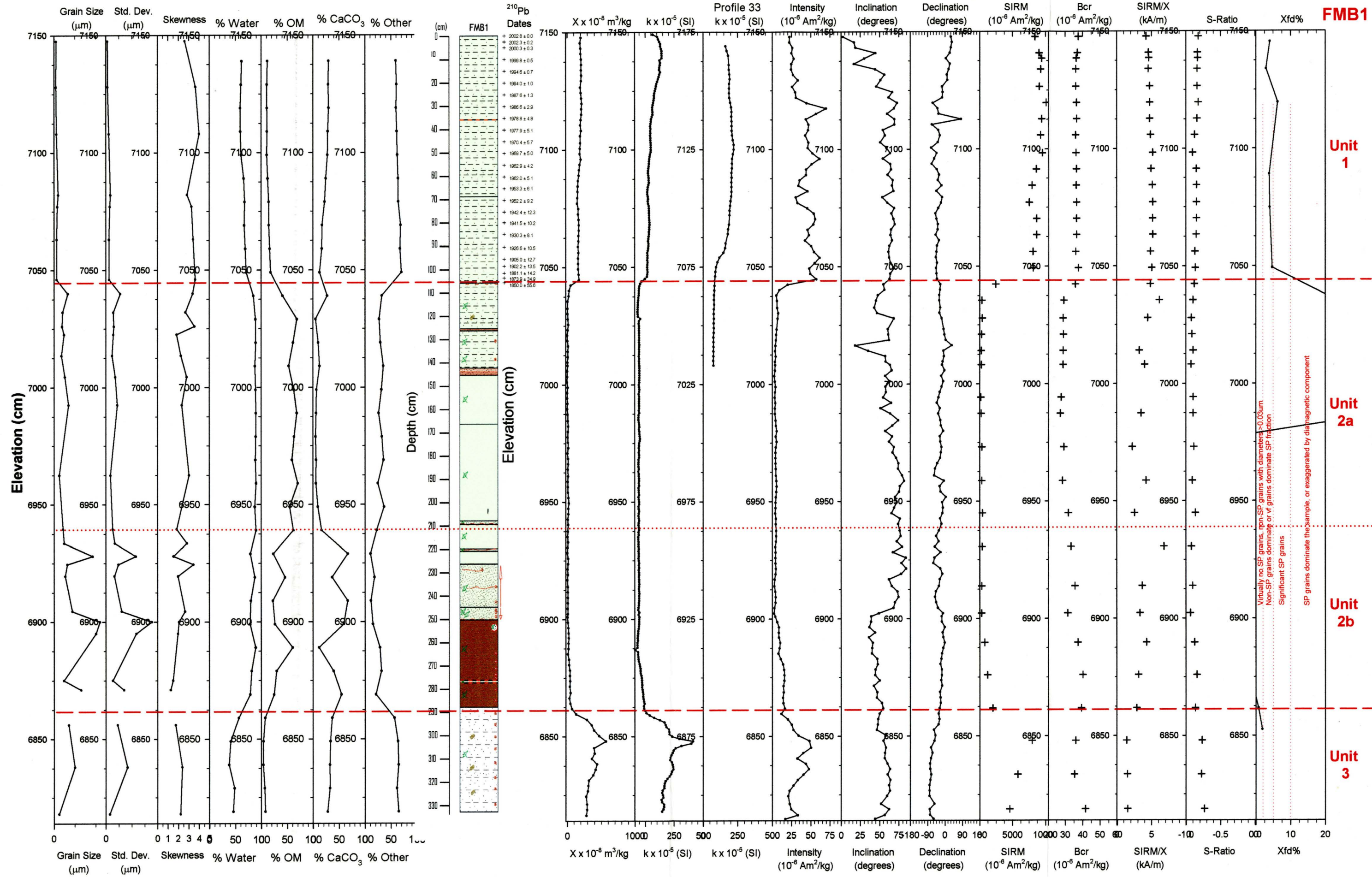
3.4.1 Lithology

Unit 1

The first unit consists of gyttja with variable amounts of fine sand to clay content that is influenced by the proximity to shoreline areas. The amount of water in the sediment varies between 60% to 80% of the total core mass, while the organic matter content remains below ~ 10%, the carbonate content gradually increases towards the top of the sediment column until maximum levels of ~25% are reached, and the remaining mineral content is 55% to 70%. Sediments near the beach barrier have fine sand to medium silts suspended in the gyttja matrix, areas near the medial edges of the lagoon have silts suspended in a gyttja matrix with ample carbonate nodules and some leaf fragments, sediments in the deepest regions of the lagoon have fine silts mixed with the gyttja matrix, while sediments in the northern shallow reaches of the lagoon demonstrate a general fining upwards sedimentary succession in cores FMB9 through to FMB10, FMB11, and FMB1 in the middle of transect AB (see Figure 3.1). The cores also demonstrate a fining outwards succession from FMB9 to FMB1 that combined with the fining outwards succession mentioned above is indicative of a (primitive) delta sequence.

Figure 3.4: The lithologic log for core FMB1 along with data for sediment and magnetic parameters used to identify four distinct units in Frenchman's Bay. Weight percent water, organic content, calcium carbonate and mineral content are indicated in the first four graphs. The lithologic log with relevant structures and dates obtained from ^{210}Pb radiometric dating is shown next. Then the in-situ volume magnetic susceptibility (κ) data from field profile #33 is shown next to the laboratory measured volume magnetic susceptibility data from core FMB1 since they were obtained in similar locations. The remainder of the magnetic parameters shown (χ , NRM, SIRM, Bcr, SIRM/ χ , S-ratio, $\chi_{fd}\%$) were measured using the cubet subsamples. These last magnetic parameters were bulk magnetic susceptibility (χ), the intensity, inclination and declination of the natural remanent magnetism (NRM), the saturation isothermal remanent magnetism (SIRM), the coercivity of remanence (Bcr), and the three ratios SIRM/ χ , S-ratio (IRM-100mT/SIRM), and the percent frequency dependence of magnetic susceptibility ($\chi_{fd}\%$).

*Larger copies of the lithologic logs are available in Appendix C: .



Virtually no SP grains, non-SP grains with diameters > 0.05 µm.
 Non-SP grains dominate or of grains dominate SP fraction.
 Significant SP grains
 SP grains dominate the sample, or exaggerated by diamagnetic component

Figure 3.5: The lithologic log for core FMB2 along with data for sediment and magnetic parameters used to identify four distinct units in Frenchman’s Bay. Weight percent water, organic content, calcium carbonate and mineral content are indicated in the first four graphs. The lithologic log with relevant structures and dates obtained from ^{210}Pb radiometric dating is shown next. Then the in-situ volume magnetic susceptibility (κ) data from field profile #14 is shown. The inclination and declination of the natural remanent magnetism (NRM) was measured using the cubet subsamples.

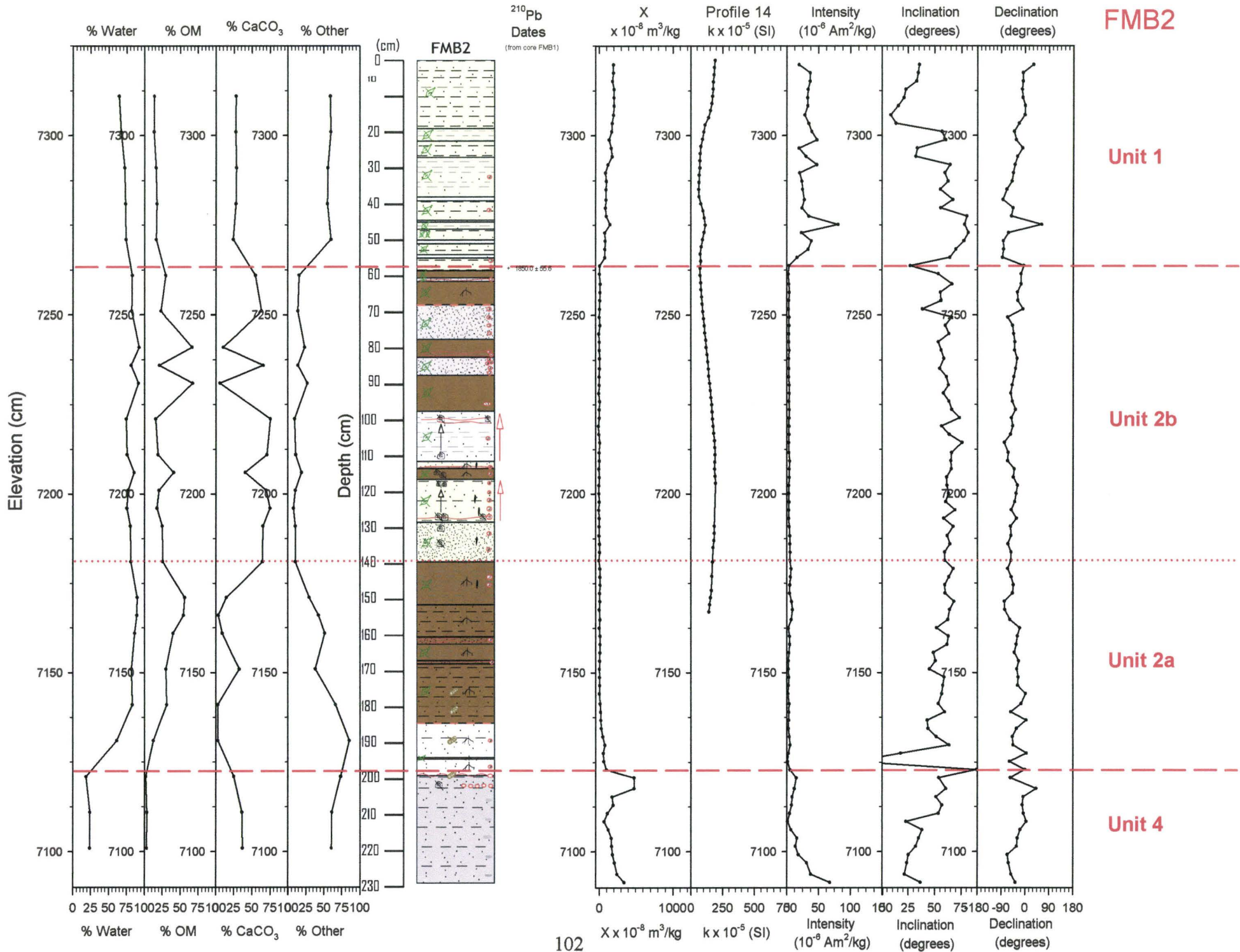


Figure 3.6: The lithologic log for core FMB3 along with data for sediment and magnetic parameters used to identify four distinct units in Frenchman’s Bay. Weight percent water, organic content, calcium carbonate and mineral content are indicated in the first four graphs. The lithologic log with relevant structures and dates obtained from ^{210}Pb radiometric dating is shown next. Then the in-situ volume magnetic susceptibility (κ) data from field profile #17 is shown. The inclination and declination of the natural remanent magnetism (NRM) was measured using the cubet subsamples.

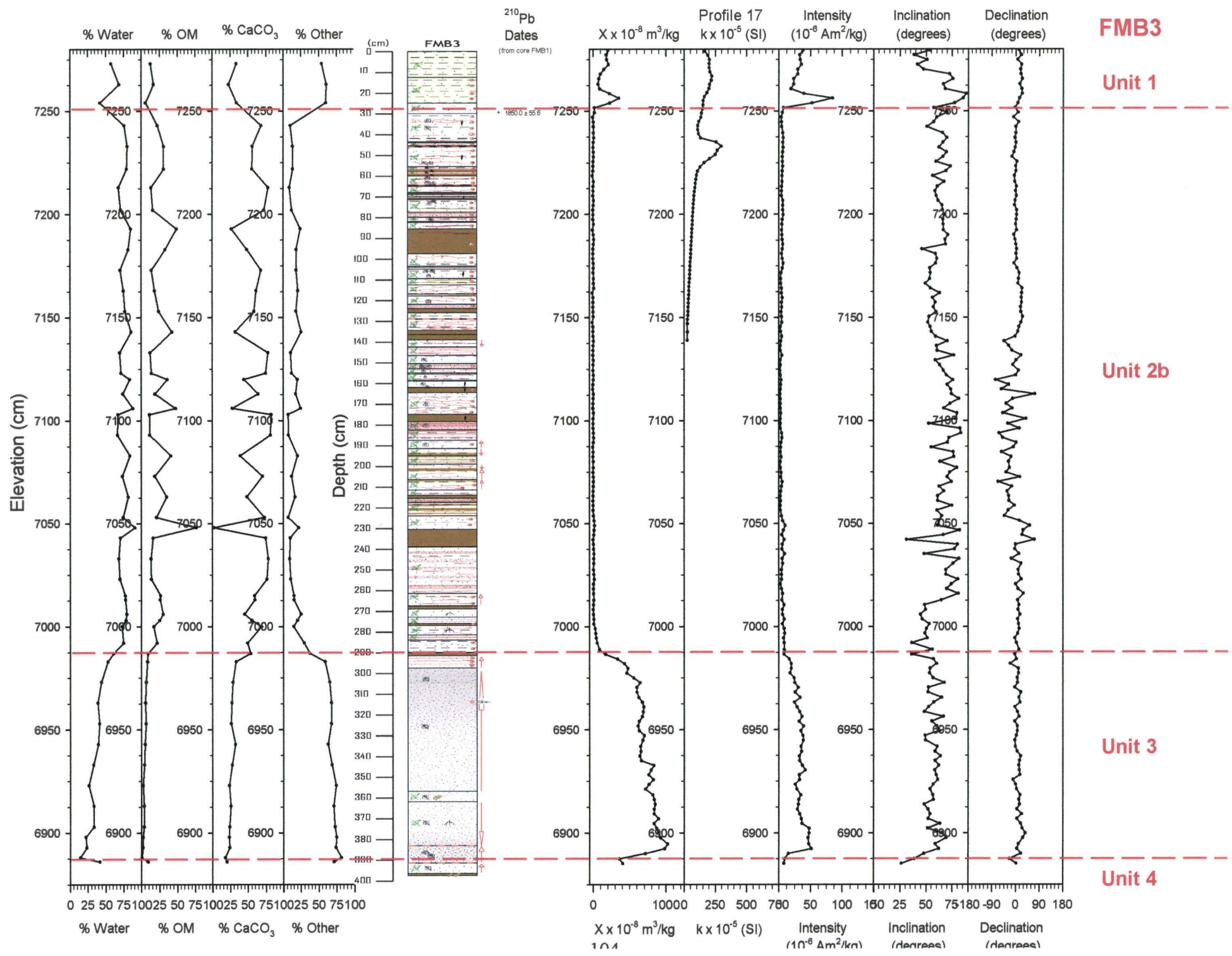
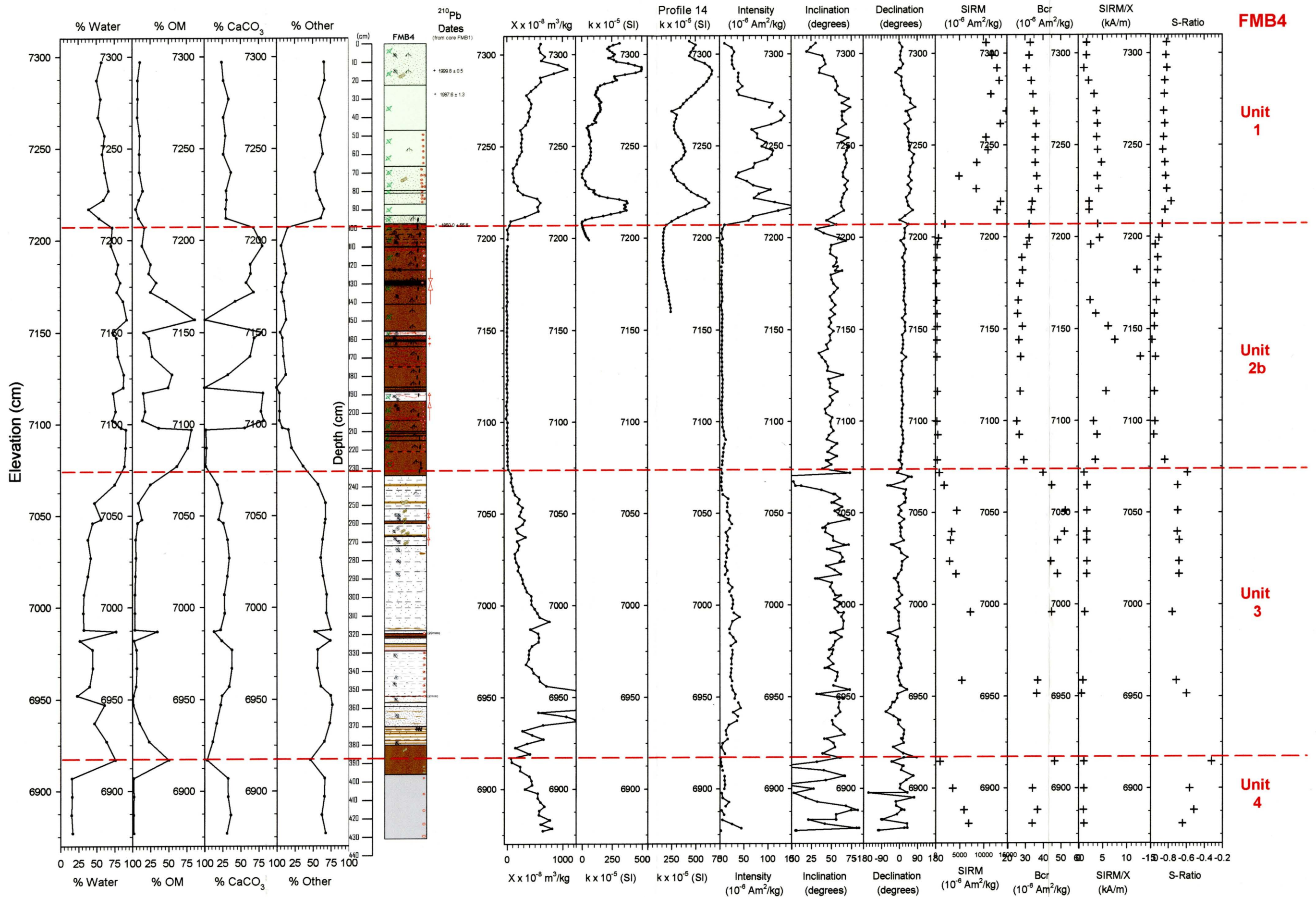


Figure 3.7: The lithologic log for core FMB4 along with data for sediment and magnetic parameters used to identify four distinct units in Frenchman’s Bay. Weight percent water, organic content, calcium carbonate and mineral content are indicated in the first four graphs. The lithologic log with relevant structures and dates estimated from ^{210}Pb radiometric dating conducted on core FMB1 is shown next. Then the in-situ volume magnetic susceptibility (κ) data from field profile #14 is shown next to the laboratory measured volume magnetic susceptibility data from core FMB1 since they were obtained in similar locations. The remainder of the magnetic parameters shown (χ , NRM, SIRM, Bcr, SIRM/ χ , S-ratio, $\chi_{fd\%}$) were measured using the cubet subsamples. These last magnetic parameters were bulk magnetic susceptibility (χ), the intensity, inclination and declination of the natural remanent magnetism (NRM), the saturation isothermal remanent magnetism (SIRM), the coercivity of remanence (Bcr), and the two ratios SIRM/ χ and S-ratio ($\text{IRM}_{100\text{mT}}/\text{SIRM}$).



Unit 2

The second unit consists of beige-coloured sandy marls with brown organic laminations that were interbedded with peat marls. The carbonate content of the organic laminated sandy marls ranges from 60 % to 80 % with approximately 20 % organic matter content for all areas except for the deepest regions where organic content was ~50 % and carbonates reached a maximum of 10 %. The amount of water in the sediment varies between 70% to 90% of the total core mass, while the mineral content made up 55% to 70% of the dry sediment mass. These organic laminated sandy marl layers commonly contained abundant gastropods, leaf fragments, and discontinuous laminae structures. The carbonate content for the layers of peat marls ranges from 10 % to 40 % with organic matter content ranging from 50 % to 85 %. These peat marls also contained rootlets, seeds, and occasionally abundant leaf fragments. McCarthy (1986) identified the initial presence of *Ambrosia* pollen (a colonization indicator) at a depth of 1.12 m. Angular microscopic green glass fragments were discovered in cores FMB1 at a depth of 200-201 cm and in FMB2 at a depth of 180-182 cm (Little et al. 2004). Red glass fragments (2) were discovered in core FMB1 at a depth of 140 cm.

Unit 3

The third unit consists of fine sandy clay to silty sand with moderate (20 % to 40 %) carbonate content and minimal (below 5 %) organic matter content. Water content in the sediment varies between 20% to 60%, while mineral content ranged from 45% to

80% of the total dry sediment mass. Occasional gastropods are found in littoral sediments while wood and leaf fragments can also be found.

Unit 4

The lowermost unit consists of carbonate-rich compacted silty clay with gravel to cobble size clasts and no organic matter (< 2 %). The water content of the sediment was ~17% of the total core mass, while mineral content of the dry sediment ranged from 60% to 70%. There is an erosional surface present at the surface of this unit, and a pebble and gravel lag at the unit surface in core FMB2.

3.4.2 Chronology

²¹⁰Pb dating was performed on a single core (FMB1) to provide estimates of sedimentation rates and ages in the upper 1 m of the core. The ²¹⁰Pb dating provided dates extending back to 1850 (±55.6) for core FMB1 (indicated on Figure 3.4). Sediment accumulation rates were also determined (see Figure 3.8) and an order of magnitude increase in sediment accumulation rates was noted since the onset of industrialization.

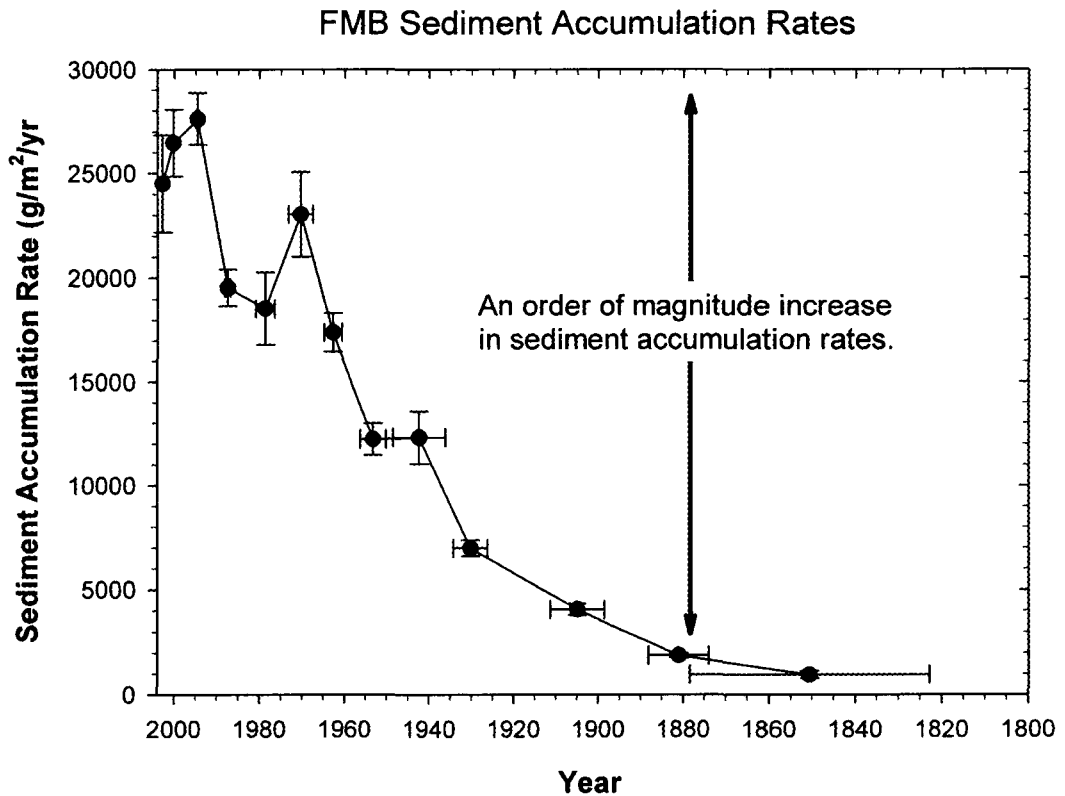
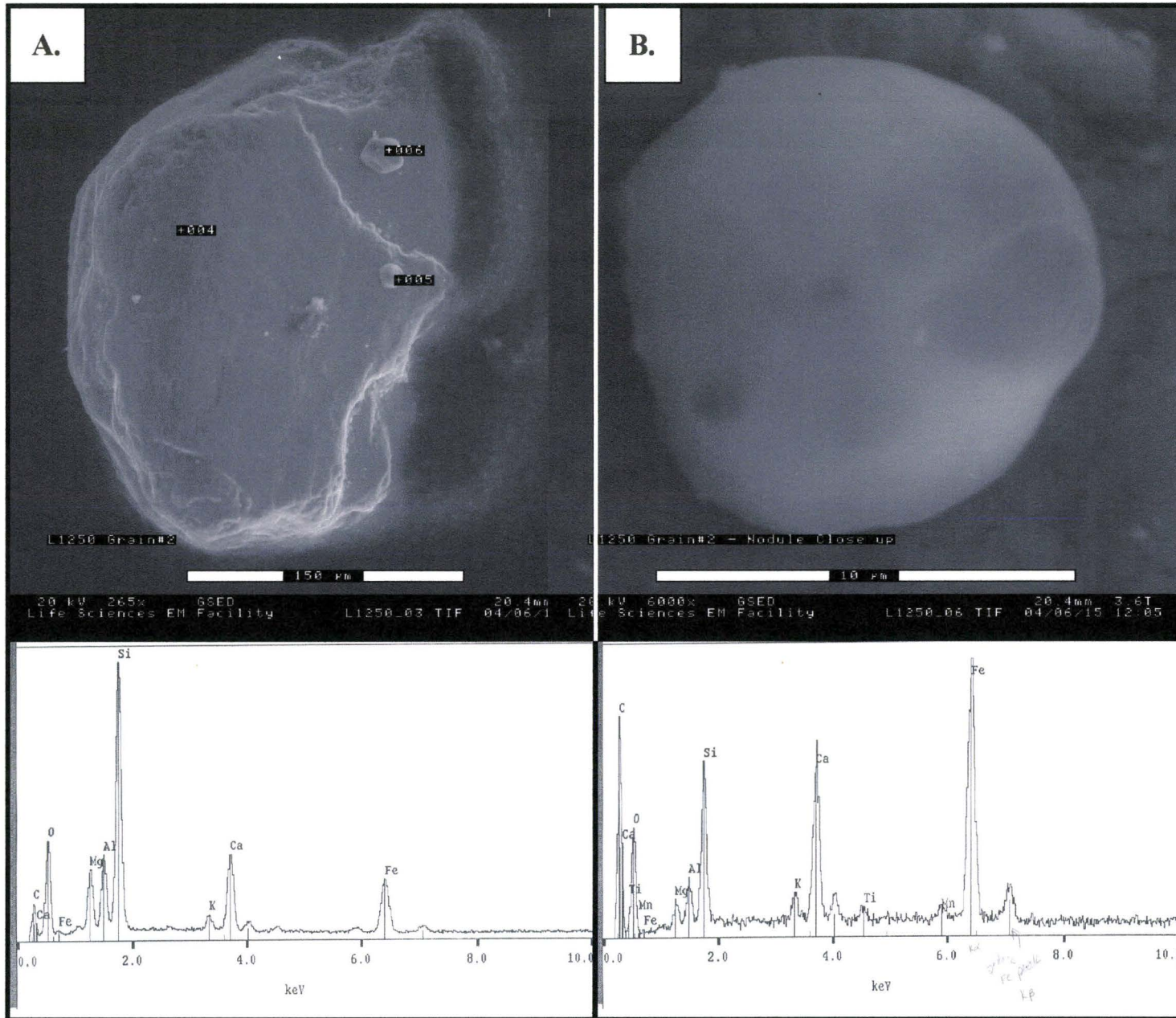


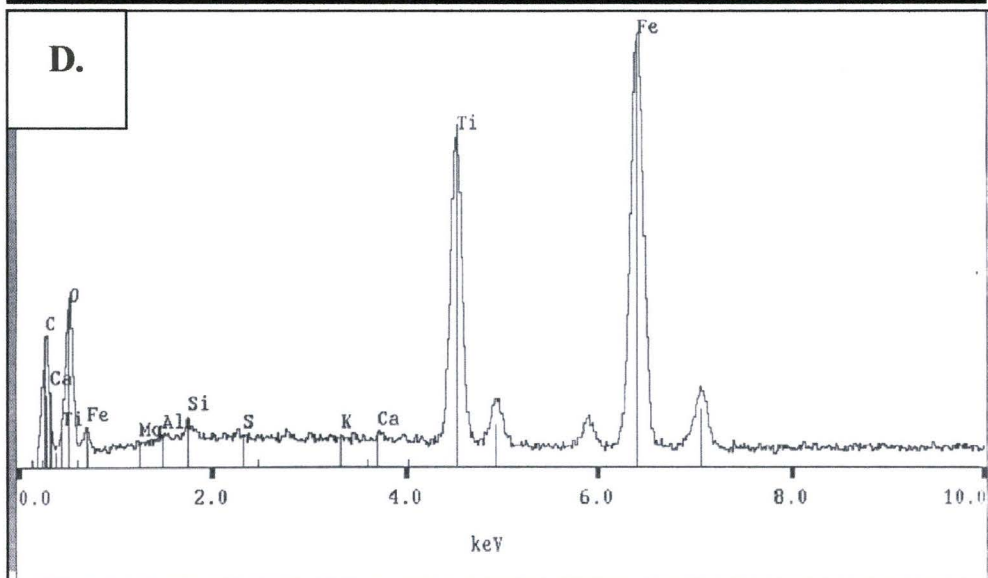
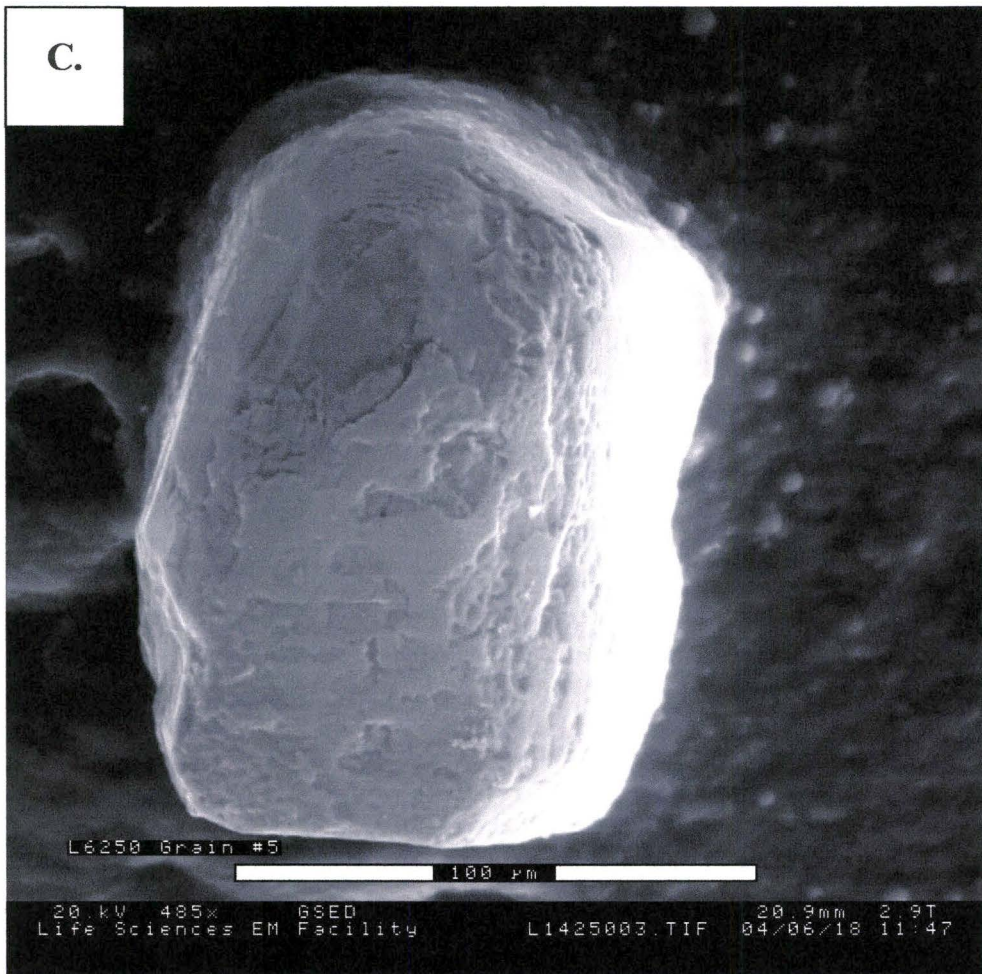
Figure 3.8: Sediment accumulation rates determined for Frenchman's Bay from ^{210}Pb analysis.

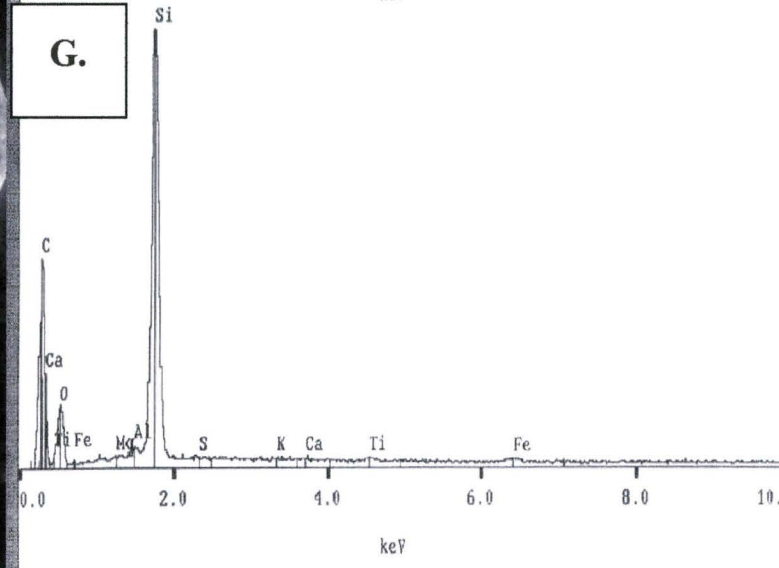
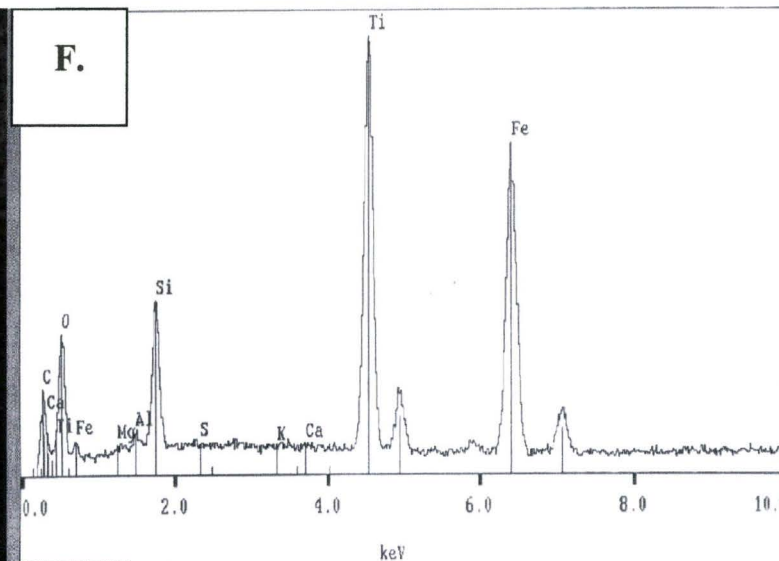
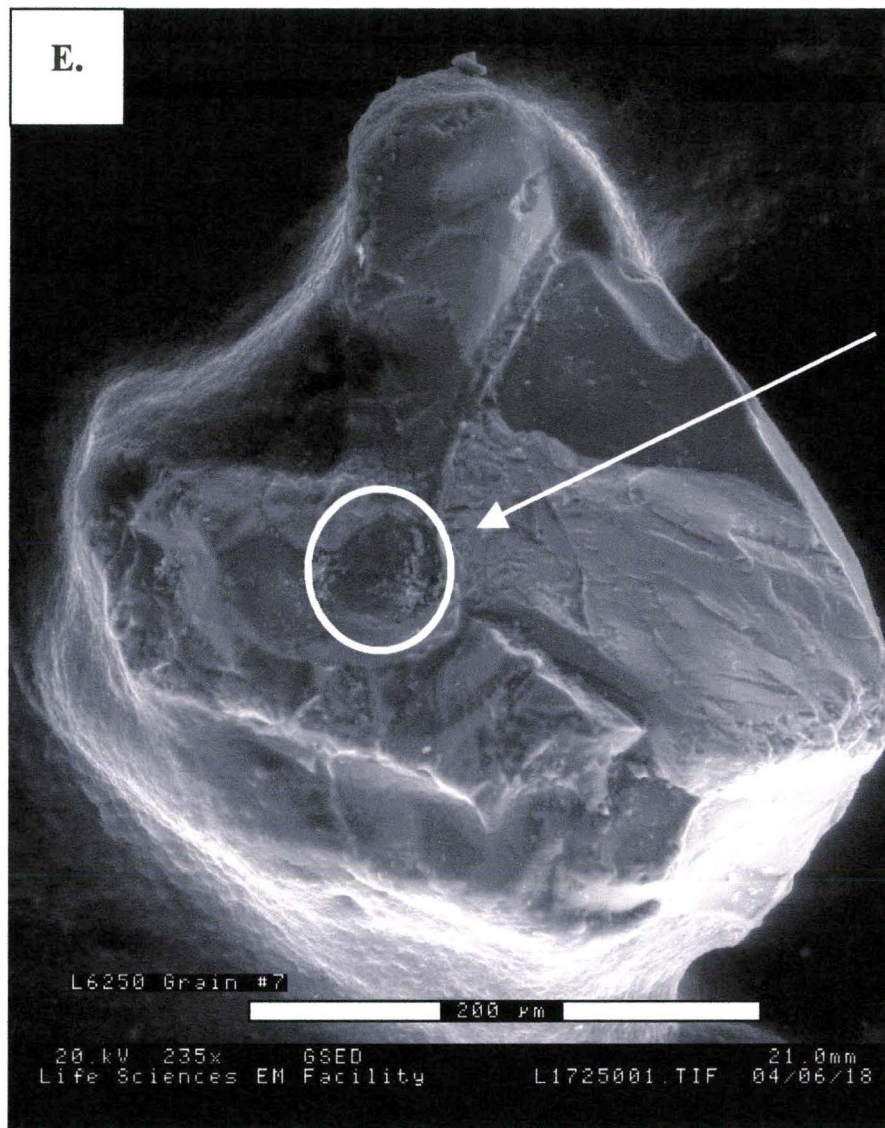
3.4.3 ESEM and XRD

The magnetic mineralogy results discussed below are supported by ESEM and XRD data, which show abundant titanomagnetite and magnetite grains within Unit 1. Figure 3.8 shows an ESEM image of a large ($>250\ \mu\text{m}$) subangular magnetite grain at unit 1 was identified as magnetite contained within an aluminosilicate matrix from the XRD spectrum (see Figure 3.9 for the ESEM image and XRD spectrum). A ~ 10 micron well-rounded iron-silicate spherule was found resting on the first grain which is indicative of atmospheric spherules

Figure 3.9: Images and XRD spectra of grains found in units 1 and 2. A. ESEM image of a large (>250 μm) subangular magnetite grain found in unit 1 with XRD spectrum that shows that the magnetite is contained within an aluminosilicate matrix. B. ESEM image of a ~10 micron well-rounded iron-silicate spherule that was resting on the grain shown in A (location identified by the label +005) with XRD spectra. C. ESEM image of a large (>250 μm) rounded magnetic mineral grain found in unit 2. The XRD spectrum for the magnetic mineral identifies it as titanomagnetite. D. ESEM image of a large (>250 μm) subangular silica grain with a ~30 micron diameter magnetic mineral inclusion indicated by the white circle. E. The XRD spectrum for the magnetic mineral inclusion identifies it as titanomagnetite. F. The XRD spectrum for the silica grain.





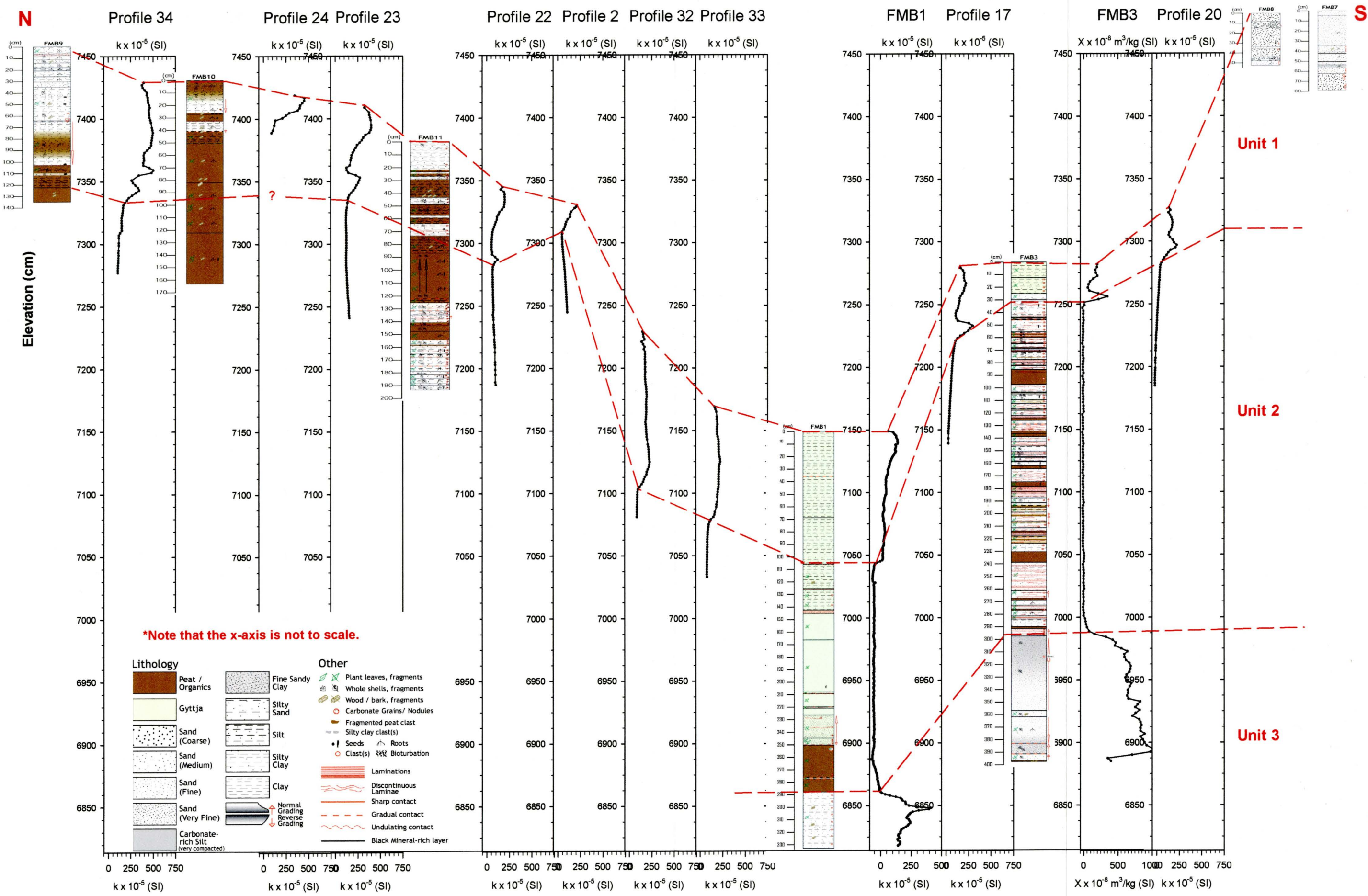


produced during combustion processes. A large (>250 μm) rounded magnetic mineral grain was also found in unit 2. The XRD spectrum for the magnetic mineral identifies it as titanomagnetite. A large (>250 μm) subangular silica grain with a ~ 30 micron diameter magnetic mineral inclusion was also found. The XRD spectrum for the magnetic mineral inclusion identifies it as titanomagnetite, while the XRD spectrum identifies the larger grain as silica.

3.4.4 Magnetostratigraphy

The magnetostratigraphic units identified in core data were mapped across the lagoon as series of profiles. Figure 3.10 shows a representative north-south transect of κ profiles and lithologic logs along the line AB (Figure 3.1) to demonstrate the use of κ profiles in conjunction with the information obtained from the sediment cores to quickly identify units of similar lithology. The base of the post-colonial sediment layer was identified by an abrupt κ increase of $50\text{-}100 \times 10^{-5}$ SI at a sediment depth of 0.5-1.2 m. This marker horizon was correlated across the lagoon and the thickness and geometry of the anthropogenic layer was determined. The maximum 1.2 m thickness of the anthropogenic layer was identified in each κ profile by noting the depth at which the $50\text{-}100 \times 10^{-5}$ SI increase in κ occurred. These anthropogenic layer thickness data were then plotted as an isopach map in Figure 3.11 A to further identify its geometry. The total volume of the post-colonial sediment layer was calculated from the isopach map and was determined to be $3.98 \times 10^5 \text{ m}^3$ with unit thickness ranging from 0.14 m to 1.2 m. The anthropogenic layer existed as a plume of sediment that was thickest at the base of

Figure 3.10: A north-south transect showing correlated sediment facies and magnetic properties. Location of the transect is shown in Figure 3.1.



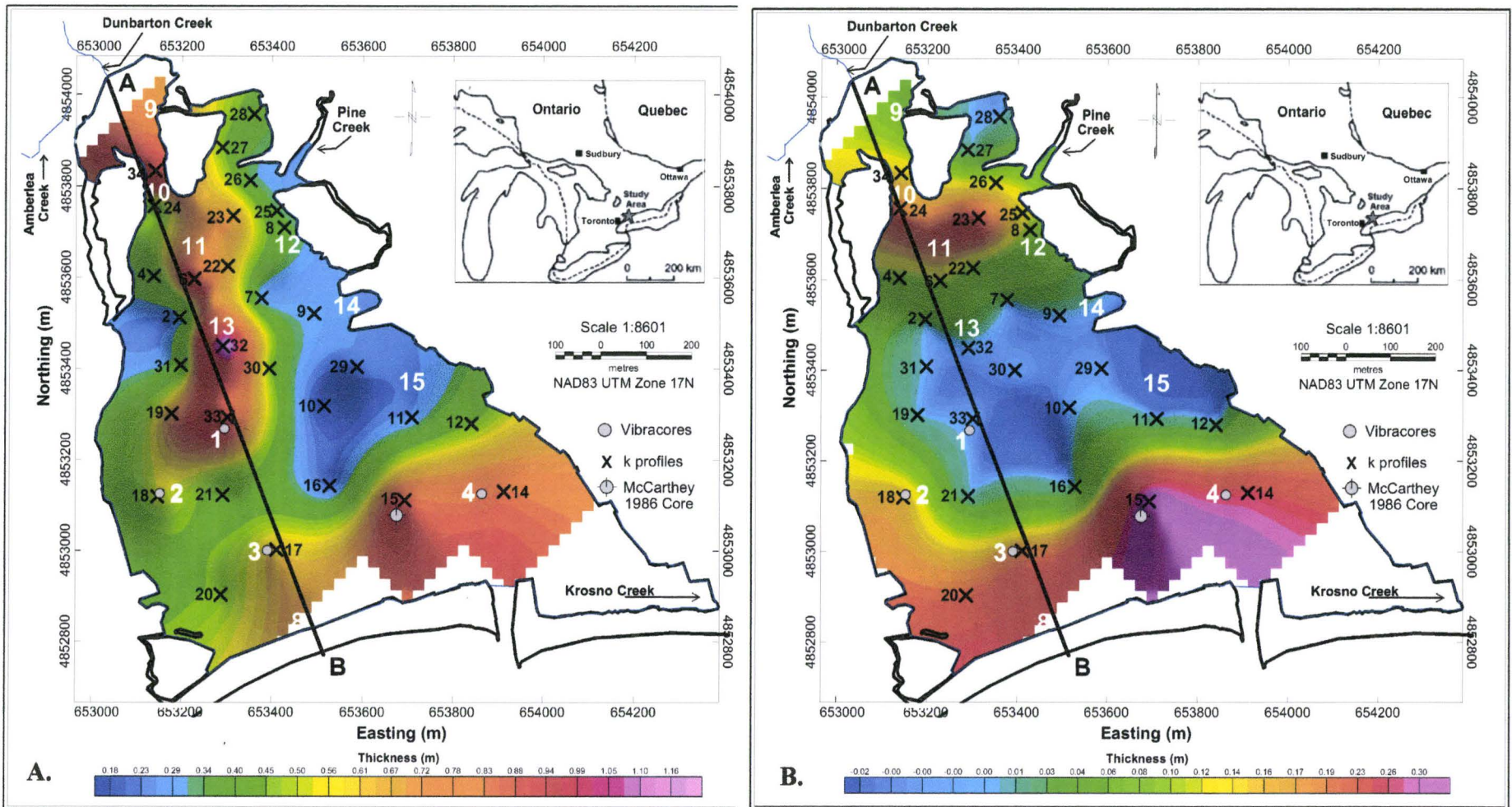


Figure 3.11: Isopach maps of A. the post-colonial sediment layer in Frenchman's Bay, and B. the location of sand and storm overwash sediments from the modern and possibly relict beach barriers.

Amberlea and Dunbarton creeks and thinned out into a bird's-foot lobed shape towards the centrally deep area of the lagoon. It was also noted that there was another shorter wavelength (8-20 cm) high intensity ($100-500 \times 10^{-5}$ SI) κ peak at depths below the post-colonial layer of ~25 cm in the north and ~5 cm to the south, but these peaks were not continuous across the lagoon. Investigation of the geometry of the signal from the isopach map (Figure 3.11 B) and the core sediments at the shorter wavelength high κ peak positions revealed that these peaks correspond to sandy and sandy silt layers in core and may represent overwash from a relict beach barrier deposit to the north, while the other signal correlates with the modern beach barrier to the south indicating that these higher κ sediments may be from storm overwash or drift from the open channel. The total volume of these potential barrier overwash sediments was calculated from the isopach map and was determined to be 9.56×10^4 m³ with unit thickness ranging from 0.02 m to 0.35 m.

3.4.5 Magnetic Properties

Magnetic Susceptibility

The magnetic susceptibility profiles (κ and χ) have a similar shape to the profiles identified by Versteeg et al. (1995) in Hamilton Harbour for urban sediments. Sediments in Unit 1 have elevated values that gradually decrease until a major shift/drop of 50 to 100×10^{-5} SI (κ) or 100 to 200×10^{-8} m³/Kg (χ) is observed at the base of the unit at sediment depths of 0.5 to 1.2 m. The middle of the sequence (Unit 2) is weakly magnetic with low κ , χ and SIRM values. There is a short wavelength (6 cm to 8 cm) κ peak

superimposed on the magnetic curves in unit 2 whose amplitude decreases from 200×10^{-5} SI to 150×10^{-5} SI as you move away from the shore and beach barrier towards the north. The shorter wavelength high κ peak corresponds to sandy and sandy silt layers in core and was observed at an average sediment depth of 50 cm in the north while the same signature was observed at a depth of 20 cm in the south. The peak was not observed in the middle section of the lagoon. These sediments are more likely related to storm overwash events redistributing the sediments from the beach barrier than the actual beach barrier since they are not deep enough to match up with unit 3. The magnetic susceptibility values rise to the greatest values in unit 3 of 450×10^{-5} SI (κ) and 6000×10^{-8} m³/Kg (χ), and then the gradual peak in values with depth cycle occurs once again in unit 4 where values increase from 5000×10^{-8} m³/Kg to $10,000 \times 10^{-8}$ m³/Kg.

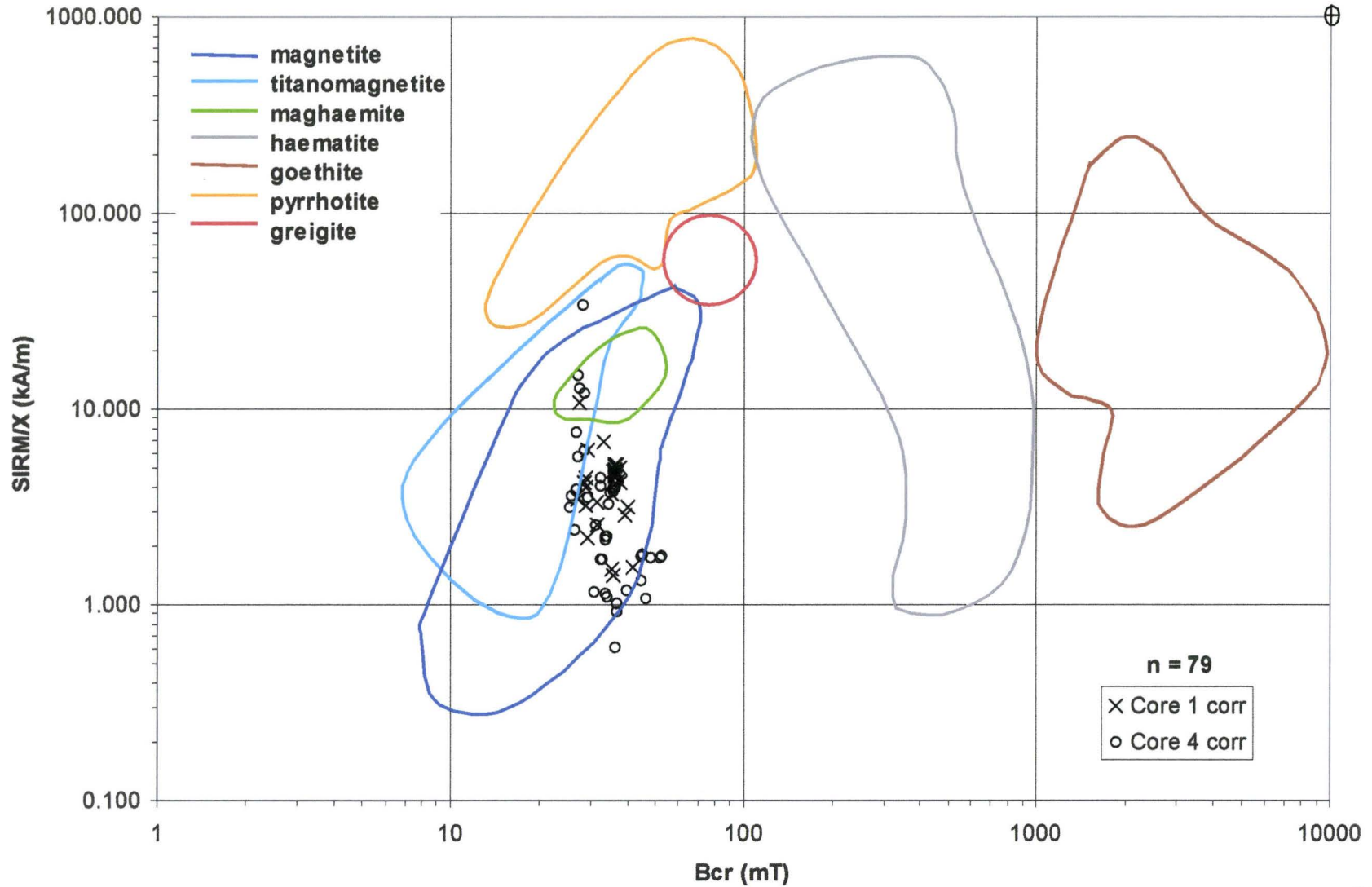
SIRM/ χ vs Bcr Biplot

A biplot of SIRM/ χ versus remanent acquisition coercivity (Bcr) for cubet subsamples from cores FMB1 and FMB4 was prepared (Figure 3.12) using the regions for magnetite, titanomagnetite, maghemite, hematite, goethite, pyrrhotite and greigite obtained from Peters and Dekkers' (2003; Fig 1) diagram that plotted data for magnetic mineral species from 16 studies. This plot identifies the dominant magnetic mineral that contributes to the magnetic signature for the sediment sample. Most of the data plot in the region for magnetite with some samples enriched in titanomagnetite, while one sample in FMB1 and two samples in FMB4 from unit 2 map in the maghaemite region.

Figure 3.12: Biplot of SIRM/ χ versus remanent acquisition coercivity (Bcr) for cubet subsamples from cores FMB1 and FMB4 using the regions for magnetite, titanomagnetite, maghemite, hematite, goethite, pyrrhotite and greigite obtained from Peters and Dekkers' (2003; Fig 1) diagram that plotted data for magnetic mineral species from 16 studies. This plot identifies the dominant magnetic mineral that contributes to the magnetic signature for the sediment sample. Most of the data plot in the region for magnetite with some samples enriched in titanomagnetite, while one sample in FMB1 and two samples in FMB4 from unit 2 map in the maghaemite region.

SIRM/X versus Bcr Plot

*Outlines of mineral species are from Peters and Dekkers (2003)



χ vs Bcr Bivariate plot

Next a bivariate plot of bulk magnetic susceptibility (χ) versus remanent acquisition coercivity (Bcr) was generated (see Figure 3.13) for cubet subsamples obtained from cores FMB1 and FMB4. This plot investigates the composition of the magnetic mineral species causing the magnetic enhancement (i.e. increase in χ , NRM and SIRM) by observing how the Bcr values change as χ increases. The data were divided according to the units identified in Figure 3.4 and Figure 3.7 based on lithology and magnetic parameters. Note that titanomagnetite has an average Bcr value of 41.4 mT while magnetite has an average Bcr value of 24.4 mT. Data from units 1, 3 and 4 from both cores generally decrease to a Bcr value of 30 mT with increasing χ , indicating that higher values of χ are related to increasing magnetite content from titanomagnetite-rich sediments. Data from unit 2 in both cores show a positive correlation between χ and Bcr values, so that the sediments become enriched in magnetically harder sediments as magnetic susceptibility increases.

S-ratio vs χ Bivariate Plot

A bivariate plot of S-ratio versus χ for cubet subsamples was generated (see Figure 3.14) from cores FMB1 and FMB4. This plot investigates the composition of the magnetic mineral species causing the magnetic enhancement (i.e. increase in χ , NRM and SIRM) by observing how the S-ratio values change as χ increases. Pure magnetite results in an S-ratio value of -1 , while contributions from harder materials increases the value of the S-ratio (i.e. away from -1). Data from unit 1 in both cores show a minor increase in

Figure 3.13: Bivariate plot of bulk magnetic susceptibility (χ) versus remanent acquisition coercivity (Bcr) for cubet subsamples obtained from cores FMB1 and FMB4. This plot investigates the composition of the magnetic mineral species causing the magnetic enhancement (i.e. increase in χ , NRM and SIRM) by observing how the Bcr values change as χ increases. The data have been divided according to the units identified in Figures 4 and 5 based on lithology and magnetic parameters. Titanomagnetite has an average Bcr value of 41.4 mT while magnetite has an average Bcr value of 24.4 mT.

X vs Bcr

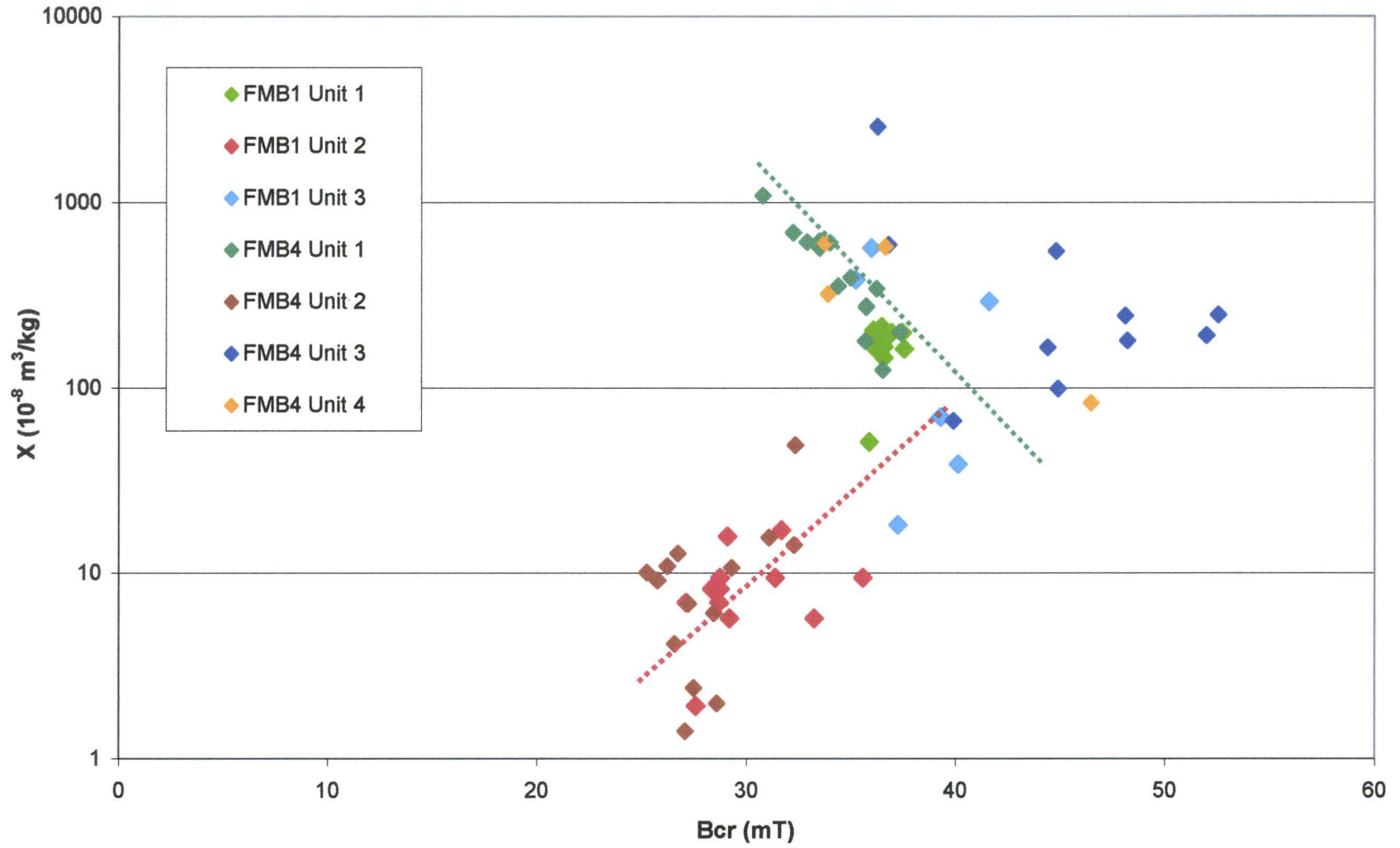
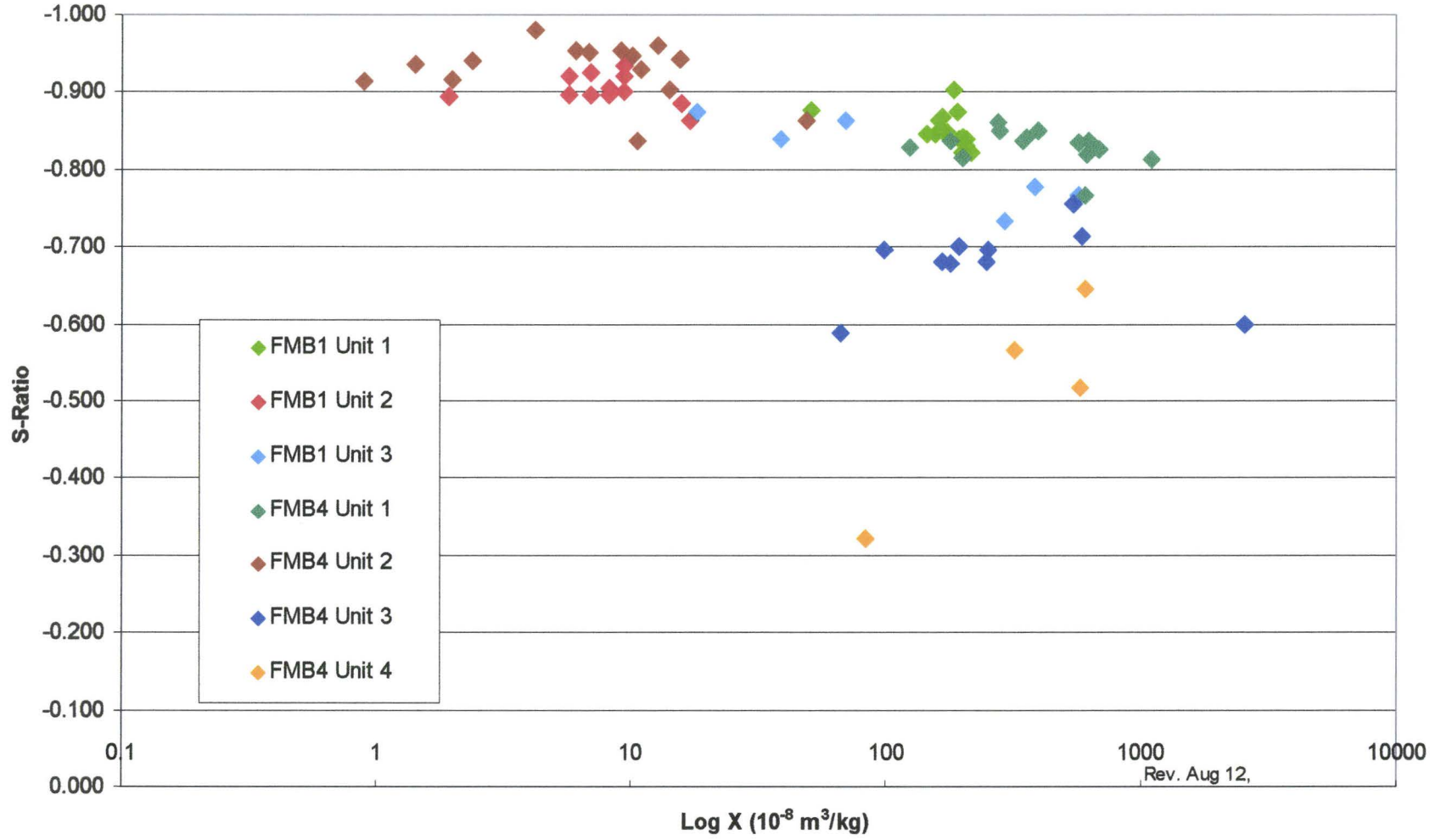


Figure 3.14: Bivariate plot of S-ratio versus χ for cubet subsamples from cores FMB1 and FMB4. The data have been divided according to the units identified in Figures 4 and 5 based on lithology and magnetic parameters. This plot investigates the composition of the magnetic mineral species causing the magnetic enhancement by observing how the S-ratio values change as χ increases. Pure magnetite results in an S-ratio value of -1 , while contributions from harder materials increases the value of the S-ratio (i.e. away from -1).

S-Ratio vs X

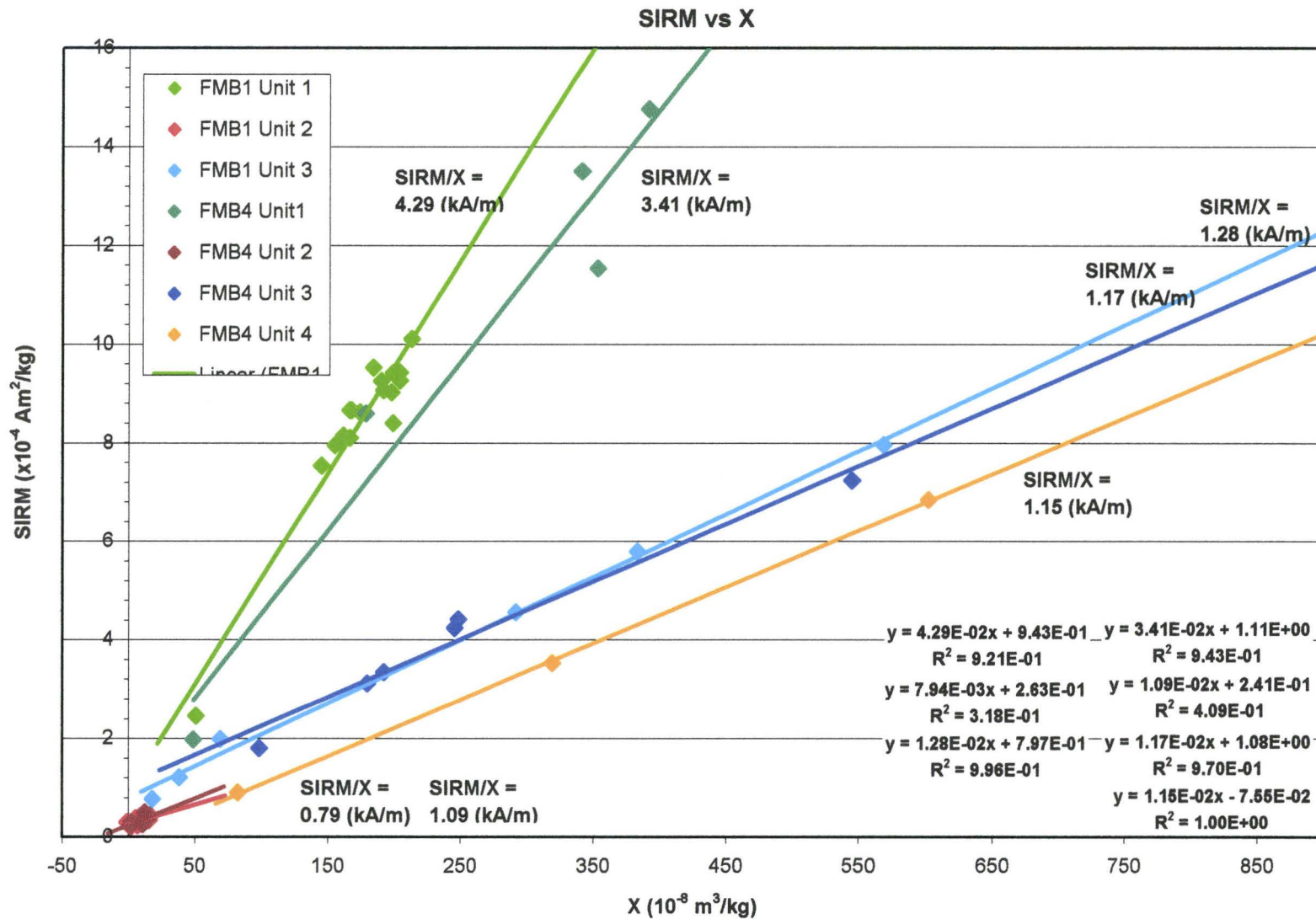


the S-ratio from -0.88 as the χ increases, therefore magnetic enhancement is still dominated by magnetite, but there are contributions from slightly higher coercivity materials (such as titanomagnetite) that increase the ratio towards -0.8 . Unit 2 has S-ratio values that average around -0.95 indicating that the magnetic signal is dominated by magnetite (though maghaemite may also be present as indicated in Figure 3.12, but it is 1,000 times weaker than magnetite so it would be masked). Unit 3 is similar to unit 1 but it shows greater variability in the S-ratio values as magnetic enhancement occurs. As χ increases the S-ratio increases from -0.88 to -0.6 indicating that harder magnetic minerals are contributing to the sediment as magnetic enhancement occurs. The scatter in values gives an indication that magnetic mineral composition is not the only controlling factor because both parameters depend on composition so if this was the only or dominant factor a linear correlation would be observed. Therefore grain size or mineral concentration is also influencing the signal in this unit. Unit 4 is the most unique in this graph; magnetic enhancement shows a decrease from S-ratios of -0.3 to -0.65 indicating that magnetically softer minerals (such as magnetite) are being added as the χ increases. The higher S-ratios identify that there are harder magnetic minerals dominating the magnetic signal in this last unit than any other unit.

SIRM vs χ Bivariate Plot

Next a bivariate plot of SIRM versus χ for cubet subsamples from cores FMB1 and FMB4 was prepared (see Figure 3.15) to examine the grain size changes of magnetic mineral assemblages between units and cores, and to evaluate the dependence of SIRM

Figure 3.15: Bivariate plot of SIRM versus χ for cubet subsamples from cores FMB1 and FMB4. This plot examines the grain size changes of magnetic mineral assemblages between units and cores, and evaluates the dependence of SIRM and χ on magnetic mineral concentration. The data have been further classified according to the units depicted in Figures 4 and 5 that were determined based upon their lithologic and magnetic properties.



and χ on magnetic mineral concentration. The data were again further classified according to the units depicted in Figure 3.4 to Figure 3.7 that were determined based upon their lithologic and magnetic properties. The strong linear correlation and minimal scatter observed for units 1, 3 and 4 in both cores (all R^2 values between 92.1 and 99.6) indicates that both SIRM and χ depend strongly on concentration and that particle size and/or mineralogy play a small role. Unit 2 exhibits a poor correlation for both cores with a great deal of scatter indicating that magnetic mineral concentration bears at most a moderate influence on SIRM and χ , therefore particle size and mineralogy may also have an influence.

Since SIRM is grain size dependant (decreases with larger sized particles), while χ is not (unless sample has superparamagnetic grains), the SIRM/ χ ratio will be higher if there are a greater number of smaller particles. Therefore slope of the linear correlations (SIRM/ χ) for each unit offer information regarding the dominant grain size assemblage for each unit. Unit 1 in core FMB1 is slightly finer grained than in core FMB4, while the magnetic mineral grain size assemblages in units 3 and 4 for both cores are approximately the same (FMB1 is slightly finer grained again). Unit 2 SIRM/ χ values of 0.79 kA/m and 1.09 kA/m, for cores FMB1 and FMB2 respectively, show distinctly coarser grained magnetic mineral sediments, with unit 2 in FMB1 having the coarser assemblage. The ESEM images shown in Figure 3.9 of small magnetic spherules in unit 1 and coarser grained magnetic minerals in unit 2 also support the SIRM/ χ findings of coarser grains in unit 2 than unit 1, which reflects the influence of increased

concentrations of small magnetic spherules in the upper layer. SIRM/ χ values greater than 70 kA/m can be interpreted as an indicator for the presence of greigite (Evans and Heller 2003; Geiss and Banerjee 2003). Since these values were not identified in any sample, greigite as a significant contributor to the magnetic signal in FMB sediments has not been identified.

χ vs. TOC+CO₃ Bivariate Plot

A bivariate plot of χ versus weight percent organic and carbonate matter was prepared (see Figure 3.16) for subsamples from cores FMB1 and FMB4. The strong correlation ($R^2=0.86$) indicates that variations in χ are strongly influenced by organic and carbonate matter content. In this case increased organic and carbonate content dilutes the magnetic signal for units 1,3 and 4. There is some scatter present, which indicates that other factors such as magnetic mineral composition and/or grain size also influence the magnetic properties of the sediment. There is great scatter for unit 2 in both cores which indicates that increased organic and carbonate content does not control the magnetic mineral concentration.

Gradient of IRM acquisition curve

The gradient of IRM acquisition curve (Figure 3.17) is plotted using the change (a positive increase) in IRM after each higher magnitude applied field is applied to the sample. This curve is useful because the magnitude of the applied field at the centre of any gaussian curve on the graph identifies the presence of a mineral magnetic species because this median applied field point represents the Bcr' value (which approximates

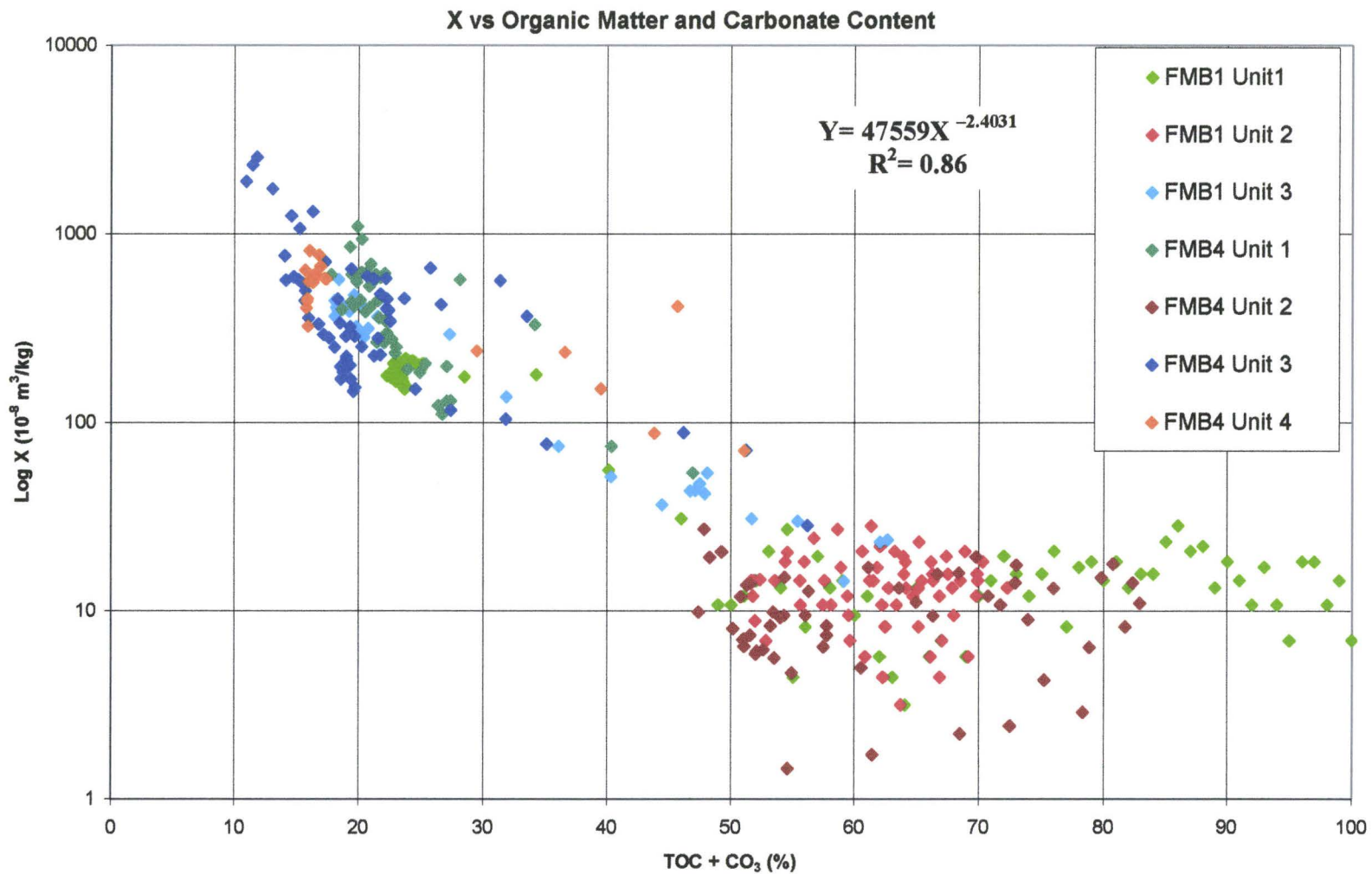


Figure 3.16: Bivariate plot of χ versus weight percent organic and carbonate matter for subsamples from cores FMB1, FMB2, FMB3, and FMB4.

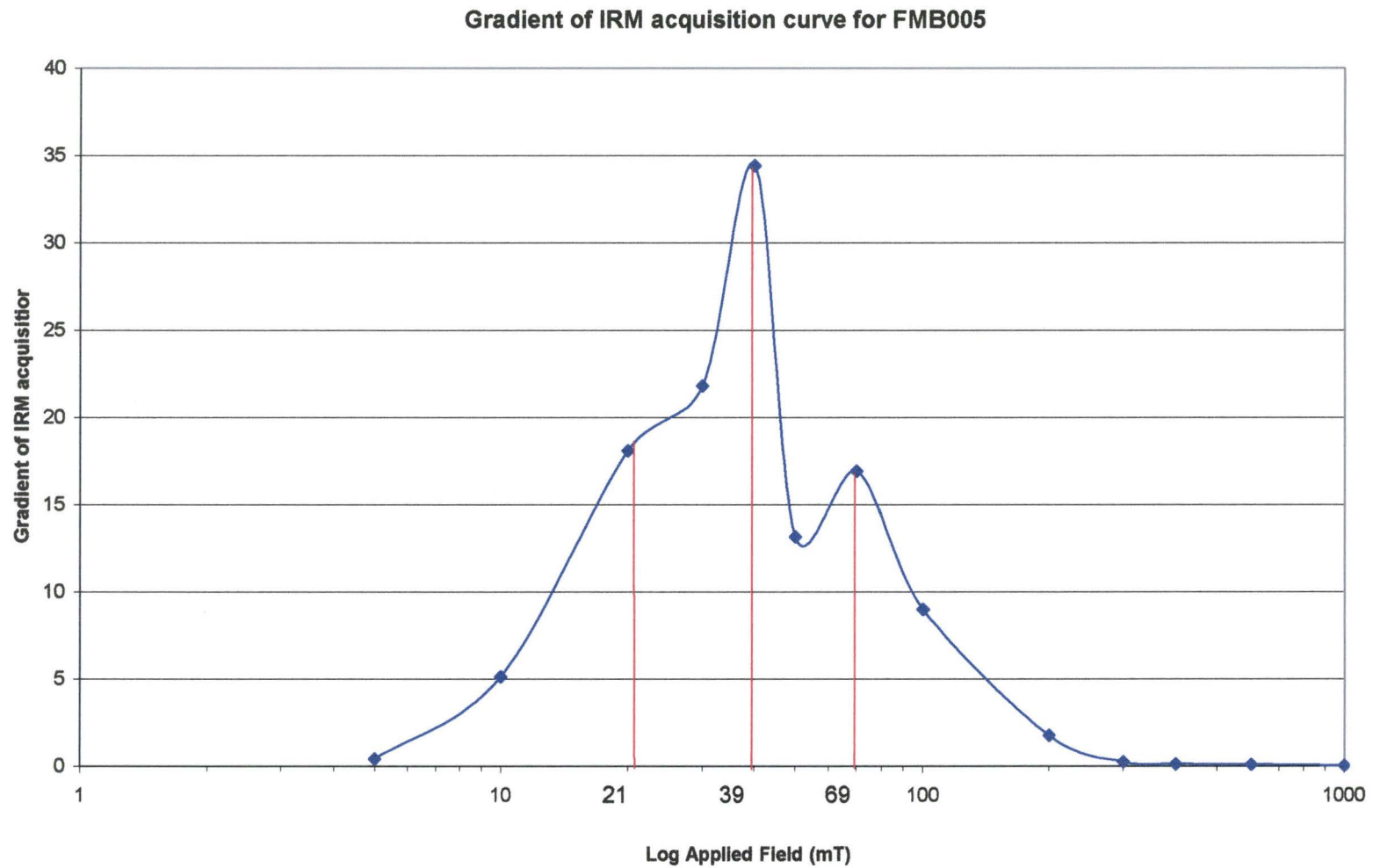


Figure 3.17: The gradient of IRM acquisition curve for a sediment sample from unit 1 (depth = 10.5 cm) in core FMB1.

Bcr). This median applied field point can then be compared against known Bcr values to identify the magnetic mineral species. The curve for the core FMB1 sediment sample from unit 1 (depth = 10.5 cm) shown in Figure 3.17 identifies the presence of magnetite, titanomagnetite and greigite with their respective Bcr values (21 mT, 39 mT, and 69 mT) in this sediment sample.

Dominant Magnetic Characteristics of Each Unit

The SIRM/ χ versus Bcr plot reveals that most of the sediment samples plot in the region for magnetite with some samples enriched in titanomagnetite.

The small magnetic grain size shift from increased fine grains at the base of unit 1 to a greater concentration of coarser grains near the top of unit 1 is reflected well in the χ , κ , NRM intensity and SIRM/ χ data. Magnetic susceptibility is not influenced by grain size (but the concentration due to the larger grains does remain significant) unless SP grains are present, while small SD grains are the most efficient remanence carriers. Therefore the high χ and κ values observed while NRM intensity and SIRM/ χ values are low indicate that the magnetism is due to larger magnetic grains than those lower in unit 1. The great variation in the NRM inclination at the top of unit 1 is due to DRM.

The middle of the sequence (Unit 2) is weakly magnetic with low κ , χ and SIRM values, which suggests a low concentration of ferromagnetic minerals. The Bcr values decrease towards 28 mT and 27 mT (in FMB1 and FMB2 respectively) indicating that the magnetic minerals are becoming dominated by magnetically softer magnetite. There is great variability in the SIRM/ χ values of unit 2 which indicates that the grain size of the

magnetic mineral assemblage varies greatly, which is supported by the great degree of scatter in Figure 3.15. Figure 3.15 shows that concentration bears at most a moderate influence on both SIRM and χ , so grain size and/or mineralogy must have a major influence on this second unit.

The sediments of Unit 3 are magnetically enriched with higher χ and κ values than those observed in units 1 and 2. The sediments from the lake are enriched in magnetic minerals because reworking of sediments at the shoreline removes finer grain sediments and leaves larger coarser grained sediments. Therefore the lake is inferred as the source for the larger magnetic mineral grains observed in unit 3. While χ and κ values are high, the NRM intensity and SIRM/ χ values are low and comparable to those observed for the upper part of unit 1, therefore the magnetic mineral grain sizes are similarly larger in unit 3. The lowest NRM intensity and SIRM/ χ values at the base of unit 3 indicate a concentration of slightly coarser magnetic minerals.

The sediments in unit 4 that have coercivity of remanence (B_{cr}) values exceeding 40 mT with S-ratios that rise to values distinctly above -1 suggests partial oxidation of magnetite or the presence of minor amounts of high coercivity minerals such as goethite or hematite.

3.5 Discussion/ Environmental Interpretation

The lithologic and magnetic evidence discussed in the previous sections have been interpreted to provide a sediment model for the formation of Frenchman's Bay, which is shown in Figure 3.18. The model will be discussed from the earliest stage for which evidence has been collected (the initial FMB basin formation 12,500 to 4000 ybp) until the final modern stage, while also identifying supporting evidence.

3.5.1 Stage 1: FMB Basin Formation (Unit 4)

The compacted sediments of unit 4 possibly define previously deposited glacial Lake Iroquois clays that were eroded 12,000 ybp during the low lake level position of Lake Ontario by a paleoriver that was located at FMB's present position (see Figure 3.18 A). There is an erosional contact at the top of unit 4 that provides evidence for the erosion of the glacial clays. The previously deposited Lake Iroquois clays would have been deposited between 13,000 and 12,500 ybp when lake levels were stable due to the Laurentian ice sheet blocking Lake Iroquois lake waters from the St. Lawrence outlet. When the Laurentian ice sheet retreated (~12,000 ybp) and opened up the St. Lawrence outlet, the ancient Lake Iroquois waters were released, which allowed lake levels to decline to their lowest level, and a paleoriver developed at the FMB position. The much lower lake levels would have triggered significant erosion within the paleoriver valley due to the lower water baseline, which would carve out the basement of the future Frenchman's Bay lagoon. The decrease in water level would also change the elevation and position at which wetlands would be found since wetlands form within ~1 m of the

lake water level. There is evidence that wetlands formed along the shore of the low lake from the peats that are preserved above the glacial clays at the top of unit 4.

The magnetic profiles for cores FMB3 and FMB4 show that the peats present at the top of unit 4 have some magnetic minerals while the peats observed in unit 2 essentially do not. Since both are interpreted to have formed from organic matter produced in wetlands with further organic enrichment from primary productivity, the difference is due to the availability of magnetically rich sediment from Lake Ontario. When the peats at the top of unit 4 were formed, the beach barrier had not yet been built (since coarse-grained sediments present in beach barrier sediments were not present anywhere in the bay area) so sediment at the shoreline of the lower lake was not blocked from washing into the wetlands (peats). The sediments from the lake are enriched in magnetic minerals because reworking of sediments at the shoreline removes finer grain sediments and leaves larger coarser grained sediments. This inference is supported by the $SIRM/\chi$ values that are the lowest for unit 3 indicating large magnetic mineral grain sizes. The higher NRM intensity values in unit 1 versus those in unit 3 and unit 4 when the χ values in all three units are similar also indicates that unit 3 and unit 4 consist of larger grain sizes that are less efficient at acquiring a remanence while χ does not depend on grain size unless SP grains are present. Unit 1 and unit 2 are dominated by smaller grain size magnetic minerals (indicated by higher $SIRM/\chi$ values) until a depth of 35 cm when both the $SIRM/\chi$ and NRM values decrease indicating larger grain size magnetic minerals in the top section of unit 1 that are less efficient at acquiring NRM. These larger

grain sizes in the top 35 cm are probably due to coarse magnetic minerals washed into the lagoon from railroads, roads and sewers.

3.5.2 Stage 2: Rapid Lake Level Rise

Beginning in 5,000 ybp, increases in basin water supply occurred when the upper Great Lakes drainage returned through Lakes Erie and Ontario, but the outlet channels were unable to release the waters fast enough, so lake levels temporarily rose in addition to the rise due to isostatic rebound until outlet channels could adjust (Anderson and Lewis 1985). Between 4,000 and 3,000 ybp the rise in lake level accelerated during the cooler wetter neoglacial phase of climate in Southern Ontario (Eyles 2002). At the FMB location this resulted in the flooding of the base of the river valley to produce a shallow bay (see Figure 3.18 B).

3.5.3 Stage 3: Formation of Beach Barrier (Unit 3)

Lake levels continue to rise but at greatly reduced rates. Due to prevalent winds and the long fetch of Lake Ontario, strong longshore drift currents from the west would have been present and able to transport coarse-grained sand sediments obtained by erosion of Scarborough sands from the bluffs to the west into the bay. The direction of the prevalent winds (indicated on Figure 3.18C), is sub parallel to the shoreline and mouth of the bay, therefore the deposition of sands via longshore drift would be deflected by the western shore and occur in an approximately triangular area indicated in Figure 3.18 C. These coarse sand sediments are observed at the base of unit 3. Once coarse sediments started to build up along the entrance to the bay the grain size of sediment that

could be transported into the bay decreased because the presence of previously built up sediment served to impede the energy of the incoming waters. Therefore, as a beach barrier developed across the mouth of the bay, the sediments on the newly formed lagoon side of the barrier were deposited in a fining upwards sequence observed in unit 3. Sediments on the lake side of the barrier would be much coarser due to the influence of the high-energy longshore drift and the reworking of sediments.

3.5.4 Stage 4: Stable Oligotrophic Lagoon (Unit 2)

Once a beach barrier was formed across the mouth of the bay (see Figure 3.18 D), coarse sediments could not be supplied to the lagoon from the lake unless a high-energy storm event occurred and was able to break through the barrier via a washover channel or storm surge. Besides impeding the input of sediments from the lake, the barrier also allowed the energy of the lagoon waters to decrease substantially (without the influence of longshore drift or lake currents) so that the sediment regime changed to fine silts and clays, and the peat and organic matter indicate that wetlands formed in the newly stable environment. Sedimentation could still be deposited along the shores of the lagoon, but the sediment size and depositional rates would be greatly reduced and baffled by the wetland vegetation and distance from the shore. Around this time it is evident that the catchment was stabilized by vegetation since detrital inputs decreased while organic and carbonate inputs to FMB increased. It is interesting to note that the unique bathymetry of FMB seems to be controlled by the shape of the original paleoriver valley being filled by the sediments from unit 3 and inputs from shore (see blue line in Figure 3.18D).

The unit of peat marls also contains the initial presence of *Ambrosia* pollen (McCarthy 1986) and glass shards at the top of the unit (Little et al. 2004), therefore it records the onset of colonization in the watershed. The initial presence of *Ambrosia* is used as a colonization indicator. The first known attempt to make glass in Canada was in 1819 (CMCC 1999), therefore sediment deposited above the glass fragments in cores FMB1 and FMB2 is interpreted as being deposited after European settlement of the watershed and after 1819 if glass was not transported earlier from European ports.

Marl precipitation is highly temperature dependant (increased temperature decreases the solubility of calcium carbonate) and forms authigenic sediments when stable catchment vegetation reduces detrital inputs (Nichols 1999; Nolan et al. 1999). Submergent vegetation such as *Myriophyllum* or *Chara* facilitate photosynthetic precipitation of CaCO_3 which slowly accumulates on the lagoon floor to form a chalky deposit (Eyles et al. 2002). Therefore the presence of marl indicates increased aquatic productivity and/or water temperature in a predominantly authigenic sediment regime (Nolan et al. 1999). Calcium carbonate is diamagnetic, with a weak negative magnetic susceptibility, and therefore variations in the ratio of marl to detrital sediments govern concentration dependant magnetic parameters (Nolan et al. 1999; Walden et al. 1999). The presence of mostly marls and organic matter with minimal detrital inputs is reflected well in all of the core magnetic susceptibility (κ and χ) profiles since the values centre around 0×10^{-5} SI (κ) and 0×10^{-8} m^3/kg (χ). During warmer conditions establishment of vegetation within the catchment decreases detrital sedimentation, organic productivity

would increase and marl precipitation could occur which could all contribute to lower magnetic mineral concentrations and lower κ values. These conditions existed with minor temperature and lake level variations when the interbedded marls and peat marls of unit 2 were deposited in a low energy oligotrophic lagoon.

Clayey calcareous oozes, or marls, form at depths above the calcium carbonate compensation depth (Boggs 1995). The reduced calcium carbonate values observed in core FMB1 (<10% versus 60% to 80%) indicate that at the time of formation the sediments could have been at a depth below or near the carbonate compensation depth so that precipitation of calcium carbonate would have been greatly reduced, and possibly halted. The gradual changes from higher CaCO_3 values at the top and bottom of unit 2 suggests that the water level may have risen just above the carbonate compensation depth at the base of unit 2, but then deposition of sediments over the years shallowed the waters enough so that carbonates could once again be deposited in unit 1.

There are peat layers within the second unit that show sharp decreases in calcium carbonate content while organic matter and mineral content increase. This is interpreted to be due to short-term decreases in temperature that increased the solubility of calcium carbonate in the water column so precipitation stopped but the vegetation (or lake productivity) would have taken longer to respond so organic matter was still deposited along with any mineral inputs from the catchment causing their relatively increased concentrations.

3.5.5 Stage 5: The Modern Lagoon (Unit 1)

Slow lake level rise and increased suspended and dissolved sediment load in stream waters due to anthropogenic stresses have choked out submergent plants, benthic invertebrates and cyanobacteria so that production of organic matter was greatly reduced in the lagoon. A reduction in submergent and emergent plants has decreased the amount of sediments that are trapped in the wetlands at the edge of the lagoon so that coarser sediments have been deposited further into the lagoon. As discussed previously, the increased sediment load to streams from more magnetic anthropogenic inputs partially due to greater overland flow to streams, has developed an urban fill delta stemming dominantly from the mouths of Amberlea and Dunbarton creeks. Pine plays a smaller role because agriculture and urban development started ~ 40 years later and at a much slower rate. The influence of large storms (such as the possible 1954 Hurricane Hazel event recorded at an elevation of 7032 cm in core FMB1 with a peak in κ , χ , SIRM, and grain size) depositing magnetically rich and coarse grained sediments in the form of overwash sands into FMB is still observed in the sediment record.

Locke and Bertine (1986) determined that the magnetic susceptibility signal due to magnetite content in sediments first increased in the mid-1800's in New England, around 1900 for Lake Michigan cores, and in the 1920's in Panama samples, which are all coincident with the onset of colonization and industrialization for each area. Specifically, the percent content of magnetic spherules (derived from a coal-combustion origin) increased 20 – 40% with the onset of industrialization. Versteeg et al. (1995) also

identified this relationship in sediments in Hamilton Harbour. This relationship is also observed in the sediments of unit 1 which ^{210}Pb dates identify as deposited after 1850 ± 56 ybp, and is especially strong in the sediments of the urban fill delta. ESEM and XRD work discussed in section 3.3.4 also identify the presence of $10 \mu\text{m}$ magnetite spherules and angular $> 250 \mu\text{m}$ titanomagnetite grains (probably derived from storm sewers, Hwy, or railroad) in FMB sediments which further identifies the onset of industrialization and urbanization influence record in unit 1 sediments. Recent higher magnetic susceptibility values observed in the FMB record are related to more detrital magnetic mineral inputs from the catchment following urbanization. These higher magnetic mineral inputs resulted from new sources of minerals from building materials, combustion processes associated with cars and wood fires and decreased vegetation in the catchment caused by rapid residential developments that caused soils and sediments to be less stable and be washed into FMB tributaries and into the lagoon by overland flow.

Nelson et al. (1991; p. 14) suggest that active currents within FMB throughput most of the incoming sediment (mostly dissolved load clay) to the lake. Evidence for this throughput of sediments to the lake exists in the geometry of the east side of the beach barrier. As sediments exit FMB and pass into Lake Ontario the strong longshore drift currents (from the west) rework the sediments and force them to be deposited on the windward side of the eastern spit. The concave shape of the eastern spit shoreline demonstrates that longshore drift causes significant erosion of these sediments after they have been deposited. A number of hardened shoreline features have been added in the

west (seawalls, groynes, rip rap, docks; Skibicki, 1991) to decrease severe erosion from longshore drift currents and storms, but erosion at the toe of the spit has increased to balance the sediment-starved waters emerging past the structures towards the east.

During the last 100 years, lake level has fluctuated up to 1.4 m in Lake Ontario, though these fluctuations have been reduced to 0.6 m since the opening of the regulated St. Lawrence Seaway in 1959 (St.LawrenceSeawayMgtCorp. 2004). Frenchman's Bay has a maximum water depth of 3.9 m with a general average depth of 2 m and would be strongly influenced by lake level changes. Low lake level will increase shoreline erosion (especially in shallow areas), rework previously existing sediments, and shift the sediment regime to a coarser grained assemblage throughout the lagoon. High lake levels increase accommodation space in FMB and erosion along upper reaches of stream channels so that there will be increased pressure for dredging of silts and clays in nearshore zones due to the additional supply of sediments to the lagoon. This variation in lake level has been reflected in the grain size assemblage of the sediments, which have coarsened during lower lake levels.

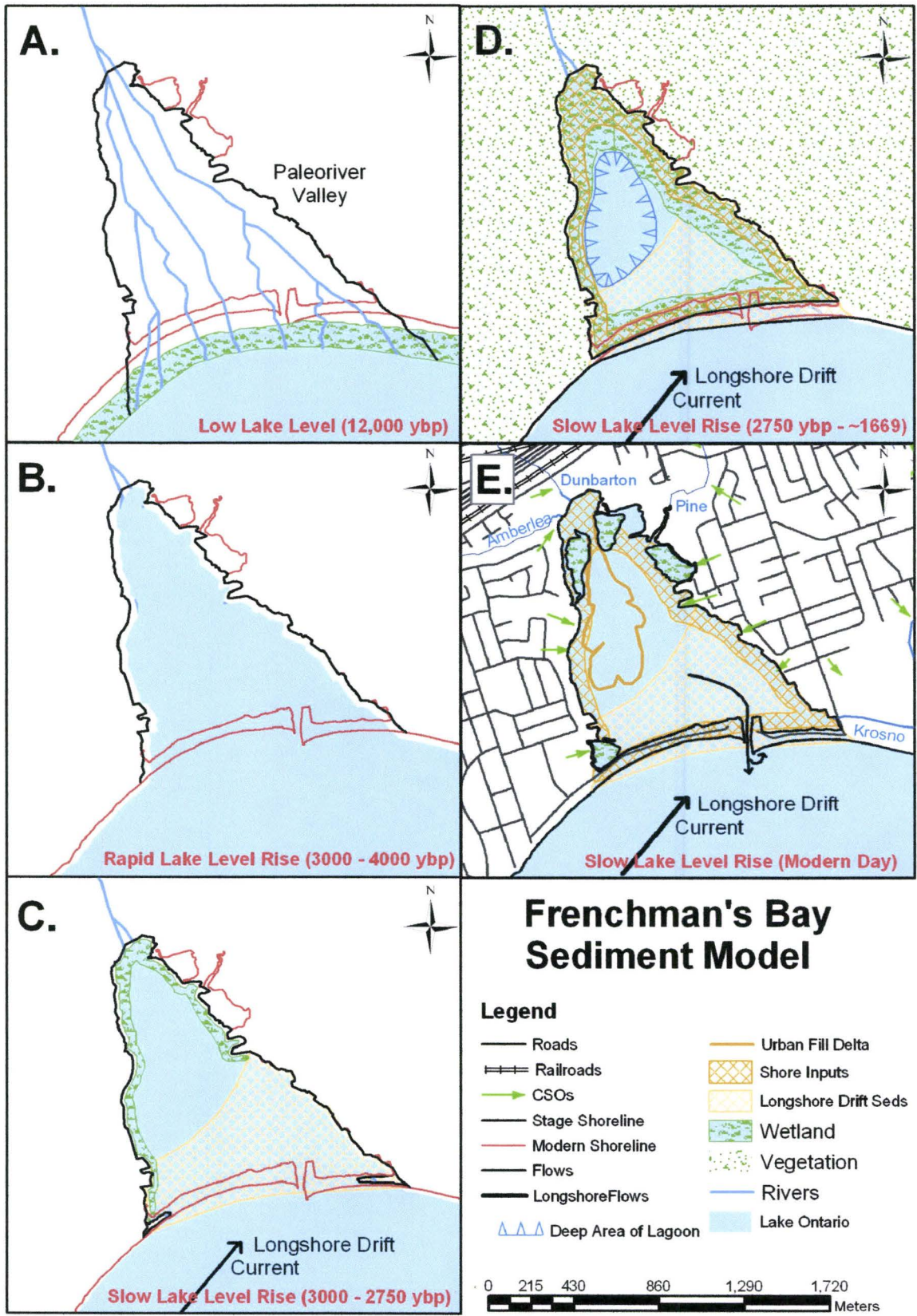


Figure 3.18: Frenchman's Bay Sediment model.

Water Level History

The sequence identified in Figure 4 that changes from stable shallow lagoon peaty marls to deep water gyttja sediments identifies that lake levels have been rising causing transgression of the beach barrier and lagoon. McCarthy (1986) also identified a transgression in FMB and other embayments along Lake Ontario using radiocarbon dates. The water rise causes drowning of wetland vegetation which is deposited as peats that is followed by silty clays once the organics have been removed. This process has been artificially enhanced in recent years when anthropogenic stresses cause increased sediment load in the streams that chokes the wetland vegetation. Deposition of peats and organic matter is followed by more angular and coarser-grained sediment after these events. The interfingering of peaty marls with clastic sediments that coarsen upwards in the south identifies that the beach barrier is translocating towards the north under rising lake level pressure. It should be noted that any sedimentary evidence for the drowning of marshes due to regional lake level rise observed in Lake Ontario has been overprinted in the record by the degradation of marsh vegetation due to anthropogenic activity since the early 1900s. This prevents the use of heavily anthropogenically-influenced lagoons or embayments to track lake-level changes.

3.6 Conclusion

The stratigraphic succession in the lagoon consists of a thick upper sequence of marly gyttja and organic-rich silty muds overlying Holocene organic-rich discontinuously laminated marls, that are above sandy silts interpreted as pre-colonial late Holocene sands

with moderate carbonate content and elevated mineral and magnetic susceptibility values. Investigation of all of the lithologic, magnetic, and microfossil parameters together (that could otherwise present multiple solutions on their own) served to refine multiple depositional options into one plausible sediment deposition model for Frenchman's Bay. The model identifies that the lagoon developed when longshore drift of scarborough sediments from the west built up a beach barrier across an embayment that had formed previously when rapid lake level rise flooded a paleoriver valley. The succession mentioned above traces the evolution of Frenchman's Bay from a young lagoon that received high concentrations of detrital minerals from an unstable catchment following deglaciation to a stable oligotrophic state where abundant organic matter and carbonate was deposited as temperatures increased and catchment vegetation stabilized. A final evolution under anthropogenic influences occurred as an order of magnitude increase in sediment rates (since the onset of industrialization) and new source sediments from agricultural, residential and industrial activities combined to form a modern 'urban-fill delta' in the northwest area of a now eutrophic lagoon. The magnetic susceptibility profiles also identified several discrete sand incursion layers within the marl units that likely record periodic storm overwash events.

Chapter 4: CONCLUSIONS

The overall objective of this thesis is to document the historical environmental change and more recent anthropogenic impacts in Frenchman's Bay. Although fieldwork was conducted at the same location (Frenchman's Bay), after first presenting background material this work was divided into two papers prepared for publication in academic journals. The paper presented in Chapter 2 focused on the feasibility of the new lake-base *method* that employed a proto-type probe developed for this project in order to map urban sediments, while the paper in Chapter 3 discussed the paleoenvironmental findings of the multi-parameter study.

An overview of the project was provided in Chapter 1, which included three objectives: i) mapping lagoon bottom sediments of FMB and construction of a depositional model to explain the observed stratigraphy; ii) evaluating the use of a rapid in-situ proto-type probe as a method for mapping anthropogenic sediments in the lagoon; and iii) reconstructing paleoenvironmental changes and human impacts on FMB using a multi-parameter magnetic and sediment physical property database. A discussion of the physical setting, geology, historical background and previous work conducted within the Frenchman's Bay study site was offered to familiarize the audience with the field site. Since environmental magnetism is a relatively unique and significant area of study explored in this thesis, a moderate discussion of background magnetic theory was supplied so that specific magnetic properties could be quickly discussed and interpreted in later chapters. Next the background theory and rationale for the methodologies applied

in later chapters was also described and included potential limitations that could be encountered.

An alternate approach to time consuming ex-situ magnetic susceptibility measurements was investigated in Chapter 2 when near continuous in-situ measurements of sediment volume magnetic susceptibility (κ) were obtained using a probe driven into the lake bottom. An inexpensive proto-type probe was constructed using a Bartington MS2-F sensor mounted in waterproof housing with an extendable 10 m handle. Laboratory testing first determined that the effective sensing volume is a 2.2 cm radius around the probe tip, ~1 cm thick beds could be identified, and that edge effects from sensor shoulders are negligible. The probe was then used to measure the thickness and distribution of a post-colonial sediment layer in Frenchman's Bay. Volume susceptibility profiles were collected at 35 locations by driving the probe up to 2.5 m into the lagoon bottom sediments at 2 cm measurement intervals. The base of the post-colonial sediment layer present in the lagoon was identified by an abrupt increase in magnetic susceptibility at 0.5-1.2 m depth. The marker horizon was correlated across the lagoon and the thickness and volume of the anthropogenic layer was estimated. The results demonstrate that in-situ susceptibility measurements using a sediment probe can provide a rapid and highly repeatable method for correlating shallow stratigraphic boundaries within unconsolidated lake bottom sediments.

Coastal environments in the lower Great Lakes have been modified significantly by post-colonial land use changes and the growth of industry. In Chapter 3 the sediment

magnetic record of these changes was investigated in a small coastal lagoon (Frenchman's Bay) lying at the eastern limits of the Greater Toronto Area in western Lake Ontario. A total of 11 vibracores (2 - 4.5 m length) were retrieved from the lagoon and the lithofacies were logged in detail and magnetic property, micropaleontologic and textural analyses were performed on core samples. Magnetic analyses included measurements of volume and bulk magnetic susceptibility (κ , χ) and remanence parameters (NRM, SIRM, B_{cr}) on 8 cm³ sub-samples. The stratigraphic succession in the lagoon consists of a thick upper sequence of marly gyttja and peat-rich silty marls overlying Holocene laminated marls. Magnetic property analyses identify an uppermost high magnetic susceptibility ($\chi \cong 200\text{-}300 \times 10^{-8} \text{ m}^3/\text{Kg}$) gyttja unit that extends to 1-1.5 m depth. The base of the unit has a ²¹⁰Pb age of 1850 (± 55.6), which corresponds with the main phase of land clearance and onset of industrialization of the harbour. The ²¹⁰Pb analysis also determined that there was an order of magnitude increase in sediment accumulation rates since the onset of industrialization. Magnetic and ESEM analyses identify titanomagnetite, maghemite and magnetite spherules, indicating that soil erosion and also coal burning are the predominant sources of magnetic particles. The underlying unit consists of peaty marls with abundant plant fragments recording a more extensive marsh. The third, lowermost unit consists of more carbonate-rich laminated marls (magnetic susceptibility $\chi \cong 6000 \times 10^{-8} \text{ m}^3/\text{Kg}$) deposited in a low energy oligotrophic lagoon.

Isopach mapping of the magnetostratigraphic units clearly identifies that the anthropogenic layer (Unit 1; post-1850) is thickest within a central basin which has acted as trap for sediment carried into the lagoon by several streams. The total volume of contaminated anthropogenic sediment is estimated at $3.98 \times 10^5 \text{ m}^3$. Isopach maps also identify a thin ($< 2 \text{ m}$) wedge of sand ($9.6 \times 10^4 \text{ m}^3$) near the southern shore of the bay that records periodic overwash and growth of the beach barrier.

Investigation of all of the lithologic, magnetic, and microfossil parameters together (that could otherwise present multiple solutions on their own) served to refine multiple depositional options into one plausible sediment deposition model for Frenchman's Bay. The model identifies that the lagoon developed when longshore drift of scarborough sediments from the west built up a beach barrier across an embayment that had formed when rapid lake level rise flooded a paleoriver valley. European settlement, modern agriculture and urbanization have all had a dramatic effect on the lagoon and watershed. Hardened shorelines and surfaces due to urbanization and increased sources of urban sediment has led to increased sedimentation rates and the development of an 'urban-fill delta' in the northwest area of Frenchman's Bay. These results demonstrate the utility of magnetic property measurements as a tool in paleoenvironmental reconstruction of lake basins, and the further advantage of multiparameter studies when multiple solutions are possible with the investigation of single parameters.

Chapter 5: REFERENCES

- Anderson, T. W. and C. F. M. Lewis (1985). Postglacial Water-Level History of the Lake Ontario Basin. Quaternary Evolution of the Great Lakes. P. F. Karrow, Geological Association of Canada. **Special Paper 30**: 231 - 252.
- Beckwith, P. R., J. B. Ellis, D. M. Revitt and F. Oldfield, (1986), Heavy Metal and Magnetic Relationships for Urban Source Sediments: *Physics of the Earth and Planetary Interiors*, **42**: 67 - 75.
- Boar, R. R. and D. M. Harper, (2002), Magnetic susceptibilities of lake sediment and soils on the shoreline of Lake Naivasha, Kenya: *Hydrobiologia*, **488**: 81-88.
- Boggs, S. (1995). Principles of Sedimentology and Stratigraphy. New Jersey, Prentice-Hall.
- Breiner, S. (1973). Applications Manual for Portable Magnetometers. California, GeoMetrics.
- Butler, R. F. (1992). Paleomagnetism: Magnetic Domains to Geologic Terranes. Oxford, Blackwell Science Inc.
- CanadianHydrographicService, (2003), Historical monthly mean water levels from the coordinated network of gauging stations for each of the Great Lakes.: Dept. Fisheries and Oceans Canada, [Online] Available: http://biachss.bur.dfo.ca/danp/network_means.html May 31.
- Chan, L. S., C. H. Yeung, W. W.-S. Yim and O. L. Or, (1998), Correlation between magnetic susceptibility and distributions of heavy metals in contaminated sea-floor sediments of Hong Kong Harbour: *Environmental Geology*, **36**: 77 - 86.
- CMCC, (1999), Canadian Glass: Canadian Museum of Civilization Corporation (CMCC), [Online] Available: <http://www.civilization.ca/hist/verre/vecan01e.html> April 1.
- Cornett, D. J. and J. Lardner (2004). Aging Environmental Samples Using ²¹⁰Pb. Deep River, MyCore Scientific Inc.: 6.
- Coulter (2001). Manual for Beckman-Coulter LS 230 Laser Particle Size Analyser.
- Dean, W. E., (1981), Carbonate Minerals and Organic Matter in Sediments of Modern North Temperate Hard-Water Lakes: *Society of Economic Paleontologists and Mineralogists*, **31**: 213 - 231.
- Desenfant, F., E. Petrovsky and P. Rochette, (2004), Magnetic signature of industrial pollution of stream sediments and correlation with heavy metals: Case study from South France: *Water Air and Soil Pollution*, **152**: 297 - 312.

- Dunlop, D. J. and O. Ozdemir (1997). Rock Magnetism Fundamentals and Frontiers. Cambridge, Cambridge University Press.
- Ekdahl, E., J. L. Teranes, T. P. Guilderson, C. L. Turton, J. H. McAndrews, C. A. Whittkop and E. F. Stoermer, (2004), Prehistorical record of cultural eutrophication from Crawford Lake, Canada: *Geology*, **32**: 745 - 748.
- Evans, M. E. and F. Heller (2003). Environmental Magnetism: Principles and Applications of Enviromagnetics. London, Academic Press.
- Eyles, N. (2002). Ontario Rocks - Three Billion Years of Environmental Change. Markham, Fitzhenry & Whiteside Limited.
- Eyles, N. and P. Chow-Fraser (2003). Remediation of an Urban-Impacted Watershed and Lagoon: Frenchman's Bay, City of Pickering, Ontario. Innovation Trust and the City of Pickering Final Report.
- Eyles, N., P. Chow-Fraser, J. I. Boyce, M. Meriano, T. Seilheimer, M. Doughty and K. Howard (2002). Remediation of an urban-impacted watershed and lagoon: Frenchman's Bay, City of Pickering.: 70pp.
- Geiss, C. E. (1999). The development of rock magnetic proxies for paleoclimate reconstruction, University of Minnesota: 273.
- Geiss, C. E. and S. K. Banerjee, (2003), A Holocene–Late Pleistocene geomagnetic inclination record from Grandfather Lake, SW Alaska: *Geophys. J. Int.*, **153**: 497–507.
- Gerrie, V., K. Blasco and S. Collins (2003). Geophysical SURcey Interpretation Report: Borehole physical property surveys for Region of York, Peel, and Durham. Toronto, Quantec Logging Services Inc.: 43.
- Heiri, O., A. F. Lotter and G. Lemcke, (2001), Loss on Ignition as a Method for Estimating Organic and Carbonate Content in Sediments: Reproducibility and Comparability of Results: *Journal of Paleolimnology*, **25**: 101 - 110.
- Heller, F., Z. Strzyszcz and T. Magiera, (1998), Magnetic record of industrial pollution in forest soils of Upper Silesia, Poland: *Journal of Geophysical Research*, **103**: 17,767 - 17,774.
- Hilfinger, M. F., H. T. Mullins, A. Burnett and M. Kirby, (2001), A 2500 year sediment record from Fayette Green Lake, New York: evidence for anthropogenic impacts and historic isotope shift: *Journal of Paleolimnology*, **26**: 292 - 305.
- Hoffmann, V., M. Knab and E. Appel, (1999), Magnetic susceptibility mapping of roadside pollution: *Journal of Geochemical Exploration*, **66**: 313 - 326.
- Hunting (1954). Digital Aerial Photographs, Southern Ontario 1954 - West Index, Hunting Survey Corporation Limited.

- King, J., S. K. Banerjee, J. Marvin and O. Ozdemir, (1982), A Comparison of Different Magnetic Methods for Determining the Relative Grain Size of Magnetite in Natural Materials: Some Results From Lake Sediments: *Earth and Planetary Science Letters*, **59**: 404 - 419.
- Kodama, K. P., J. C. Lyons, P. A. Siver and A. M. Lott, (1997), A mineral magnetic and scaled-chrysophyte paleolimnological study of two northeastern Pennsylvania lakes: Records of fly ash deposition, land-use change, and paleorainfall variation: *Journal of Paleolimnology*, **17**: 173 - 189.
- Last, W. M. and J. P. Smol (2001). Volume 1: Basin Analysis, Coring, and Chronological Techniques. Dordrecht, The Netherlands, Kluwer Academic Publishers.
- Last, W. M. and J. P. Smol (2001). Volume 2: Physical and Geochemical Methods. Dordrecht, The Netherlands, Kluwer Academic Publishers.
- Little, M., D. Findlay, A. Krueger, C. Clark, J. Boyce, S. Donato and E. G. Reinhardt, (2004), Arcellacean (thecamoebian) changes in Frenchman's Bay, Pickering, Ontario, and the impact of urbanization on water quality: GAC MAC Joint Annual Meeting, **Poster Session SS9-1**.
- Locke, G. and K. K. Bertine, (1986), Magnetite in Sediments as an Indicator of Coal Combustion: *Applied Geochemistry*, **1**: 345 - 356.
- McCarthy, F. (1986). Late Holocene water levels in Lake Ontario: Evidence from Grenadier Pond. Department of Geology. Scarborough, University of Toronto: 114.
- Morris, W. A., J. K. Versteeg, D. W. Bryant, A. E. Legzdins, B. E. McCarry and C. H. Marvin, (1995), Preliminary Comparisons Between Mutagenicity and Magnetic Susceptibility of Respirable Airborne Particulate: *Atmospheric Environment*, **29**: 3441 - 3450.
- Morris, W. A., J. K. Versteeg, C. H. Marvin, B. E. McCarry and N. A. Rukavina, (1994), Preliminary Comparisons Between Magnetic Susceptibility and Polycyclic Aromatic Hydrocarbon Content in Sediments from Hamilton Harbour, Western Lake Ontario: *Sci. Total Envir.*, **152**: 153 - 160.
- Moskowitz, B. M. (1991). Hitchhiker's Guide to Magnetism. Environmental Magnetism Workshop. Minneapolis, Institute for Rock Magnetism.
- Murray, M. R., (2002), Is Laser Particle Size Determination Possible for Carbonate-Rich Lake Sediments?: *Journal of Paleolimnology*, **27**: 173 - 183.
- Nelson, J. G., A. J. Skibicki, R. E. Stenson and C. L. Yeung (1991). Urbanization, Conservation and Sustainable Development: The Case of Frenchman's Bay, Toronto, Ontario. Waterloo, Heritage Resources Centre, University of Waterloo: 102.
- Nichols, G. (1999). Sedimentology and Stratigraphy. Oxford, Blackwell Science Ltd.

- Nolan, S. R., J. Bloemendal, J. F. Boyle, R. T. Jones, F. Oldfield and M. Whitney, (1999), Mineral magnetic and geochemical records of late Glacial climate change from two northwest European carbonate lakes: *Journal of Paleolimnology*, **22**: 97 - 107.
- Oldfield, F., (1990), Magnetic measurements of recent sediments from Big Moose Lake, Adirondack Mountains, N.Y., USA: *Journal of Paleolimnology*, **4**: 93 - 101.
- Oldfield, F. and N. Richardson, (1990), Lake sediment magnetism and atmospheric deposition: *Philosophical Transactions of the Royal Society*, **B327**: 325 - 330.
- Patterson, R. T., A. Dalby, A. Kumar, L. A. Henderson and R. E. A. Boudreau, (2002), Arcellaceans (thecamoebians) as indicators of land-use change: settlement history of the Swan Lake area, Ontario as a case study: *Journal of Paleolimnology*, **28**: 297 - 316.
- Peters, C. and M. J. Dekkers, (2003), Selected room temperature magnetic parameters as a function of mineralogy, concentration and grain size: *Physics and Chemistry of the Earth*, **28**: 659 - 667.
- Petrovsky, E., A. Kapicka, N. Jordanova, M. Knab and V. Hoffmann, (2000), Low-field magnetic susceptibility: a proxy method of estimating increased pollution of different environmental systems.: *Environmental Geology*, **39**: 312 - 318.
- Pickering, (2001), Pickering Waterfront: City of Pickering, [Online] Available: <http://www.cityofpickering.com/>
- PlantownConsultantsLtd. (1975). The North Pickering Project: Evaluation of Phase III modified concept plans. Interim Report 2 for the Ministry of Housing Ontario. Pickering, Plantown Consultants Ltd.
- Pozza, M. R., J. I. Boyce and W. A. Morris, (2004), Lake-based magnetic mapping of contaminated sediment distribution, Hamilton Harbour, Lake Ontario, Canada: *Journal of Applied Geophysics*, *Accepted*.
- Reynolds, R. L. and J. W. King, (1995), Magnetic records of climate change: *Reviews of Geophysics*, **33**.
- Reynolds, R. L., J. G. Rosenbaum, P. v. Metre, M. Tuttle, E. Callender and A. Goldin, (1999), Greigite (Fe₃S₄) as an indicator of drought - The 1912-1994 sediment magnetic record from White Rock Lake, Dallas, Texas, USA: *Journal of Paleolimnology*, **21**: 193 - 206.
- Robertson, D. J. and D. E. France, (1994), Discrimination of remanence-carrying minerals in mixtures, using isothermal remanent magnetization acquisition curves: *Physics of the Earth and Planetary Interiors*, **82**: 223-234.
- Rummery, T. A., (1983), The use of magnetic measurements in interpreting the fire histories of lake drainage basins: *Hydrobiologia*, **103**: 53 - 58.

- Schultes, K., (2004). Environmental Scanning Electron Microscopy (ESEM) and Xray Diffraction (XRD). [Personal Communication]. Life Science Electron Microscopy Unit, McMaster University.
- Shenggao, L., (2000), Lithological factors affecting magnetic susceptibility of subtropical soils, Zhejiang Province, China: *Catena*, **40**: 359 - 373.
- Skibicki, A. J. (1991). Frenchman's Bay Resource: Cultural and Institutional Aspects. Urbanization, Conservation and Sustainable Development: The Case of Frenchman's Bay, Toronto, Ontario. C. L. Yeung. Waterloo, Heritage Resources Centre, University of Waterloo: 69 - 102.
- Smol, J. P., (1992), Paleolimnology: an important tool for effective ecosystem management: *Journal of Aquatic Ecosystems Health*, **1**: 49-58.
- Snowball, I. F., (1994), Bacterial magnetite and the magnetic properties of sediments in a Swedish lake: *Earth and Planetary Science Letters*, **126**: 129-142.
- St.LawrenceSeawayMgtCorp., (2004), THE MONTREAL/LAKE ONTARIO SECTION OF THE SEAWAY - History: Saint Lawrence Seaway Development Corporation The St. Lawrence Seaway Management Corporation, [Online] Available: <http://www.greatlakes-seaway.com/en/pdf/mlo.pdf>
- Stenson, R. E. (1991). Frenchman's Bay: Abiotic Report. Urbanization, Conservation and Sustainable Development: The Case of Frenchman's Bay, Toronto, Ontario. C. L. Yeung. Waterloo, Heritage Resources Centre, University of Waterloo: 1-28.
- Stockhausen, H., (1998), Some new aspects for the modelling of isothermal remanent magnetization acquisition curves by cumulative log Gaussian functions: *Geophys. Res. Lett.*, **25**: 2217.
- Thompson, R. and F. Oldfield (1986). Environmental Magnetism. London, Allen and Unwin.
- TRCA, (1999), The Frenchman's Bay Watershed: Toronto and Region Conservation Authority, [Online] Available: <http://www.frenchmansbayfestival.com/Theme%20page.htm>
- Verosub, K. L. and A. P. Roberts, (1995), Environmental Magnetism - Past, Present, and Future: *Journal of Geophysical Research-Solid Earth*, **100**: 2175 - 2192.
- Versteeg, J. K. (1994). The Characterization and Distribution of Contaminated Sediments in Hamilton Harbour as Determined by Magnetic Property Analysis. Department of Geology. Hamilton, McMaster University.
- Versteeg, J. K., W. A. Morris and N. A. Rukavina (1995). Mapping Contaminated Sediment in Hamilton Harbour, Ontario. Environmental Geology of Urban Areas: 241 - 248.

- Versteeg, J. K., W. A. Morris and N. A. Rukavina, (1995), The utility of magnetic properties as a proxy for mapping contamination in Hamilton Harbour sediment.: *Journal of Great Lakes Research*, **21**: 71 - 83.
- Walden, J. and K. Addison, (1995), Mineral magnetic analysis of a 'weathering' surface within glacial sediments at Glanllynau, North Wales: *Journal of Quaternary Science*, **10**: 367 - 378.
- Walden, J., F. Oldfield and J. Smith, Eds. (1999). Environmental Magnetism: A Practical Guide. London, Quaternary Research Association.
- Yeung, C.-L. (1991). The Biological and Water Quality Status of Frenchman's Bay. Urbanization, Conservation and Sustainable Development: The Case of Frenchman's Bay, Toronto, Ontario. C. L. Yeung. Waterloo, Heritage Resources Centre, University of Waterloo: 29-68.

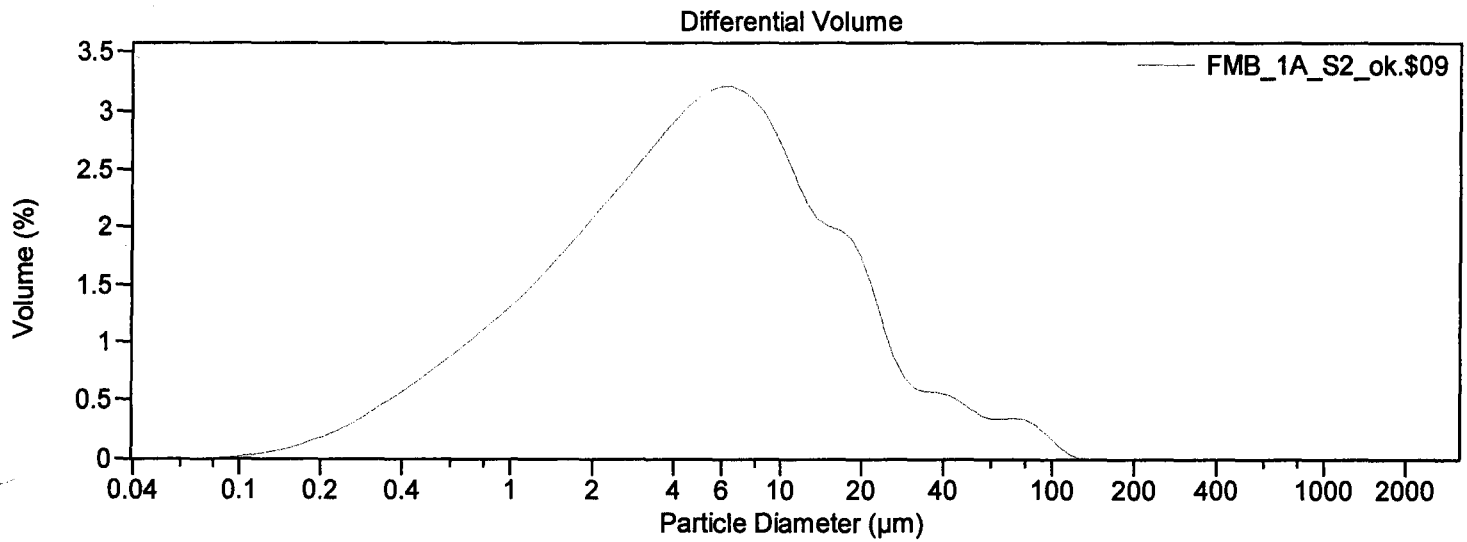
Appendix A:

LITHOLOGIC LOG TEMPLATE

Appendix B:

**EXAMPLE PRINTOUT FROM THE BECKMAN-COULTER LS
230 LASER PARTICLE SIZE ANALYSER**

name:	FMB_1A_S2_ok.\$09	Group ID:	FMB_1A_
Sample ID:	S2		
Run number:	9	Operator:	CTC
Comments:	with peroxide and HCl		
Optical model:	Fraunhofer.rfd PIDS included		
Model:	230 VSM+		
Start time:	15:52 5 Dec 2002	Run length:	121 seconds
Temp speed:	100		
Obscuration:	12%	PIDS Obscur:	79%
Medium:	Water		
Firmware:	3.01	Firmware:	2.02 0



Volume Statistics (Arithmetic)

FMB_1A_S2_ok.\$09

Calculations from 0.0400 µm to 2,000 µm

Volume:	100%	S.D.:	13.42 µm
Mean:	9.189 µm	Variance:	180.2 µm ²
Median:	4.890 µm	C.V.:	146%
Mode:	5.878 µm	Skewness:	3.640 Right skewed
		Kurtosis:	16.61 Leptokurtic

	10	25	50	75	90
< n	0.838	2.009	4.890	10.46	20.47

Appendix C:

DETAILED LITHOLOGIC LOGS FOR FRENCHMAN'S BAY

